DISCLAIMER NOTICE

THIS DOCUMENT IS THE BEST QUALITY AVAILABLE.

COPY FURNISHED CONTAINED A SIGNIFICANT NUMBER OF PAGES WHICH DO NOT REPRODUCE LEGIBLY.

TIROS METEOROLOGY

ARNOLD H. GLASER

ALLIED RESEARCH ASSOCIATES, INC.
43 LEON STREET · BOSTON 15, MASSACHUSETTS

31 MARCH 1961

FINAL REPORT

UNDER

CONTRACT NO. AF 19(604)- 5581

ARPA ORDER NO. 26-59

ARPA PROJECT CODE NO. 2600

GEOPHYSICS RESEARCH DIRECTORATE
AIR FORCE CAMBRIDGE RESEARCH LABORATORY
OFFICE OF AEROSPACE RESEARCH
UNITED STATES AIR FORCE BEDFORD, MASSACHUSETTS

AFCRL 613

TIROS METEOROLOGY

ARNOLD H. GLASER

ALLIED RESEARCH ASSOCIATES, INC.
43 LEON STREET · BOSTON 15, MASSACHUSETTS

31 MARCH 1961

FINAL REPORT

UNDER

CONTRACT NO. AF 19(604)- 5581

ARPA ORDER NO. 26-59

ARPA PROJECT CODE NO. 2600

GEOPHYSICS RESEARCH DIRECTORATE
AIR FORCE CAMBRIDGE RESEARCH LABORATORY
OFFICE OF AEROSPACE RESEARCH
UNITED STATES AIR FORCE BEDFORD, MASSACHUSETTS

FOREWORD

The work resulting in this report was performed by Allied Research Associates, Inc., Boston, Massachusetts, and was sponsored by the Geophysics Research Directorate, Air Force Cambridge Research Laboratory, Office of Aerospace Research, under Contract No. AF 19(604)-5581, through support provided under Advanced Research Projects Agency Order No. 26-59, Project Code No. 2600.

This report contains contributions from the following authors: R. J. Boucher, C. J. Bowley, C. Dean, A. H. Glaser, A. L. Goldshlak, R. J. Newcomb, R. B. Smith and R. Wexler. Editing and introductory material were provided by R. J. Boucher, A. H. Glaser and R. J. Newcomb.

ABSTRACT

TIROS II has continued the meteorological observational series begun so brilliantly with TIROS I. Further analyses of pictures from both TIROS I and II show how the cloud patterns respond to physical processes. In a cold air outbreak off the northeast coast of the United States it was observed that the cloud edge accurately mirrored the shape of the coast line, displaced some 75 miles to sea. This was found to be the distance required to bring the appropriate heat and moisture to a reasonable mixing condensation level.

In another case, a wake behind a mountain peak was observed in clouds limited by an inversion. It is possible to show that this is an analog to the supersonic wake behind an obstacle.

One of the most striking features of TIROS pictures has been the strong pattern exhibited by cyclonic storms. It has been possible to trace the life history of cyclones as evidenced by these patterns. It is evident from the sequence of patterns that there is much about the life history of the cyclone that is not adequately described by conventional models.

A review of techniques of TIROS data reduction indicates that substantial progress has been made in facilitating the use of satellite meteorological information.

TABLE OF CONTENTS

LIST OF ILLUSTRATIONS

SECTION I

INTRODUCTION

TIROS I was launched from Cape Canaveral on 1 April 1960. It fulfilled its prime function, that of telemetering back to the earth pictures of cloud cover in the earth's atmosphere, with eminent success. To carry on the observational program thus begun, TIROS II was launched from Cape Canaveral into a nearly identical orbit on 23 November 1960. Once again, teams of meteorologists watched the pictorial information as it came down from the satellite at two data acquisitions stations, one at Belmar, New Jersey, and the other at the Pacific Missile Range Station at Point Mugu, California. Trained meteorologists abstracted from the newly-received pictures meteorologically significant information which was forwarded by facsimile and teletype communications to meteorological activities all over the world.

An unfortunate accident during launch beclouded the wide-angle lens of TIROS II. While pictures were still received, they were of reduced contrast and resolution. It was possible to restore much of the contrast by the adjustment of the ground equipment. Resolution seemed to increase with the passage of time, suggesting that the beclouding had resulted from the condensation of slightly volatile material, probably from a rocket exhaust, on the surface of the lens. The narrow-angle lens escaped such contamination. It is interesting to note that this loss of resolution caused less difficulty with meteorological utilization of the images than might have been anticipated.

An important advance in data reduction procedures of TIROS II was the use of machine-drawn latitude-longitude grids at the Point Mugu data acquisition station. There, a small digital computer, furnished with the necessary position and attitude parameters of the satellite, automatically drew an appropriate latitude-longitude grid upon which the picture could be projected to indicate locations of features. A later version of this program permitted entry of only orbital parameters and times of picture taking, the computer performing the necessary interpolations, extrapolations,

and computations to properly locate each picture. The use of this system greatly accelerated the data reduction operation, permitting the transmission of relatively fresh information to meteorological forecast activities. As a result of the success of this venture, the computer equipment will be present at all data acquisitions stations for the projected TIROS III satellite.

TIROS II carried, in addition to the camera equipment, infrared sensors for measurement of the radiation emitted from the surface and the atmosphere of the earth in various wave length bands. These sensors functioned satisfactorily, and data processing is in progress. Real-time data processing was not possible, and accordingly, the infrared observations can not yet be properly evaluated. TIROS II had a magnetic attitude control device that permitted, by ground command, limited changes in the orientation of the spin axis. This was basically a coil wrapped around the satellite. The magnetic dipole produced by current through the coil, interacting with the earth's field, resulted in predictable long-period motion of the axis in space.

This report is the second evaluation of the status and potential of satellite meteorology as seen by Allied Research Associate scientists. The first report (Ref. 1) was published after the end of the TIROS I operation. There is little in the original evaluation that needs revision at this time. Once again we can give but small samples of the tremendous wealth of material contained within the pictures from the two satellites.

We have acquired a somewhat better feeling for the problems of satellite meteorology and their relative difficulty. We have a somewhat more seasoned view of the potentialities of the satellite, and at least some feeling for the probable form that the eventual operational meteorological satellite system will assume.

Our enthusiasm for the television meteorological satellite and the branch of meteorology that it has so abruptly opened is undiminished. We trust that the objectivity with which we attempt to approach the material of the following sections does not obscure our feeling of excitement about the great potentialities and accomplishments of the TIROS satellites.

SECTION II

EVALUATION OF TIROS II IMMEDIATE OPERATIONAL USE PROJECT

2.1 Introduction

Meteorological utility of the TIROS II satellite was somewhat reduced below that of TIROS I because of relatively poor resolution of the pictures obtained from the wide-angle camera. Resolution of the narrow-angle camera was good. Again, as in the TIROS I experiment, over ninety percent of the meteorological analysis effort during the Immediate Operational Use program was confined to wide-angle picture sequences.

This section will be concerned with some of the more recent highlights of the TIROS II Immediate Operational Use program. Particular note should be taken of Section 2.4.3, Data Utility. Despite the low resolution of the wide-angle camera pictures, significant meteorological information was found and considerable utility was derived. This usability of relatively low-grade material is an indication of the general value of meteorological satellite surveillance.

2.2 Picture Resolution

2.2.1 Narrow-Angle Camera

Picture resolution obtained from the narrow-angle camera was comparable to that of TIROS I. Figure 1 is a portion of a narrow-angle photograph taken on orbit 078 and read out at Point Mugu, California, on 28 November 1960.

San Clemente and San Nicolas Islands are visible in the photograph. San Clemente Island is 20 miles long and ranges from a minimum of 2 miles to a maximum of 5 miles in width. San Nicolas Island is 10 miles long and 4 miles wide. The lower figure, 1b, is a map indicating the orientation and location of the two islands.

Figure 2 shows a narrow-angle photograph from TIROS II and a corresponding map of the area visible in the photograph. The picture was taken at 17:40:59 Z on 25 November 1960 during revolution 033, and read out at

EXAMPLE OF NARROW-ANGLE CAMERA RESOLUTION
ORBIT 078 POINT MUGU, CALIFORNIA

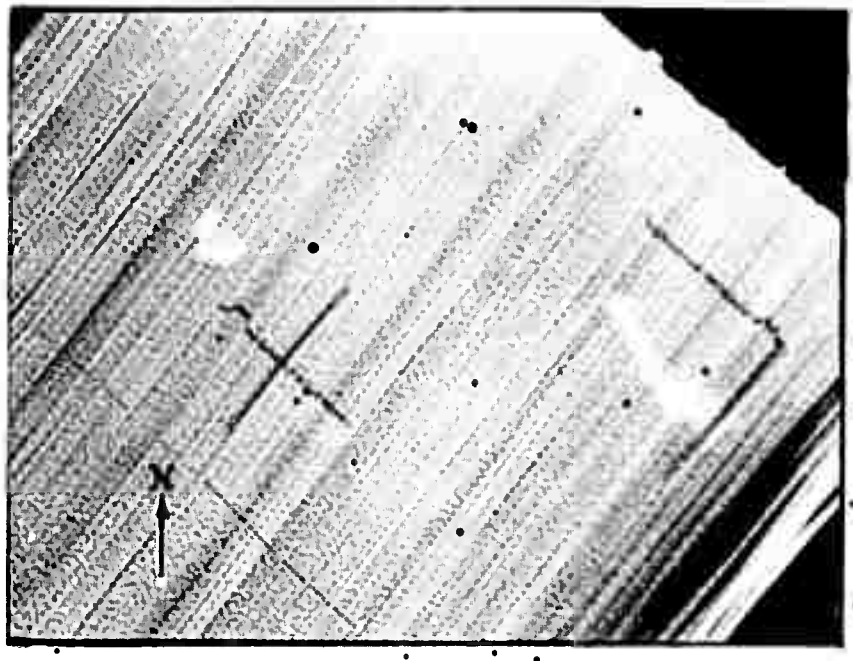

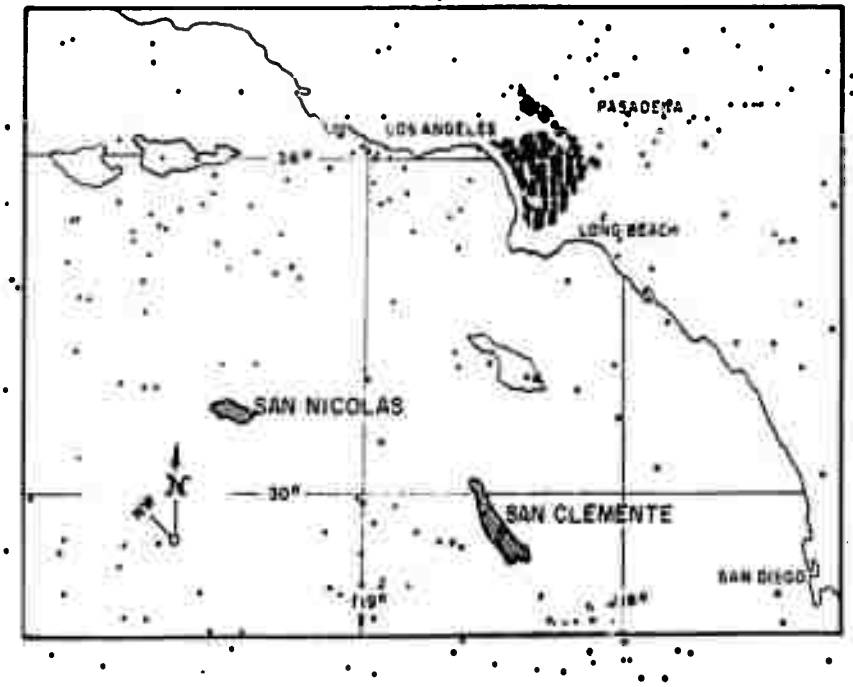

ORIENTATION OF SAN NICOLAS AND SAN CLEMENTE ISLANDS

EXAMPLE OF NARROW-ANGLE CAMERA RESOLUTION
ORBIT 033 • BELMAR, NEW JERSEY

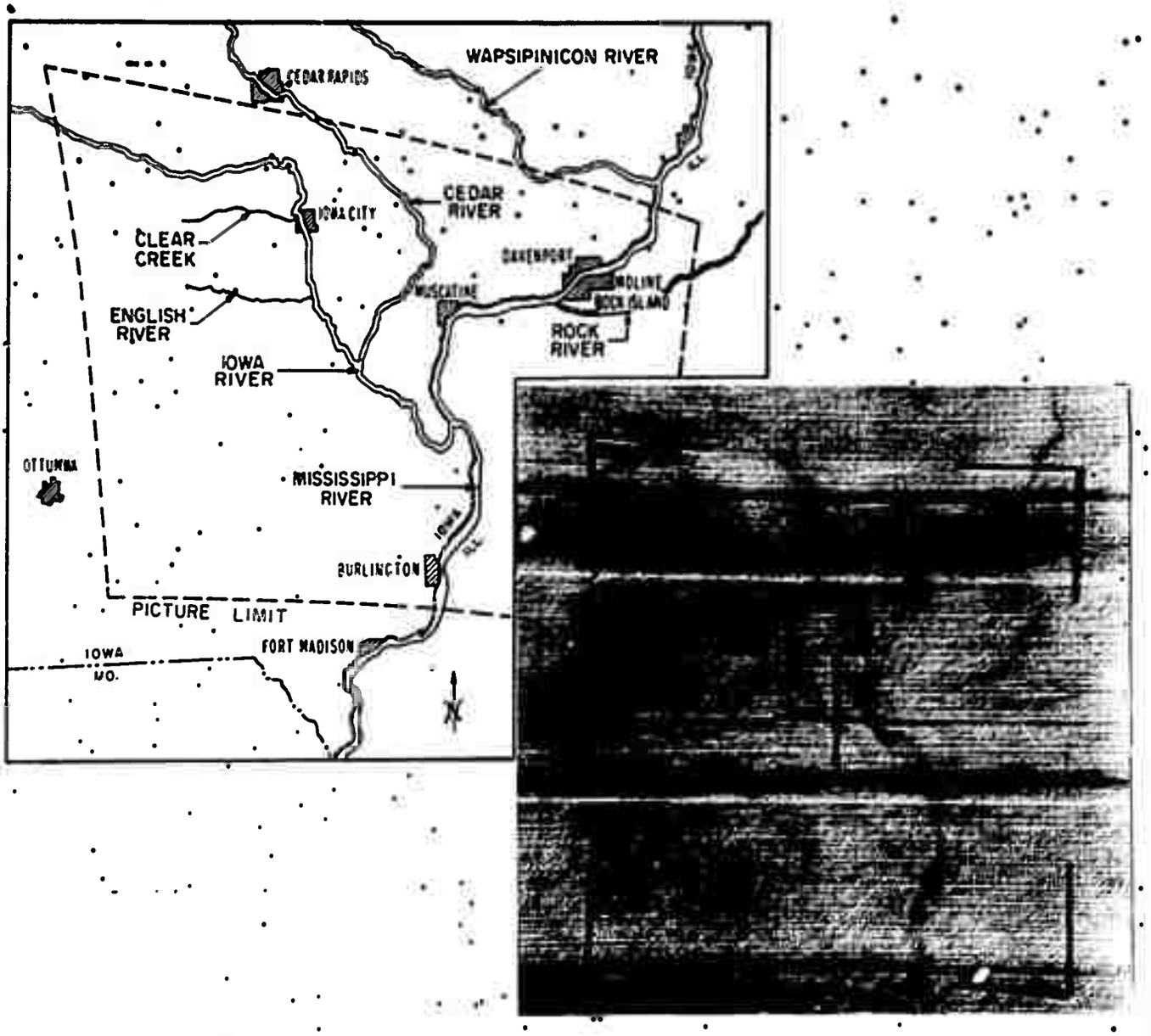

Belmar, New Jersey. Satellite altitude was approximately 450 miles and the nadir angle was 34.5 degrees. The slant range, from satellite to object at the principal point (41.3 N latitude and 91.2 W longitude), was about 550 miles. The satellite subpoint was at 40.5 N latitude and 85.2 W longitude.

The dark lines in the photograph represent the lower reflectivity of river bottoms on and near the Iowa-Illinois border. The Mississippi River is clearly visible, as well as the junction of the Cedar and Iowa Rivers. The English and Rock Rivers are also visible. A "V" shaped section of the Wapsipinicon River appears in the upper part of the photograph between the Mississippi and Cedar Rivers. On first generation negative and positive transparencies it was possible to identify Clear Creek and another creek (or river) northeast of Burlington and joining the east band of the Mississippi River. The photograph shown in Figure 2 is at best third generation quality due to the processes required for reproduction in this report. As a result the picture quality has been reduced, making image identification more difficult and apparently degrading the high resolution capability of the narrow-angle optical system.

It should perhaps be mentioned that resolution and identification are not identical. An image of an object may be resolved but it may not be identifiable. Identification is a function of contrast, shape, reflectivity and familiarity with the object as well as of resolution.

2.2.2 Wide-Angle Camera

The picture resolution obtained from the TIROS II wide-angle camera was inferior to that of TIROS I. It is probable that the inferior picture quality was a result of an optical mishap rather than a faulty vidicon.

Figure 3 is a wide-angle photograph taken during orbit 928 on 25 January 1961 from an altitude of approximately 425 miles. Visible landmarks on the northeast coast of the United States are Long Island, New York, and Cape Cod, Massachusetts (see Figure 3a for orientation). The dark area represents the coastal waters of the Atlantic Ocean. Both of the above landmarks appear gray as a result of a snow cover. The reflectivity from the snow surface rendered these landmarks visible for the first time during the TIROS experiments.

The more easily identifiable landmark is Long Island. Identification of Cape Cod is more difficult since the edges of the land appear "out of focus".

EXAMPLE OF WIDE-ANGLE CAMERA RESOLUTION
LONG ISLAND, NEW YORK AND CAPE COD, MASSACHUSETTS

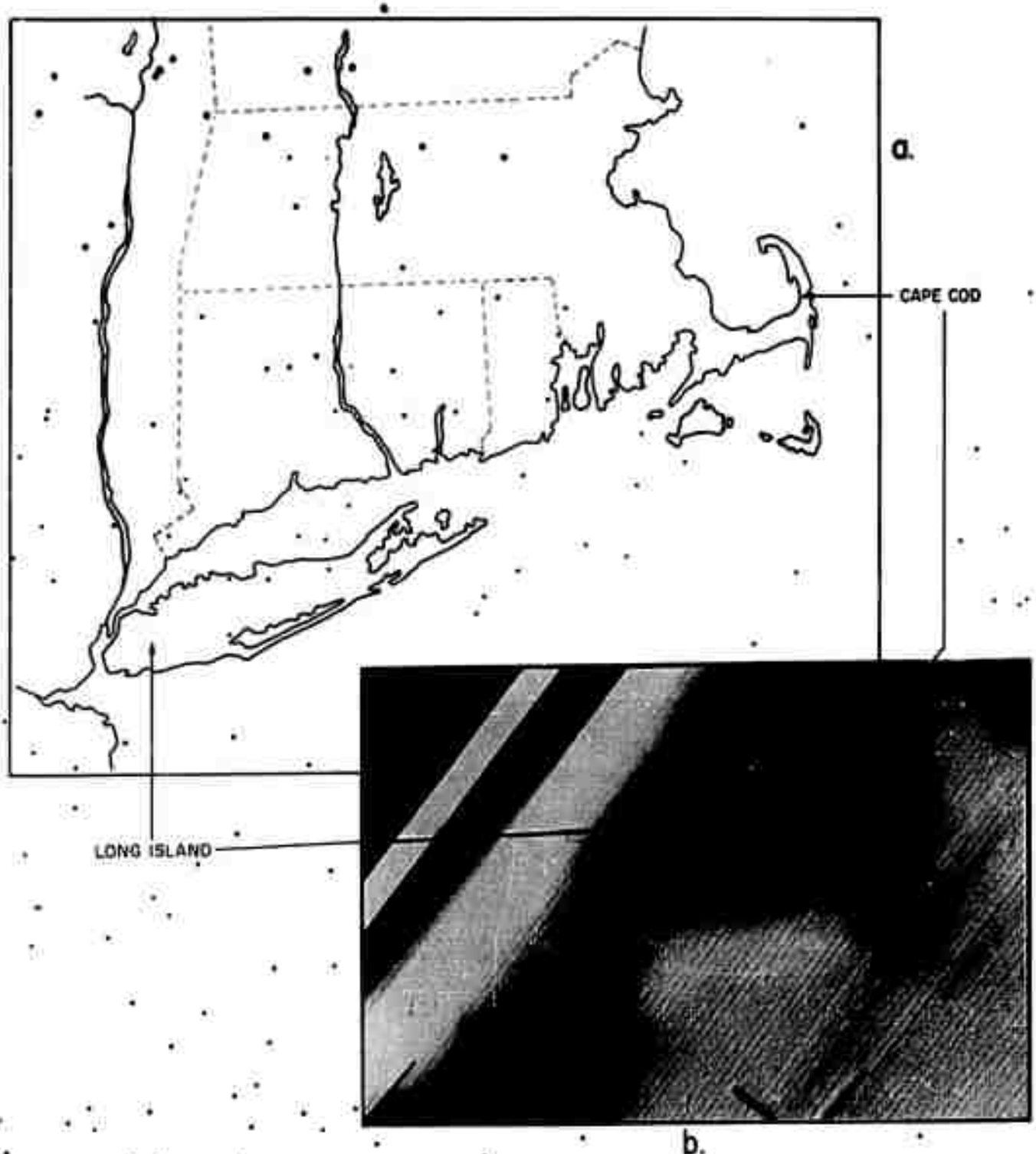

The width of the Cape ranges from two to eight miles. It is probable that the threshold of resolution lies somewhere towards the lower limit of the above range.

On Figure 4 in Section 3.3 two small, nearly parallel gray lines are faintly visible south of Lake Ontario. It is probable that these gray images are Lake Seneca and Lake Cayuga, the two largest lakes of the Finger Lakes in upstate New York. Each lake is approximately 35 to 40 miles long and four to five miles wide. Assuming proper identification of the lakes, the threshold of resolution for the wide-angle camera would be below four miles.

2.3 Latitude-Longitude Perspective Grids

During the early phase of the TIROS II Immediate Operational Use program, latitude-longitude perspective grids were generated, on an experimental basis, at the Point Mugu data acquisition site. A Bendix G-15 computer was used in conjunction with an incremental graph plotter. Program inputs included satellite position and attitude.

Advantages provided by the use of latitude-longitude perspective grids were as follows:

a) Rectification time, from data acquisition to initial transmission of nephanalysis over facsimile, was reduced by at least twenty-five percent (one half-hour).

b) Transfer of cloud patterns was possible from the image projected on the grid directly to a normal Mercator map suitable for immediate facsimile transmission, thus avoiding use of transfer grids and oblique Mercator maps.

c) A preview of location of anticipated landmarks was afforded thus guiding the analyst in "what to look for" on particular frames and sequences.

d) Aid was provided to the analyst in mentally orienting himself to proper perspective view of images.

The latitude-longitude grids could also be used to verify the time at which a picture was taken. This feature was especially useful in determining the time of the first remote picture, when it was suspected that the picture-taking sequence did not start as programmed. Timing discrepancies

are indicated by a poorly fitting grid - i.e., apparent displacement of landmarks in the picture from appropriate latitude-longitude grid coordinates and grid horizon improperly fitting the image horizon (indicating an incorrect nadir angle). The assumption, of course, is made that the computer has been provided with proper inputs for the period in question. Details of required input data are discussed elsewhere in this report.

Extrapolation of position and attitude data for required inputs was not particularly difficult once the trend lines were determined. Linear extrapolations were usually quite sufficient for a 24-hour period. However, when the Magnetic Attitude Control switch was activated, thus changing slightly the space orientation of the satellite, it was frequently not possible to apply properly simple extrapolation techniques.

Some additional comments concerning the utilization of the latitude-longitude perspective grids appear in Appendix II of this report.

The machine program used at that time (and since modified) to generate the latitude-longitude perspective grids required a fair number of "type-ins" for each grid desired. In order to properly prepare the input data, a great deal of repetitious work such as numerical and graphical interpolations and reading of nomographs was necessary. This data-preparation procedure consumed a certain amount of the analyst's time, especially when a large number of grids were to be produced.

To economize the analyst's time, a supplemental machine program was devised at the Point Mugu data acquisition site which accepted fewer and more readily available inputs. The computer output from this supplemental program was precisely the required input for the grid program.

Briefly, the supplemental program required two groups of "type-ins". The first group contained the orbital elements of TIROS II as obtained from the NASA Computer Center. Since the orbital elements are quasi-conservative over a period of days, this input group need not be altered more than once or twice a week, depending upon the amount of modification and availability of information from the Computing Center. The orbital elements were "typed-in" only once a day when the computer was started.

The second group of "type-ins" simply consisted of data for the particular orbit and specific times for which grids were to be generated. These "type-ins" were required for each orbit for which grids were to be drawn. The supplemental program proved to be a usable and valuable time and

labor saving system during the Immediate Operational Use program. Further refinement of computation and grid drawing programs has been achieved; these new programs are to be used in later work with TIROS II.

2.4 Operational Utility of Tiros II Data

2.4.1 Operational Data

The raw data obtained from the TIROS II satellite were not directly applicable to the immediate operational requirements of most "users". Accordingly, usable abstracted presentations of the raw data were prepared at each of the two data acquisition sites. This information was distributed, through appropriate channels, to interested "user" agencies and to the meteorological world at large.

The operational data were prepared at the acquisition sites in three forms to accomodate the variety of receiving equipment operated by potential "users". A nephanalysis was prepared from rectified cloud pictures and copied onto an appropriate base map suitable for facsimile transmission. Significant features of the nephanalysis were then coded and transmitted via teletype circuits. The third form of operational data was simple verbal messages describing the general features observed from the completed nephanalysis. This form of information was intended for distribution via teletype or telephone; what it lacked in completeness was compensated for by ease of transmission and decoding.

During the period between launch date and 1 February 1961, TIROS II had completed about one thousand revolutions around the Earth. Conditions were favorable to permit picture-taking on slightly over half of the total number of orbital revolutions. Nephanalyses were prepared and transmitted for sixty-five percent of the available picture sequences. The remaining thirty-five percent of the passes which contained pictures were deemed to be of insufficient quality to prepare usable nephanalyses.

2.4.2 Data Distribution

Nephanalyses prepared at each acquisition station were forwarded by facsimile directly to the U. S. Weather Bureau in Suitland, Maryland. Initial retransmission of all the TIROS II nephanalyses was the responsibility of the Weather Bureau. Interested agencies to which retransmission was directed included the U. S. Weather Bureau, the U. S. Air Force, the U. S.

Navy, some foreign countries and international meteorological centers. Coded and verbal message nephanalyses were also transmitted via teletype.

TIROS II nephanalyses were relayed on the U. S. Weather Bureau's High Altitude Facsimile Network. This circuit provided rather limited distribution. Early in January 1961 the speed of the National Facsimile Network was doubled, permitting as many as two to seven transmissions of TIROS II facsimile maps. This latter facsimile circuit had the advantage of wider distribution which included all Weather Bureau and military weather stations in the continental United States, as well as commercial organizations which subscribed to the services of this facsimile circuit.

In addition to the initial retransmission of the facsimile maps by the Weather Bureau, most military agencies retransmitted the nephanalyses over their own service circuits. For example, the U. S. Air Force relayed nearly three hundred nephanalyses to Air Weather Service units in the United States, thus serving the requirements of the Strategic Air Command, Military Air Transport Service, Tactical Air Command and Air Defense Command. Air Weather Service units stationed outside of the continental United States received nearly three hundred nephanalyses, most of which were relayed via teletype. Some facsimile maps were received by overseas units via radio facsimile.

The United States Naval distribution of TIROS II nephanalyses consisted of maps relayed to the Pacific area through the San Francisco Fleet Facsimile Broadcast; maps for Atlantic and European coverage were channeled through the Washington Fleet Facsimile Broadcast and the Port Lyautey Fleet Facsimile Broadcast. The Sixth and Seventh Fleet and the Antarctic Support Force Commands were serviced with TIROS II data by message summaries over radioteletype from the Pacific Missile Range at Point Mugu, California, and Fleet Weather Central, Suitland, Maryland.

International distribution of TIROS II data included at least the British Meteorological Service, the Australian Meteorological Service and the International Antarctic Analysis Center in Australia. It is possible that African and/or other European agencies received some TIROS II data by copying Naval radio facsimile transmissions, but at this time no confirmation or acknowledgment had been received from those agencies.

2.4.3 Data Utility

Prior to the launch of TIROS II, requests for evaluations and comments were issued to the anticipated field "users" of the TIROS II nephanalyses. As yet only a portion of these critiques has been prepared since the TIROS II project has not yet completely ended.

The following commentaries have been compiled for the National Aeronautics and Space Administration. The commentaries originally appeared in the Appendix to NASA Presentation on Meteorological Satellites made by Dr. Morris Tepper to the U. S. Senate Committee on Aeronautics and Space Sciences, 1 March 1961.

2.4.3.1 Examples of Operational Uses

2.4.3.1.1 U. S. Weather Bureau

A) International Aviation Forecast Centers such as those at Idlewild International Airport, New York, and Miami International Airport have made use of TIROS nephanalyses received over the High Altitude Facsimile Network. The International Aviation Forecast Center at Miami, in particular, made some use of TIROS nephanalyses in preparing forecasts for air routes between New York and northern South America and between Miami and Panama City, Bogota, and Mexico City. General area forecasts for the Caribbean and southern North Atlantic areas were made from conventional meteorological analyses corroborated by or compared with TIROS nephanalyses.

B) Mr. F. W. Burnett, Director, National Weather Analysis Center, has stated, "TIROS II cloud pictures have confirmed and helped relocate frontal positions on several occasions, mainly during November and early December 1960."

2.4.3.1.2 U. S. Air Force

TIROS II data were used to establish, modify, and extend conventional nephanalyses; establish, confirm or modify surface frontal analyses; and for briefing enroute weather to pilots. One series of charts covering approximately 30 days was used in direct support of an exercise which involved over-water deployment of aircraft and aerial refueling. In another instance, a TIROS nephanalysis led to the reanalysis of a front over the Mediterranean. Pilots were briefed on the basis of a new frontal position

and subsequently reported thunderstorm activity associated with the "TIROS front". Several requests for special area coverage were received. Where satellite attitude and illumination permitted, these requests were honored.

2.4.3.1.3 U. S. Navy

See section on Evaluation and Specific Cases Cited by the various Weather Services.

2.4.3.1.4 International

A) International Antarctic Analysis Center: Mr. T. I. Gray, U. S. Weather Bureau representative, has written that nephanalyses received via teletype are being plotted on maps there. The data are then used to refine weather analyses in the Australia to Antarctica region. Nephanalyses have been used in direct support of the Antarctic resupply mission.

B) The Australian Meteorological Service is using the data in conjunction with their map analysis and in special research projects concerning storm systems over Australia.

C) No comments or evaluations have been received from the British Meteorological Service to date.

2.4.3.2 Evaluations

2.4.3.2.1 U. S. Weather Bureau

A) Mr. F. W. Burnett, Director, National Weather Analysis Center, states, "The cloud shield on one occasion definitely suggested a frontal wave position between Bermuda and the West Indies which was entered on the analyses and later confirmed as it passed to the southeast of Bermuda."

"The cloud shield confirmed the analyzed position of a Pacific typhoon on one occasion."

"Cloud pictures off the east coast of Africa at low latitudes suggested a closed circulation. The nephanalyses were simply plotted on the surface chart as part of the analysis. Conventional data were not available to either confirm or deny the existence of this circulation nor were subsequent pictures for this area available to follow continuity."

"In general, most of the pictures available over the portions of the hemisphere which concern us have been over areas of relatively good data coverage, making their primary use one of confirming existing analyses."

B) Comments from the Flight Advisory Weather Service, Weather Bureau Airport Station, Anchorage:

"Because of occasional poor reception on radio facsimile, only one or two pictures were received which fell in our area of interest. These accorded well with the general synoptic situation on the traditional weather charts. A satellite which makes frequent routine passes over the North Pacific and/or Arctic will furnish this office valuable meteorological information, assuming that facsimile reception also becomes more dependable. Sporadic passes are of only limited value. Once routine pictures become available, they will be useful in pinpointing cloud structures for individual flight planning on long-haul flights as well as in depicting jet stream location and areas of probable significant turbulence."

C) Comments from Weather Bureau Airport Station, Albuquerque:

"While we have received various TIROS transmissions on the facsimile circuit, the areas depicted rarely have been those of any concern to this office. On January 30th we did receive a depiction that was of vital concern to us, namely, the area along the peninsula of Baja, California. Unfortunately, that transmission was not as clear and legible as would be desired, but it did show that the cloud area over our part of the country was much more extensive than could be determined from our usual surface observations and weather charts."

D) Comments from Weather Bureau Airport Station, Honolulu:

"Because sparseness of data is our chief problem in analysis and forecasting in the Pacific Ocean region, we have been trying to make operational use of TIROS facsimile cloud pictures. In a portion of our 'Significant Weather' forecast chart for 0000Z January 14, 1961, the cloud forecast in the area around 5°N 165°W was based largely on our interpretation of the TIROS pictures. We have indicated these nephanalyses on the forecast chart regularly distributed to aviation interests."

2.4.3.2.2 U. S. Air Force

A) "Evaluation sheets received from Air Weather Service units indicate that the nephanalyses were useful in almost all phases of weather support to air operations and that approximately 50 percent of the nephanalyses transmitted met the criteria of timeliness and coverage in the areas of interest. All nephanalyses meeting these criteria found useful application in routine analysis."

B) "The reported utility of the nephanalyses in routine weather support is encouraging and gratifying. The general reaction from the field has been: (1) The nephanalyses have been useful in spite of the random sampling characteristics of the satellite, (2) more frequent views of the same areas at regular intervals are needed, (3) an estimate of cloud tops is required, and (4) the time between observation and relay of processed data must be reduced to increase utility."

C) "While there has been no report of a spectacular 'save', the application of satellite nephanalyses to solution of daily problems in analysis and forecasting has been quietly spectacular."

2.4.3.2.3 U. S. Navy

Comments received from fleet units have been most enthusiastic. The comments received have been similar to those quoted below:

A) From the Sixth Fleet in the Mediterranean:

"Summary of orbit 143 was a better description of major cloud patterns over the Mediterranean than could be derived from available synoptic reports."

B) From Fleet Weather Central, Guam:

"Limited test suggests an immediate operational potential in the location and intensity of the intertropical convergence zone, early detection of tropical disturbances, and a basis for analysis in areas of sparse or no data."

C) From Fleet Facility, Yokosuka:

"Observation of cyclonic and convective systems over remote or infrequently observed areas shows promise of extremely valuable data."

D) From the aircraft carrier, USS Yorktown:

"Summaries received indicate that information is valuable for verification or amplification of local analyses, particularly over areas from which there are few reports. It is considered that the ability to indicate the extent of tropical distribution is of great value."

E) From Fleet Weather Central Pearl Harbor:

"The potential of TIROS data is considered excellent."

F) From the USS Independence (CVA-62):

"Four facsimile charts were received from the Fleet Weather Facility, Port Lyautey, during the period 30 November to 4 December 1960. Only three of these charts contained sufficient data for analyses and are evaluated as follows:

(1) "The facsimile charts were received 8 to 12 hours after verification time of the cloud data. In each case, the facsimile charts did verify the positions of the fronts as analyzed from surface charts. In one case, cloud cover was shown in an area of sparse surface reports, thereby aiding in the reanalysis of that area."

(2) "In one case the cloud cover shown by TIROS was used operationally to send aircraft on navigation flights to an area relatively free of clouds."

(3) "Since the ship was located in the fringe area of usable data, forecasts for ship operations did not utilize TIROS data. However, the data was utilized in preparing forecasts for long-range navigation flights."

(4) "The following potential operational uses are envisioned to be of great value to the ship, particularly when direct read out of the television pictures will be available on board:

(a) "Optimum ship routing on long oceanic voyages similar to the service now offered by long-range reconnaissance aircraft to ships moving through Arctic Sea ice."

(b) "Short distance movements to open areas to afford air operations of gunnery exercises."

(c) "Celestial navigation flights will be scheduled into areas relatively free of clouds."

(d) "Direct read out will show areas free of clouds so that photo reconnaissance missions can be directed to those areas on short notice."

(e) "Many other uses of an operational nature will come into play as experience is gained in the correlation of the TIROS charts with analyzed surface and upper air charts."

G) From Fleet Weather Facility, Alameda:

(1) "The few charts and/or summaries received covering area of interest corroborated surface analyses. Orbit No. 093 modified analysis from two fronts to three fronts off west coast United States at 310800Z November 1960."

(2) "Expect increasing value as source of information on potential or existing tropical cyclones off west coast Central America and as forecasting aid for trans-Pacific cross-section forecasts."

H) From Fleet Weather Central, Kodiak:

(1) "The overcast area described in orbit 125 compared favorably with the synoptic map data as did the clear to scattered areas. The broken cumulus band described 120 miles wide along 13624 (136 W, 24 N) 13126 compared analysis of a trough off California coast very well. As a result of the timely receipt of summary the trough was extended farther south than previously analyzed."

(2) "The summary of orbit 149 compared quite favorably with the analysis. Most of summary was out of the Kodiak area; however, the 'OVC area 14702 14705, etc.,' substantiated the presence of the series of waves extending from Arizona to South Dakota."

(3) "The summary of orbit 165 compared very favorably with analysis and data. The nephanalysis depicted a heavy overcast in southerly flow, both surface and aloft, in advance of a moderate trough, and a clear to hazy area in the northwesterly flow at the front of the ridge."

I) From Fleet Weather Central, Port Lyautey:

(1) "Facsimile charts of several orbits (117, 118, 161, 233, etc.) aided in the establishment and modification of the surface analysis in the South Atlantic, South Africa, and Red Sea areas. These are areas of secondary responsibility with sparse weather coverage for Fleet Weather Central, Port Lyautey and all data received is considered highly useful."

(2) "All charts and summaries have aided in preparation of forecasts as well as permitting, at times, an opportunity to visually verify and review forecasts previously made."

(3) "To be of any use operationally, TIROS II data must be received expeditiously. The time lag, in the receipt of word summaries, continues to have improved greatly over TIROS I. It is noted, however, the time lag in receipt at this command increases considerably (as much as two hours) when data for more than one orbit is included in the same work summaries. There has been no delay in receipt of the facsimile charts. This weather central has received the facsimile chart about nine (9) hours after verifying time. Again, this is an improvement over TIROS I program."

2.4.3.2.4 International

A) The following is quoted from a letter from Mr. T. I. Gray, U. S. Weather Bureau representative, International Antarctic Analysis Center:

"The first message to cover the area between Australia and Antarctica confirmed our general analyses picture for the surface conditions and helped, in a qualitative way, to improve the curvature details. This pattern showed a very distinct trough or frontal zone and was followed by scattered cumuloform clouds over a large area

about 200 miles west of the western edge of this zone, implying anticyclonic conditions for that area. To the east, the frontal zone or trough in the vicinity of Macquarie-Campbell-picket ship was very well marked. The frontal zone passed through Victoria, at approximately the projected time from the subjective analyses, with a structure very similar to the subjective estimate from the TIROS picture. Certainly the area of this picture and several subsequent ones taken near the southernmost location of the orbit are a boon to southern hemisphere analyses. The vast areas of the southern hemisphere with no observational data becomes an argument for the operational analytical use of the data through subjective procedures."

B) Mr. Gray wrote again in January:

"Between 8 December and 16 January, 215 nephanalyses were received. The IAAC plotted these, as often as they fitted into our base charts, and used them subjectively to obtain the most probable distribution of the 1000 mb, 700 mb, 500 mb, and 300 mb features. After each series for the day had been completed, a map discussion was held and comments about the relation of the nephanalyses to the analyzed charts were exchanged. Staffing and routine work problems at the Melbourne Weather Bureau offices were responsible for a delay of a few days in their consideration of the nephanalyses; however, as soon as the messages began arriving relatively promptly, the C. O. units utilized all nephanalyses from the vicinity of Marion and Kerguelen eastward to about the date line."

C) Australia: In a report, "Synoptic Applications of Nephanalyses from Artificial Satellites," G. T. Rutherford of the Australian Central Weather Office in Melbourne summarizes the experience in Australia with the nephanalysis transmissions of TIROS II:

"A large number of nephanalyses as interpreted from TIROS II photographs have been made available to the Bureau of Meteorology from the Meteorological Satellite Laboratories of the U. S. Weather Bureau over the December to January period of 1960/61.'

'Some of these have provided general confirmation of our Southern Ocean analyses. Some have presented features which have called for re-analysis in a manner which has been verified by later

history. Others have not lent themselves to ready interpretation of current or later analyses and a full appreciation of these will require closer study. Finally a few nephanalyses have apparently been at variance with observations.'

'Interpretation of nephanalyses or cloud photographs for use in analysis will involve not only a study of cloud patterns for models to be associated with various types of fronts and cyclonic vortex-spiral systems, but also an attempt to identify the types of cloud represented and the nature of the cloud producing mechanism, i.e., weather fronts, convergence turbulence or convection.'

'The utility of satellite photographs when their interpretation is more thoroughly understood is likely to have far-reaching and scarcely foreseeable effects on extended range and day-to-day forecasting. In Australia the opportunity of participating in the TIROS II experiments has laid the ground work to this end."

2.4.4 Summary

From the cases cited in Sections 2.4.3.1 and 2.4.3.2 it appears that the TIROS II satellite provided adequate meteorological data for a variety of purposes despite the inferior picture quality relative to TIROS I. The utility of the satellite data was primarily confined to larger scale meteorological phenomena.

Increasing the utility of TIROS satellite data appears to be closely associated with improvement of image depiction and high speed rectification and transmission techniques. The inability of some users to quickly interpret and/or visualize the cloud representation on the facsimile maps may well be a strong deterrent to complete utilization of the available information. The excessive time delay (six to eight hours in most cases) between data acquisition from the satellite and data reception by operational users also hampers complete and proper data utilization. Operational users prefer the most current data available for analysis and forecast purposes. However, even delayed information obtained from TIROS II nephanalyses served as an excellent continuity and confidence check for analyses and forecasts already prepared.

SECTION III

A CASE STUDY: TIROS II

3.1 Introduction

Figures 4 and 5 are photographs taken by TIROS II during its 928th revolution around the earth at approximately 1837Z on 25 January 1961. Thearea viewed in the wide-angle photographs, from a height of about 425 miles, is the northeastern section of the United States. The total area observed is outlined in Figure 6. The United States coast line, from approximately North Carolina to Maine, is visible on the photographs as the left edge of the dark elongated area. Significant landmarks are labeled on the photograph of Figure 4.

The pictures were chosen because they exhibit a characteristic meteorological phenomenon. Note how the edge of the cloud deck over the Atlantic Ocean closely parallels the United States coast line. The effect is so striking that we undertook to determine whether, as seemed apparent, this was the product of overwater heating and moistening of a cold outbreak, and to investigate the physical conditions producing this pattern.

3.2 Synoptic Weather Situation

Figure 6 is a section of the plotted, but unanalyzed, 1200Z surface chart with pressure values omitted. A large anticyclone is centered south of the Great Lakes. A section of a cold front is shown which extends towards the northeast, culminating in an open wave centered at 45N latitude and 42W longitude. The hatched area within the picture limit boundary represents the cloud deck observed in the photographs. Surface winds are west-north-west at 10 to 20 knots veering slightly with height. Wind velocities over the ocean range from 20 to 40 knots. The distance from coast line to cloud edge measured along the wind is about 75 miles.

Reports indicate relatively clear skies over the continental areas with some widely scattered snow flurries and/or blowing snow in up-state New York. The precipitation is a localized effect of both the modification of the air flow over the Great Lakes and orographic effects. Ship reports

FIG.4

LANDMARK IDENTIFICATION AND CONGRUENCE OF CLOUD DECK EDGE AND COASTLINE

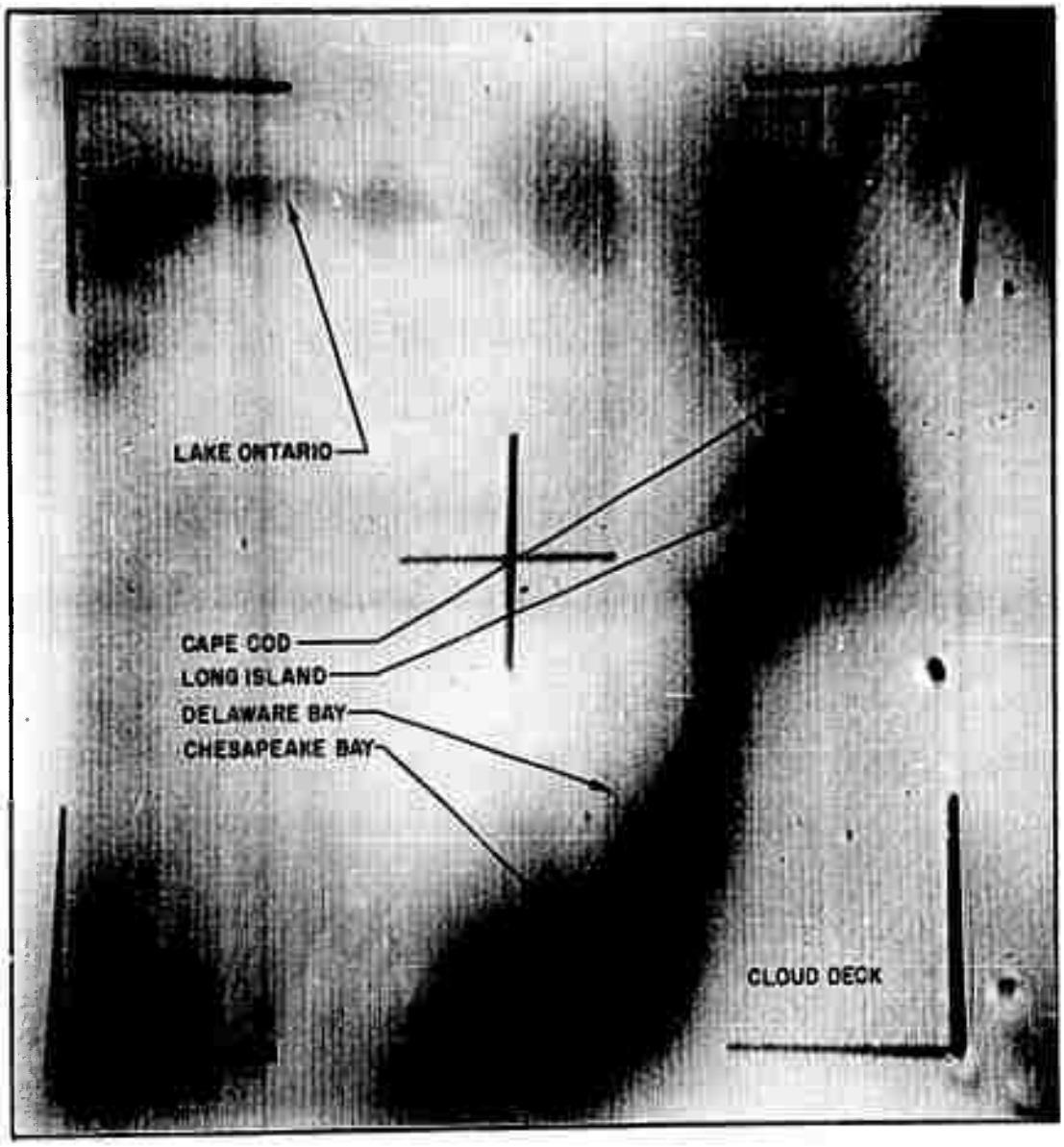

FIG.5

CONGRUENCE OF CLOUD DECK EDGE AND COASTLINE

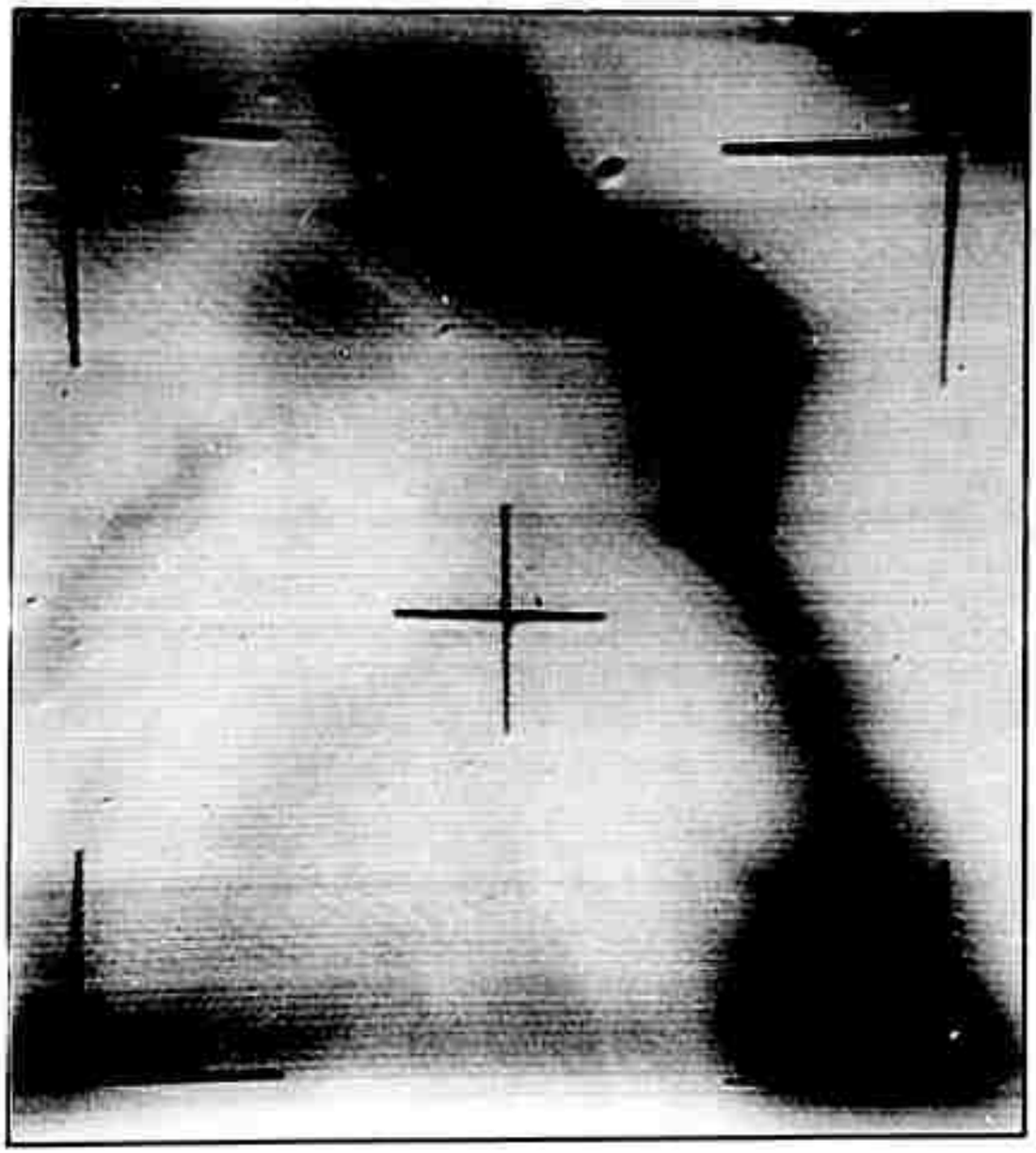

FIG. 6

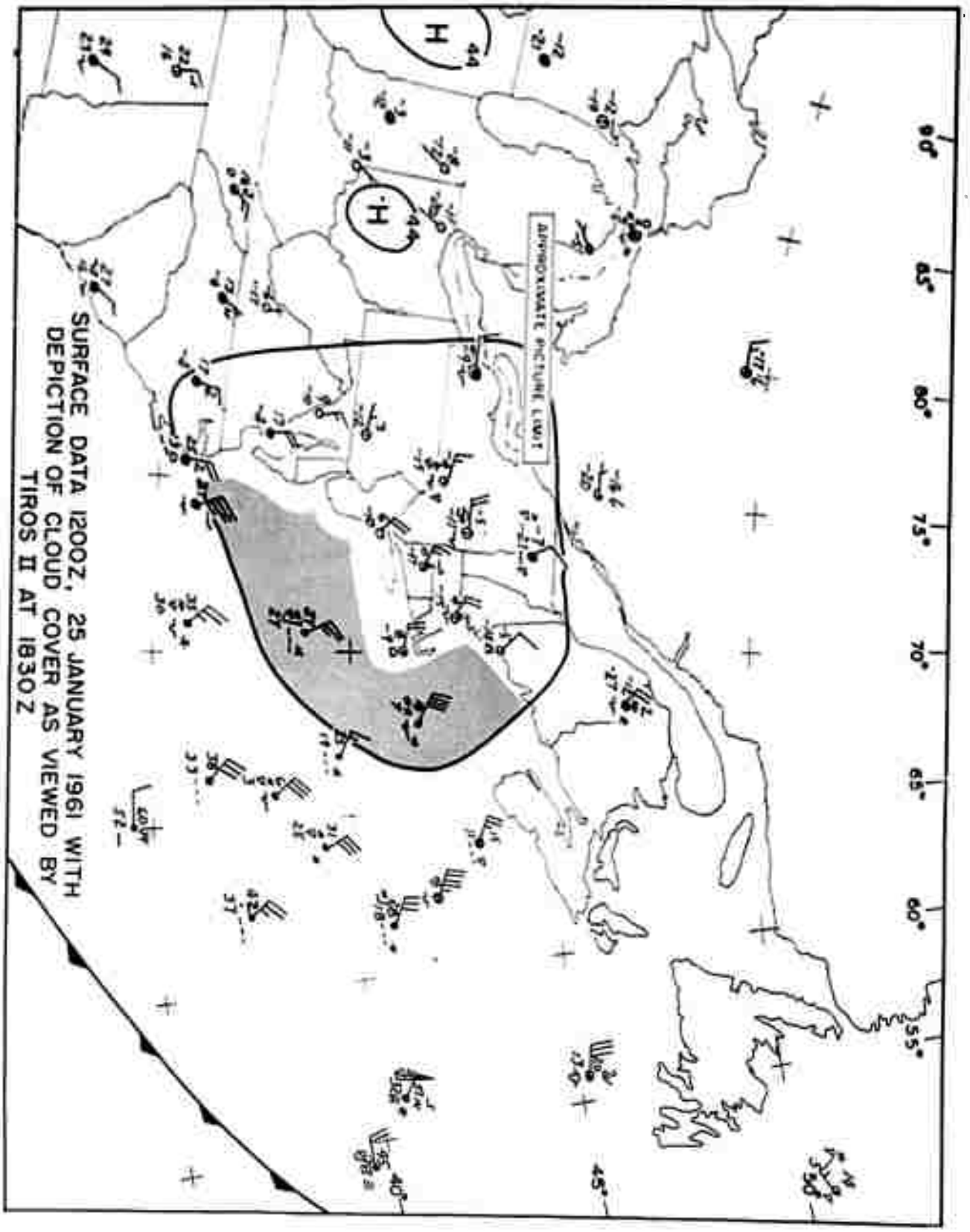

SURFACE DATA 1200Z, 25 JANUARY 1961 WITH DEPICTION OF CLOUD COVER AS VIEWED BY TIROS II AT 1830Z

from the western Atlantic indicate low overcast conditions and precipitation. Continental temperatures are extremely cold ranging from below 0°F inland to near zero along the New England coast, with much higher temperatures over the ocean. Temperature and dew point differences diminish from continental to oceanic areas as the cold air becomes heated and moistened from below. The continental surface is snow covered, providing the highly reflective and clearly distinguishable landforms in the photographs.

A conventional 850 mb level chart is shown in Figure 7. The trough associated with the surface front is just off the eastern coast line of the United States. Cold, dry air is being advected behind the trough line.

Part of the 1200Z radiosonde at Portland, Maine is shown in Figure 8 to illustrate the extremely cold, dry and stable nature of the air mass over the New England area.

Temperature contrasts across the ocean-atmosphere boundary were in excess of 20°F in the area extending east-southeast from Cape Cod to about 100 miles off-shore. Table 1 presents the actual temperatures measured at 1200Z in the above area.

TABLE I

Station	Location Lat.-Long.	Surface Water Temp. (°F)	Surface Atmospheric Temp. (°F)
Texas Tower B (TTB)	41.4N; 67.5W	38	18
Texas Tower C (TTC)	41.0N; 69.3W	40	—
Pollock Rip Lightship (492)	41.6N; 69.8W	38	14
Nantucket Lightship (493)	40.6N; 69.3W	—	18

3.3 Discussion

Subsidence and cold, dry air advection over the northeast section of the United States has produced a very stable continental air mass. The clouds produced by heating over the Great Lakes and by the orography of the Appalachians are invisible against a snow background.

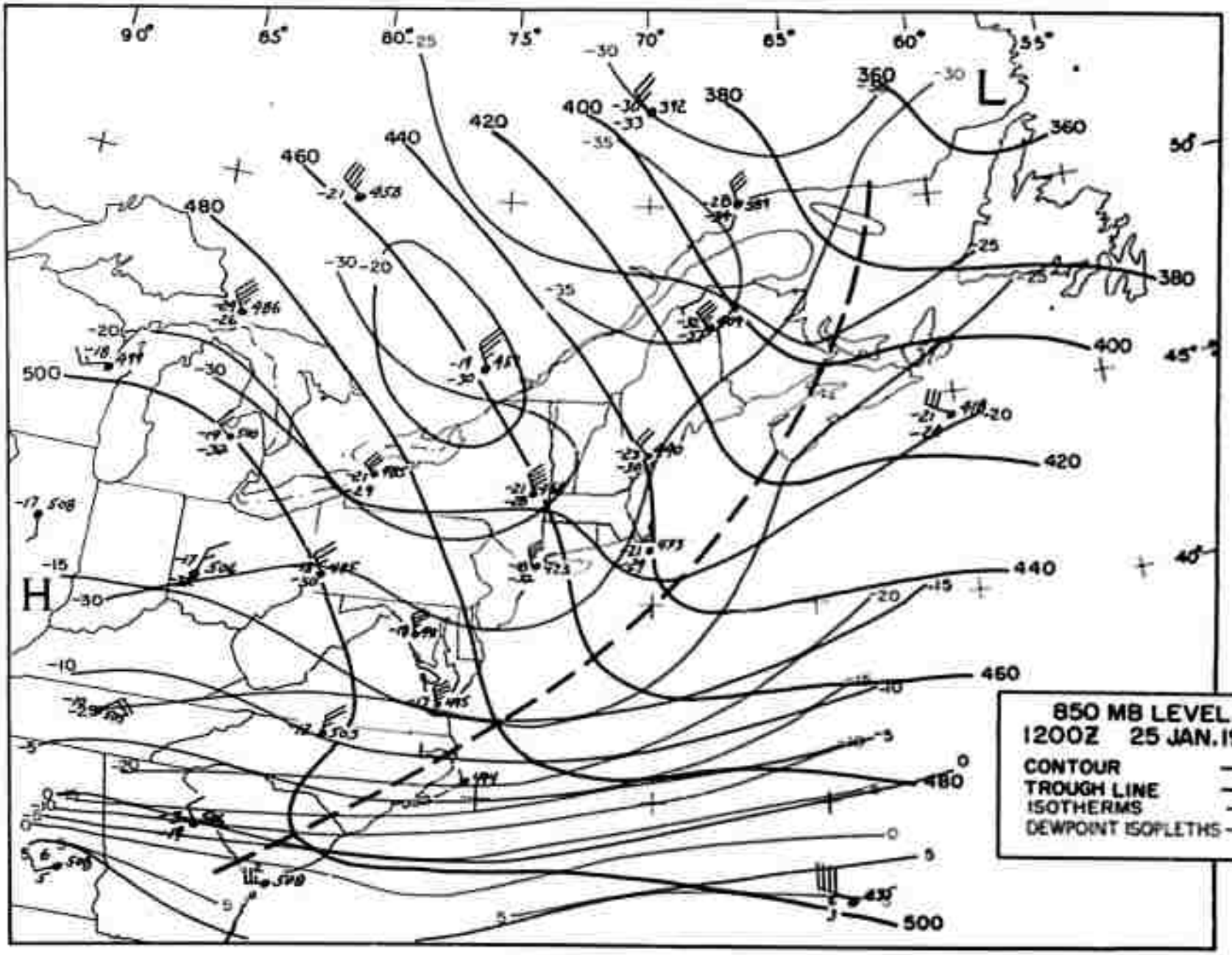
850 MB LEVEL
1200Z 25 JAN. 1961
CONTOUR
TROUGH LINE
ISOTHERMS
DEWPOINT ISOPLETHS
H
L

FIG. 7

PSEUDO — ADIABATIC DIAGRAM

PORTLAND, MAINE RADIOSONDE

1200Z 25 JANUARY 1961

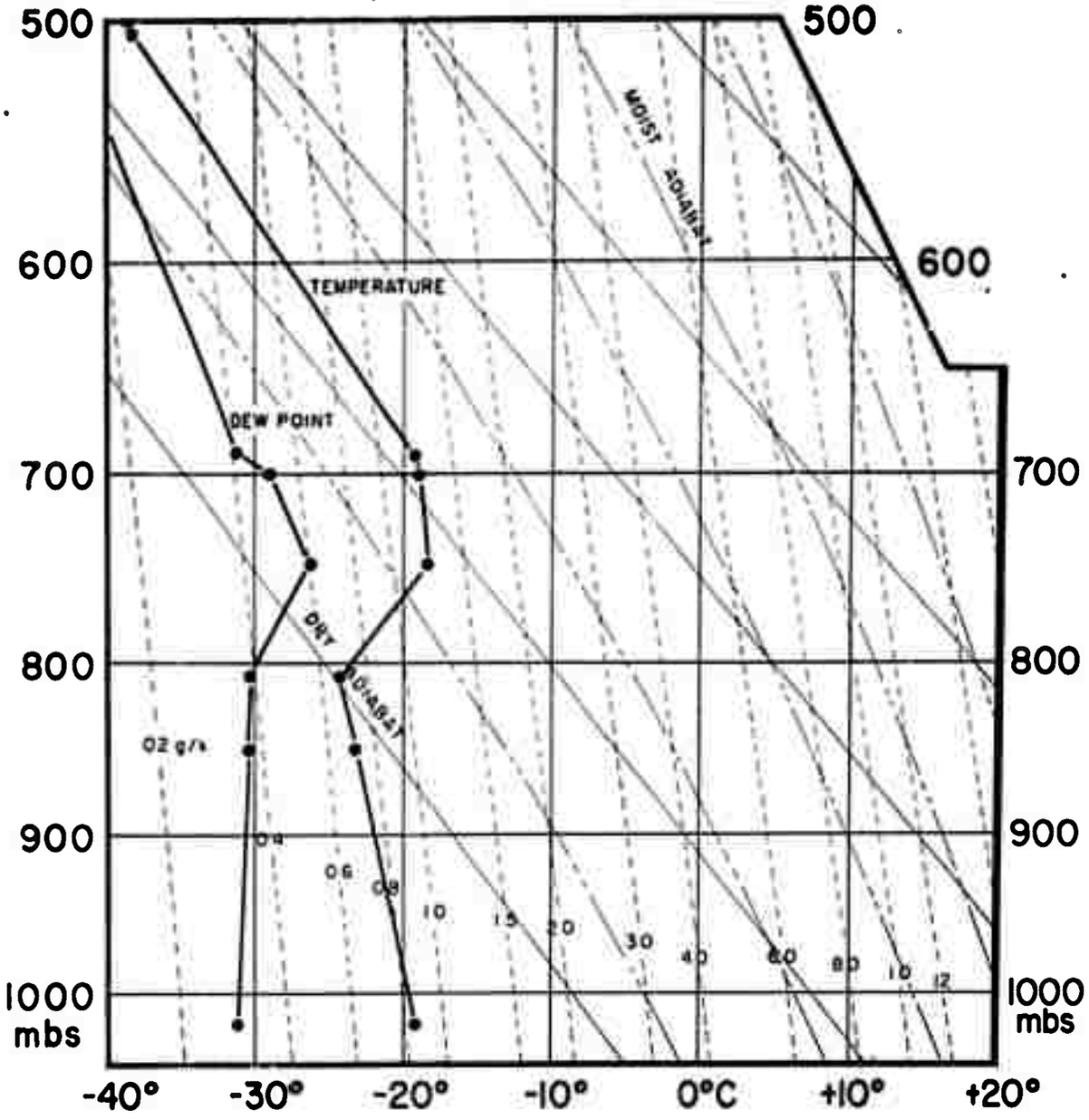

As the cold, stable air passes off the coast line it is subject to several new influences. The water surface, particularly that close to the shore line where heavy seas have not yet had an opportunity to build up, is considerably smoother than the land. As a result, the surface layers of the air accelerate. It can be seen from Figure 6 that wind speeds over the water are nearly double those over land. This acceleration results, from continuity, in downward motion of the entire atmosphere above the accelerated air. Any clouds that may have survived the orographic descent to the coast are probably wiped out at this point, although it must be admitted that thin or scattered clouds could well have escaped observation by the low-resolution camera of TIROS II.

It is difficult to make any accurate estimate of the amount of vertical motion that has occurred without a detailed knowledge of the low-level wind profiles over land and water. The reality of this vertical convergence has been demonstrated for smaller-scale situations of the same nature (Ref. 2). An indication of the magnitude of the vertical motion can be obtained by a rather simple application of the relations given in that reference. We make the following assumptions:

1. At sea the geostrophic velocity prevails from anemometer level upward.

2. Over the land the wind velocity varies linearly from anemometer level, where it is half geostrophic, to the geostrophic level at 1 kilometer. It is recognized that this assumption leads to somewhat of an overestimate of the vertical motion.

3. Purely vertical convergence occurs.

If the transport be computed through a vertical column of 1 km depth over the land, it will be found that the same transport occurs in a 3/4 km column over the sea. Accordingly, the vertical motion associated with this land-sea motion is of the order of 250 m or so. This is probably somewhat smaller in magnitude than the orographic drop from the interior highlands to the coast line.

Once the air finds itself over warmer water, heating from below commences, together with the addition of moisture. The penetration of heat from below results in the formation of an internal boundary layer in the

air over the sea. A discussion of these boundary layers may be found in Reference 3. There it is shown that internal boundary layers containing unstable air, essentially the present case, seem to behave as if the air were of neutral stability. For the case of neutral stability, relationships for the rate of growth of the boundary layer have been established. A simple expression for the thickness of the thermal boundary layer, Z, as a function of downwind distance from the surface boundary, x, is

$$Z = 0.37\, z_o^{2/9} x^{7/9}$$

where z_o is the roughness length of the surface underlying the internal boundary layer. It should be noted that wind speed and surface temperature difference do not enter in this relationship. The thickness of the boundary layer seems to be the same for temperature and for water vapor. It is approximately double this thickness for momentum(Ref. 3).

Substitution of a roughness length of 0.6 cm for the wind-roughened water (Ref. 4) gives a boundary layer thickness of 0.93 km at a downwind distance from the coast of 100 km. This is in excellent agreement with a pilot report of thick cloud tops at about 4,000 ft off the coast. Presumably, the cloud forms when the thickness of the internal boundary layer becomes sufficient to include the mixing condensation level. Since the height of the internal boundary layer is largely independent of wind speed and of the degree of instability, the cloud edge should be expected to lie at a uniform distance from the coast line.

It is to be noted that the 850 mb trough lies a relatively short distance off the coast. However, it is believed that convergence into this trough plays a minor part in establishing the low cloud deck. It may well be that at some distance off the coast the cloud development is accelerated by general convergence.

In summary, the TIROS pictures have provided for the first time a sufficiently detailed view of the cloud field in this interesting meteorological situation to permit ready identification of the processes at work. Also, the forecaster, once aware of the persistent gaps between coast and cloud in these situations, can become more specific even in the absence of satellite pictures.

SECTION IV

FURTHER RESULTS FROM TIROS I

4.1 Synoptic Interpretation of the TIROS Satellite Vortex Patterns

4.1.1 Introduction

A never ending source of awe to meteorologists, upon contemplating TIROS pictures, is the organization so obviously displayed in cloud systems. This organization is evident through a wide spectrum of sizes. Near the large end of this spectrum are the TIROS "spectaculars", the large scale vortex patterns identified with major cyclonic circulations. Their existence was not unexpected. Indeed the detection of such patterns by TV satellites had not only been correctly predicted in 1957 (Ref. 5), but the patterns themselves were recognized nearly 100 years ago by Admiral Fitz Roy, the first chief of the Meteorological Office, London. Fitz Roy's model weather systems, published in 1863 (Ref. 6), and reproduced in a recent article by Bergeron (Ref. 7), show a most striking resemblance to patterns seen in the TIROS pictures. It is a tribute to Fitz Roy's keen observation and well-directed imagination that he was able to visualize these patterns on the basis of surface observation alone.

It was somewhat beyond the fondest dream of the synoptic meteorologist that for every cyclone to come under TIROS' eye there would appear a corresponding vortex[1] pattern. Based on the TIROS I pictures this appears to be true. This 1:1 relationship between the vortex patterns in the TIROS pictures and the presence of cyclones on the earth's surface quite naturally places additional emphasis on the value of meteorological television satellites in monitoring the weather over sections of the globe where conventional weather data are sparse or otherwise unavailable. Considering the northern hemisphere alone, more than 40 separate vortices were positively identified from the TIROS I pictures, many of them remaining under observation for several orbits. The recurrence of similar cloud patterns from one cyclone to another and the apparent transition of patterns were recognized as features of possible significance in

[1] As used in this report, "vortex" will refer solely to the cloud pattern as seen in the TIROS pictures.

evaluating the particular phase of the cyclonic development being portrayed by TIROS. This section concerns itself with the results of a study of some 30 northern hemisphere vortices, selected from the TIROS I picture files, and their cyclonic counterparts as depicted on the sea level and 500 mb level synoptic weather maps of the northern hemisphere. Idealized TIROS cyclone models are derived which should aid in the utilization of satellite pictures for the diagnosis of global weather.

4.1.2 Analysis of the Data

Out of the more than forty vortices observed in the northern hemisphere during the 78-day useful life of TIROS I, thirty were selected for study on the basis of picture quality and trustworthy orbital data. Of these some twenty-one were located and oriented using techniques similar to those employed operationally for TIROS I and improved for TIROS II. Geographical coordinates were obtained for the center of each vortex and in some cases the pictures were rectified. Sea level and 500 mb synoptic analyses were obtained. The analysis consisted of: (a) determining the position of the vortex center, as seen on the picture, in relation to the low pressure center at sea level and at 500 mb; (b) comparing the features of each vortex pattern with the corresponding weather analysis.

4.1.3 Results

4.1.3.1 Location of Vortex with Reference to Low Center at Sea Level and at 500 mb

Twenty-one vortices, where location was believed accurate to within 1° latitude, were compared with the position of the corresponding sea-level low pressure centers. Figure 9 shows the results. The low position is at the center of the diagram; x's mark the relative location of the vortices. All but two vortices are within 275 miles of the low, and the mean vortex position for this sample is about 80 nautical miles SW of the low. In a number of cases the vortex pattern appeared to lag behind the surface low by about 12 hours.

Nine of the above vortices were associated with closed 500 mb lows. The vortical positions are given in Figure 10 with the 500 mb low position at the center. These positions are quite uniformly distributed about the low; in fact, the mean vortex position is very close to the center. While this may

FIG.9

POSITION OF 21 TIROS VORTICES WITH REFERENCE TO ASSOCIATED SEA LEVEL LOW CENTER

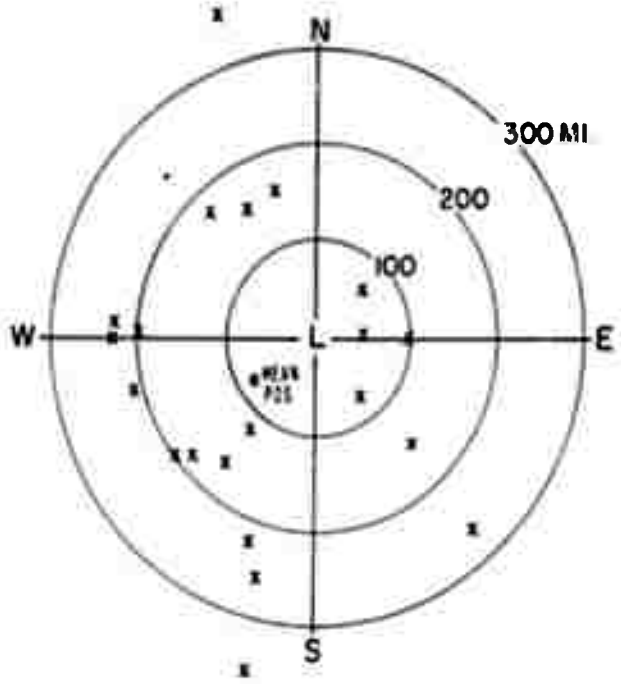

FIG.10

POSITION OF 9 TIROS VORTICES WITH REFERENCE TO ASSOCIATED 500 MB LOW CENTER

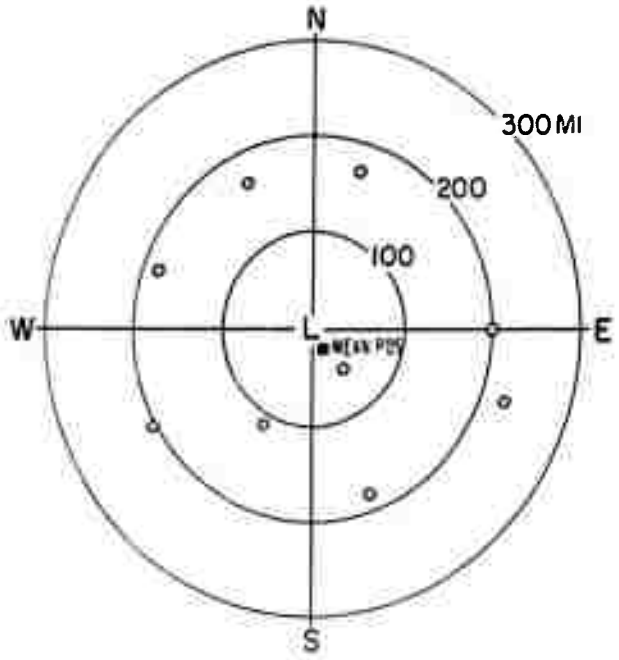

suggest that the vortex position corresponds more closely to the low at 500 mb than that at sea level, the sample of cases is too small to draw any definite conclusions.

4.1.3.2 Cyclonic Cloud Developments: The TIROS Cyclone Model

While it is admittedly dangerous to generalize on the basis of a small sample of data, the very convincing evidence found in the vortex pictures, and the logical manner in which it ties in with the synoptic data, point toward a model describing the evolution of cloud patterns attending the development and decay of a middle latitude cyclone. This model, like most, is idealized and retains only those features which appear common to all cases. It is intended as a guide in interpreting satellite pictures.

4.1.3.3 The Open Wave

The initial stage of the classical cyclone is the familiar frontal wave. Although this is a common phenomenon on weather maps, it is often accompanied by or embedded in a vast cloud sheet which presents no characteristic pattern when viewed from above. On occations however, frontal zones are found between two essentially unclouded areas. In such instances the frontal zone stands out clearly in the TIROS pictures as a long cloud band. The few waves seen along such clearly delineated fronts have appeared as a widening, bulging or bending, of the frontal band schematically shown in Figure 11 and illustrated by a TIROS I photo in Figure 12. The surface weather data indicate that the area of heaviest precipitation coincides with the highest cloud reflectivity which has been shown schematically in Figure 11. This does not mean, however, that this particular cloud configuration is characteristic of frontal waves alone. This is definitely not the case -- other very similar patterns have been observed where neither waves nor fronts existed, pointing to the need for exercising caution in interpreting the patterns. But in the few instances where a frontal wave has come under observation, with no obscuring mask of clouds, the pattern has been similar to that indicated here, even to the cloud bands north of the wave.

4.1.3.4 The Occluding Cyclone

It is not yet known at which stage of the developing cyclone the vortex pattern, not seen in the wave, first appears; but all of the examples of partially occluded cyclones examined already contain the unmistakable

MODEL CLOUD PATTERN OF FRONTAL WAVE AS DEDUCED FROM TIROS PHOTOS

FIG. 11

CLOUD PATTERN ASSOCIATED WITH FRONTAL WAVE IN THE CENTRAL NORTH PACIFIC, 24 MAY 1960, ORBIT 763, TIROS I

vortex signature in the cloud pattern. An additional feature peculiar to this stage is the appearance of a wedge or tongue of essentially clear air which intrudes into the cloud sheet (Figure 13). The forward or right-hand edge of this clear zone, as indicated in the model, closely parallels the surface cold front which invariably lies some distance under the cloud band. Thin streaks are generally present in the cloudy areas spiralling inward to the vortex center which is found in the semicircular cloudy bulge beyond the clear wedge.

The width of the clear wedge is quite variable, depending on characteristics of the air mass, whether over land or sea, the season of the year, the time of day, all factors which affect the amount of low-level convection. This probably accounts for most of the clouds seen in the otherwise clear sector. The clear sector is believed to represent a region of actively subsiding (dry) air behind the cold front, a characteristic feature of developing cyclones. In the TIROS example shown in Figure 14, the air in the clear zone was extremely dry, hence the zone is very wide and almost completely cloudless.

4.1.3.5 The Occluded Cyclone

As the cyclone matures, the clear sector of the earlier stage tends to "spiral in" toward the vortex center (Figure 15). Some measure of the age or degree of maturity of a cyclone can be obtained from the number of loops described by the "clear sector" which now becomes rather narrow and subject to cloud intrusions. At this stage the cyclone begins to lose energy, the regions of subsidence and updraft are weaker, and the system is generally running down or "coasting". Hence the features become less clear cut, less sharply defined, as exemplified by Figure 16. Even so the persistence of the characteristic features is still remarkable.

4.1.3.6 The Decadent, Filling Cyclone

As the cyclone passes maturity and reaches the decadent, filling and, usually, frontless stage the large scale regions of rising cloudy air and subsiding clear air which characterized the early developing stages have disappeared. The cyclone's existence is now principally due to its inertia. Some inflow is maintained in the low levels which in turn favors the development of convective clouds. It is now apparent from the TIROS pictures that these clouds tend to arrange themselves into long spiral bands separated by relatively large clear areas (Figure 17). The width and number of the bands,

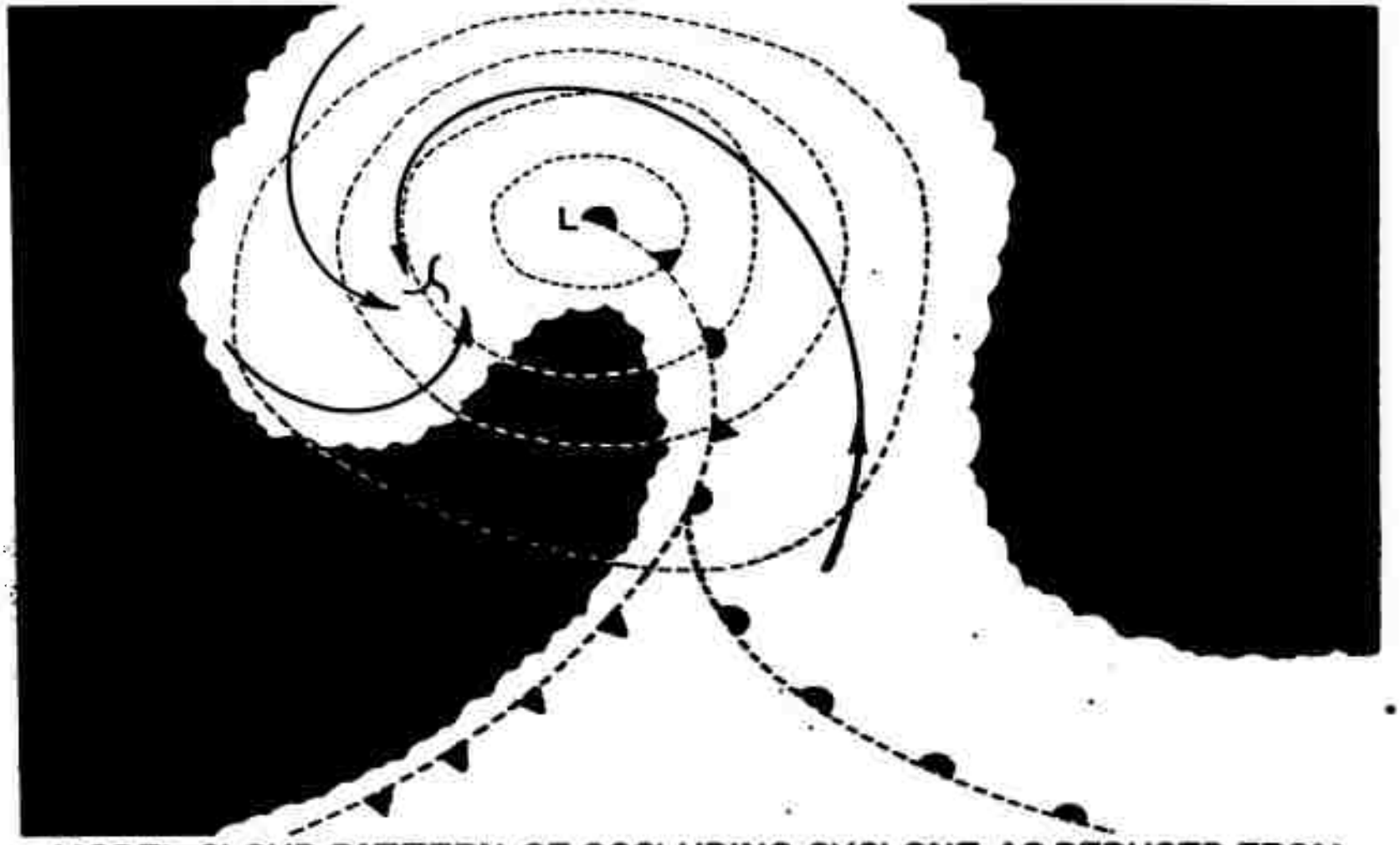

MODEL CLOUD PATTERN OF OCCLUDING CYCLONE AS DEDUCED FROM TIROS PHOTOS

FIG. 13

FIG.14

CYCLONIC VORTEX AND FRONTAL BAND ASSOCIATED WITH INTENSE OCCLUDING CYCLONE IN CENTRAL U.S., 1 APRIL 1960, ORBIT 5 TIROS I

NOTE VERY WIDE CLEAR ZONE DUE TO EXTREME DRYNESS OF SURFACE AIR SOUTH OF VORTEX

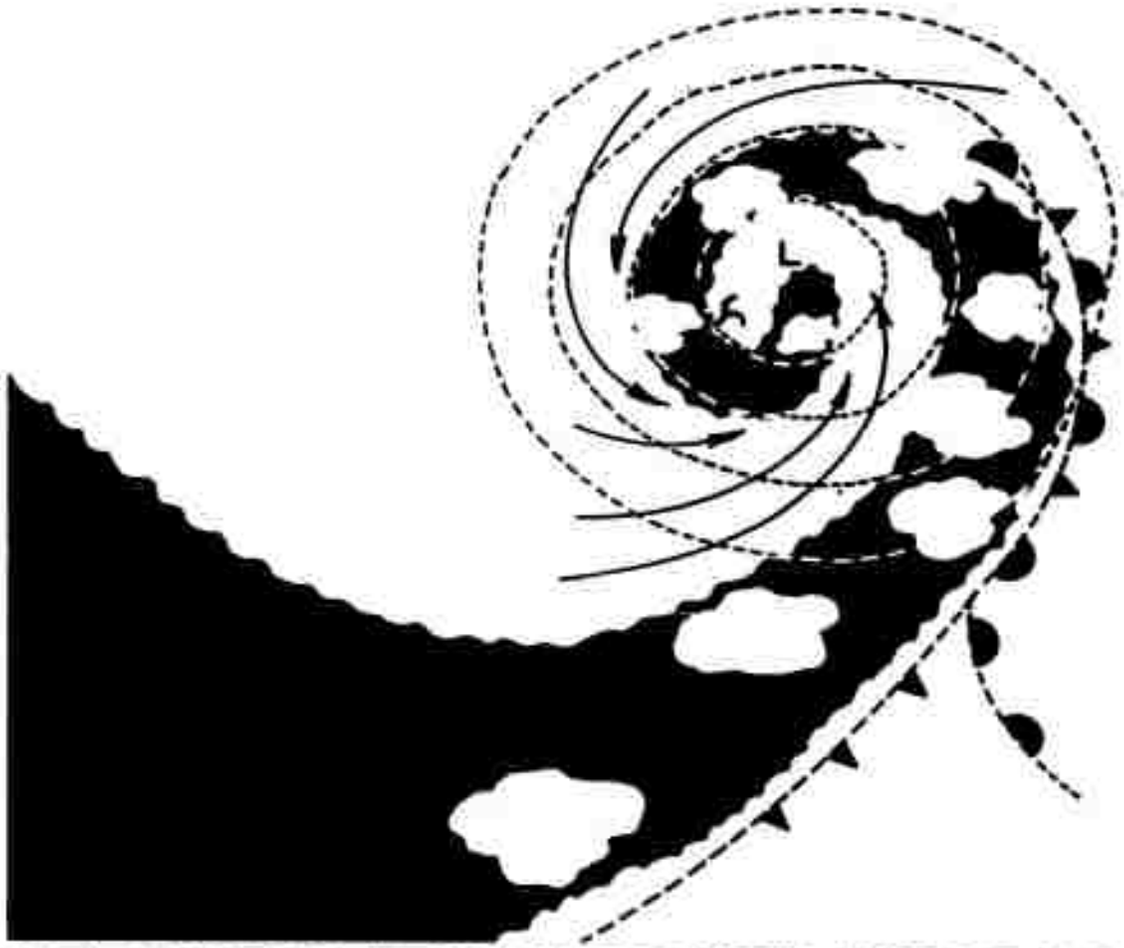

MODEL CLOUD PATTERN OF OCCLUDED, MATURE CYCLONE AS DEDUCED FROM TIROS PHOTOS

FIG. 15

VORTEX PATTERN FROM TIROS I SHOWING SPIRAL CLEAR ZONE WITH CLOUD INTRUSIONS ASSOCIATED WITH OCCLUDED CYCLONE IN THE GREAT LAKES, 22 MAY 1960, ORBIT 745 TIROS I

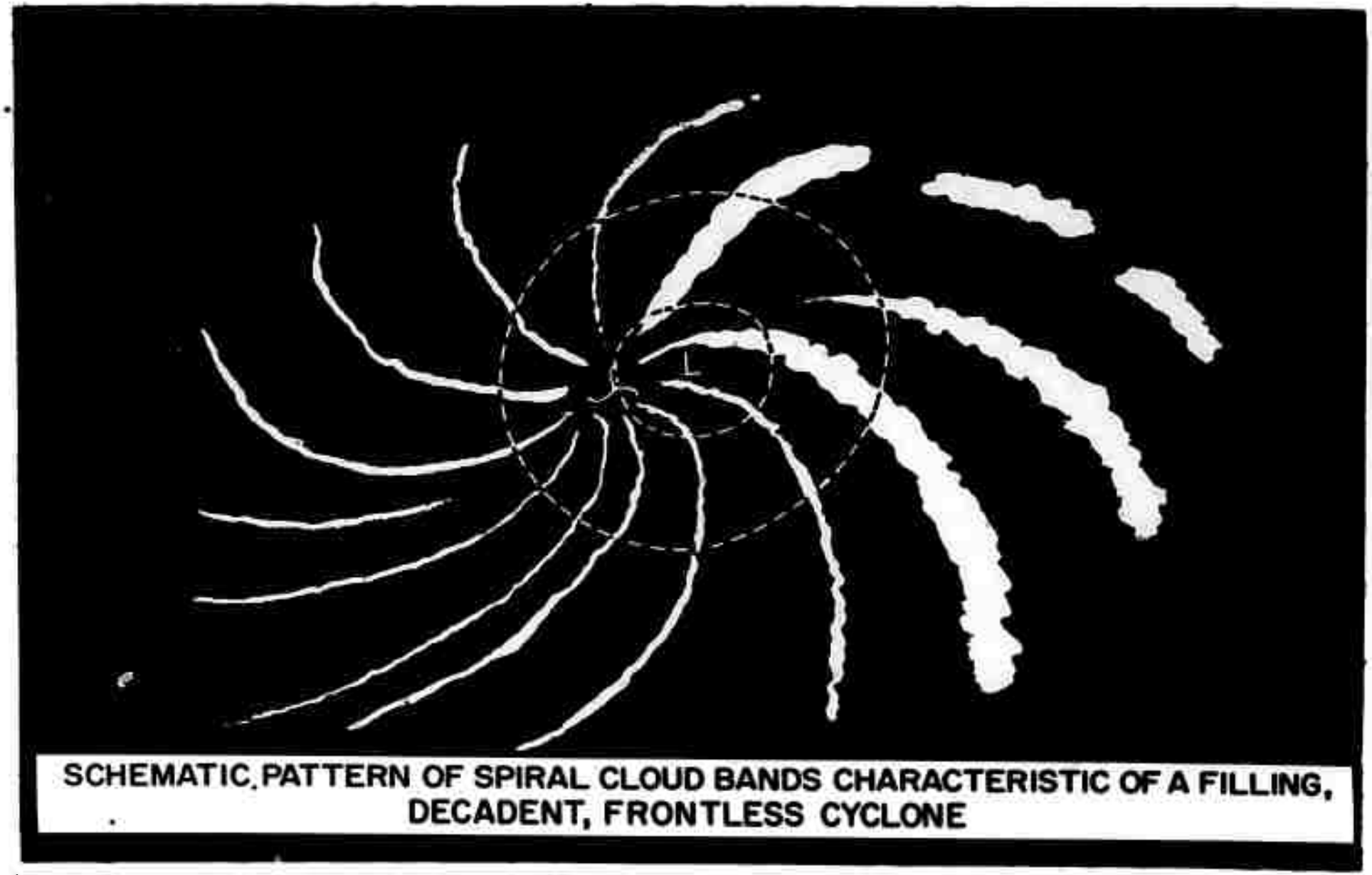

SCHEMATIC PATTERN OF SPIRAL CLOUD BANDS CHARACTERISTIC OF A FILLING, DECADENT, FRONTLESS CYCLONE

FIG. 17

their spacing and the presence or absence of unorganized cloudiness are variable features which probably again depend upon the surface conditions, mainly whether it is ocean or land, the season and time of day, and the intensity of the cyclone circulation. The example shown in Figure 18 is over land, hence the presence of considerable cumuliform cloudiness.

4.1.4 Conclusion

This brief study of TIROS vortex patterns has demonstrated the practicality of monitoring synoptic scale weather systems with the aid of an artificial satellite.

The TIROS pictures permit an accurate fix on the center of the vortex which is the cloud signature of a cyclonic circulation. Although the vortex itself bears no unique relationship to the location of either the associated sea-level low or that at the 500 mb level, it occupies a position within a radius of 2 to 3 hundred miles of both. This in itself, is useful information from a region of sparse or no data, but the TIROS pictures go far beyond merely fixing the probable location of a cyclone. The patterns, as they evolve progressively from the "kink" or bulge on a frontal band, corresponding to a nascent cyclone, through the winding spiral typical of a developing cyclone and finally display the simple nebula-like arms of a decaying storm, convey meteorological information which specifies within rather narrow limits the stage of development, the age and intensity of a cyclone and the placement of its significant features. This is an extremely useful function in the monitoring of global weather.

4.2 Observations of Wake Formation Beneath an Inversion

TIROS I photographs have revealed some very striking cloud patterns in the wakes of islands. Criss-cross patterns in stratiform clouds under inversions have been observed which are reminiscent of Mach lines in supersonic wakes.

The analogy between flow beneath an inversion and supersonic gas flow has been pointed out by Freeman (Ref. 8). In particular, it was shown that the equations governing motion beneath an inversion with winds of the order of 5 to 20 m sec^{-1} are quite similar to those governing gas flow at supersonic speeds.

Physically, disturbances affecting the height of an inversion are mirrored by changes in wind speed below the inversion. Under appropriate atmospheric

SPIRAL CLOUD PATTERN ASSOCIATED WITH OLD FILLING LOW NORTH OF CASPIAN SEA
19 MAY 1960, ORBIT 700
TIROS I

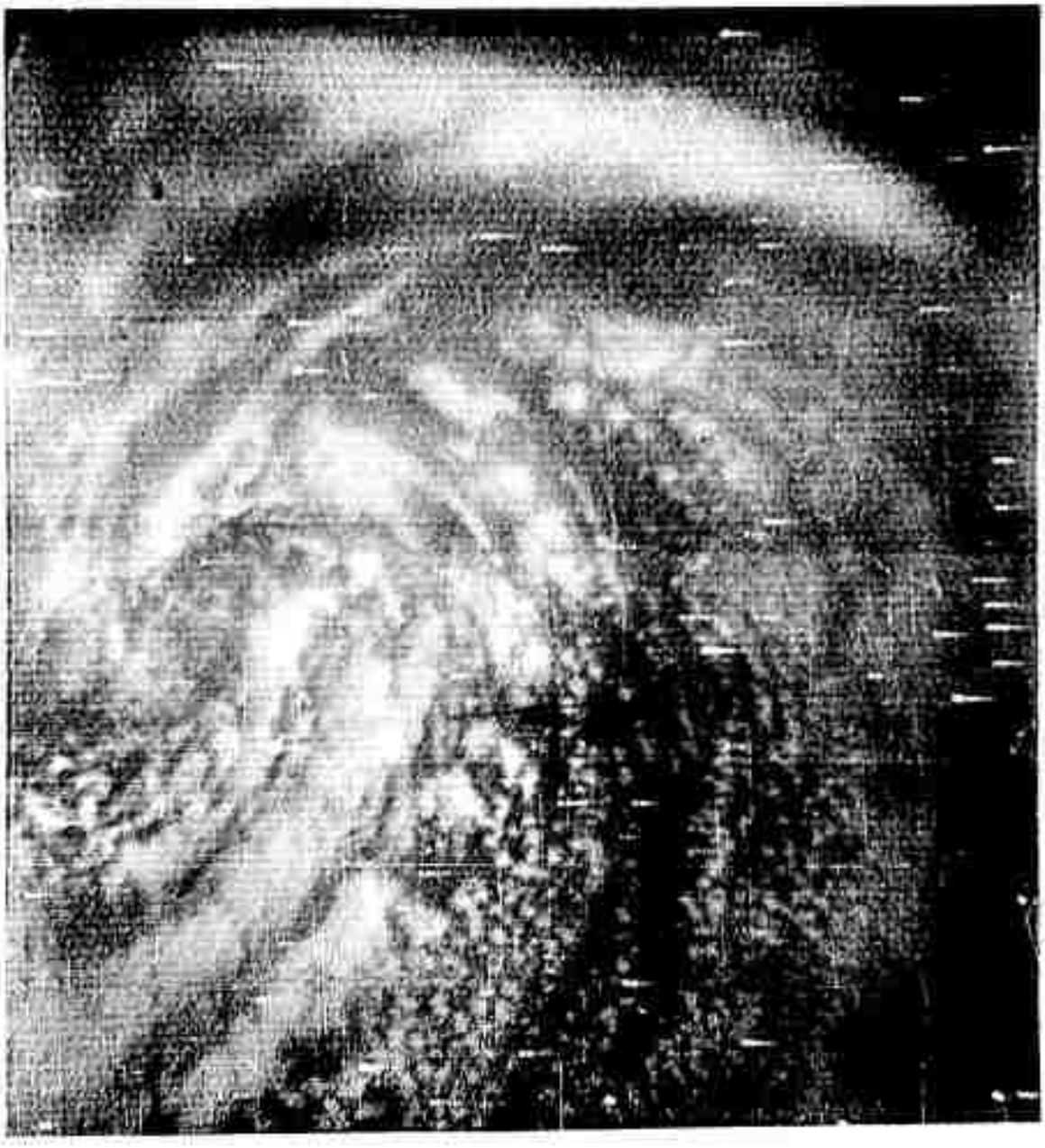

conditions, the disturbances may in turn be reflected in the cloud patterns. Regions corresponding to compression in the supersonic analogy would be marked by lifting of the inversion and cloud enhancement; conversely, supersonic rarefaction corresponds to inversion depression and cloud dissolution.

TIROS I has observed an extended wake pattern on several occasions to the lee of an island, which acted as the disturbing influence. One such wake, originating from Guadalupe Island off lower California on 18 May 1960, has been selected for the purpose of illustration.

4.2.1 Synoptic

The 19 May 1960 surface map for 0000Z, three hours after the wake observation discussed below, is shown as Figure 19. The familiar summertime thermal low over southern Nevada and the California desert is noted, with a low pressure trough extending southward into Mexico. To the west is a portion of the eastern cell of the Pacific high. Jointly, these systems give rise to northwesterly flow in the vicinity of Lower California and Guadalupe Island. A similar wind pattern is indicated on the 850 mb contour chart (not shown). Nearby pilot balloon observations show the northwesterly flow extending to about the 3 km level. A sounding from a ship, located some 420 km due north of Guadalupe, indicated a strong subsidence inversion at about 450 m with extremely dry air above.

4.2.2 Cloud Pattern

Evidence of the wake phenomenon - i.e., cloud banding - as observed by TIROS is shown (arrow) in Figure 20a, a wide angle photograph taken at about 2100Z on 18 May. Depicted in Figure 20b is the same cloud pattern rectified onto a base map containing geographic features. Of note is the coincidence of Guadalupe Island with the origin of the disturbance. A mountain on Guadalupe extends to 1600 m above sea level. Guadalupe is invisible in these photographs; even under ideal cloudless conditions, the island is infrequently seen because of its small size and low reflectivity.

In the wake of the island, extending at least 385 km downstream, is an unusual disturbed zone of rather diffuse cloud with superimposed oblique bands spaced at 55 km intervals. The breadth of the disturbance is of the order of 60 km, while the band dimensions are about 55 km by 9 km.

A narrow angle photograph, Figure 21, shows the clear area adjacent

FIG.19

SEA LEVEL MAP

19 MAY 1960 0000Z

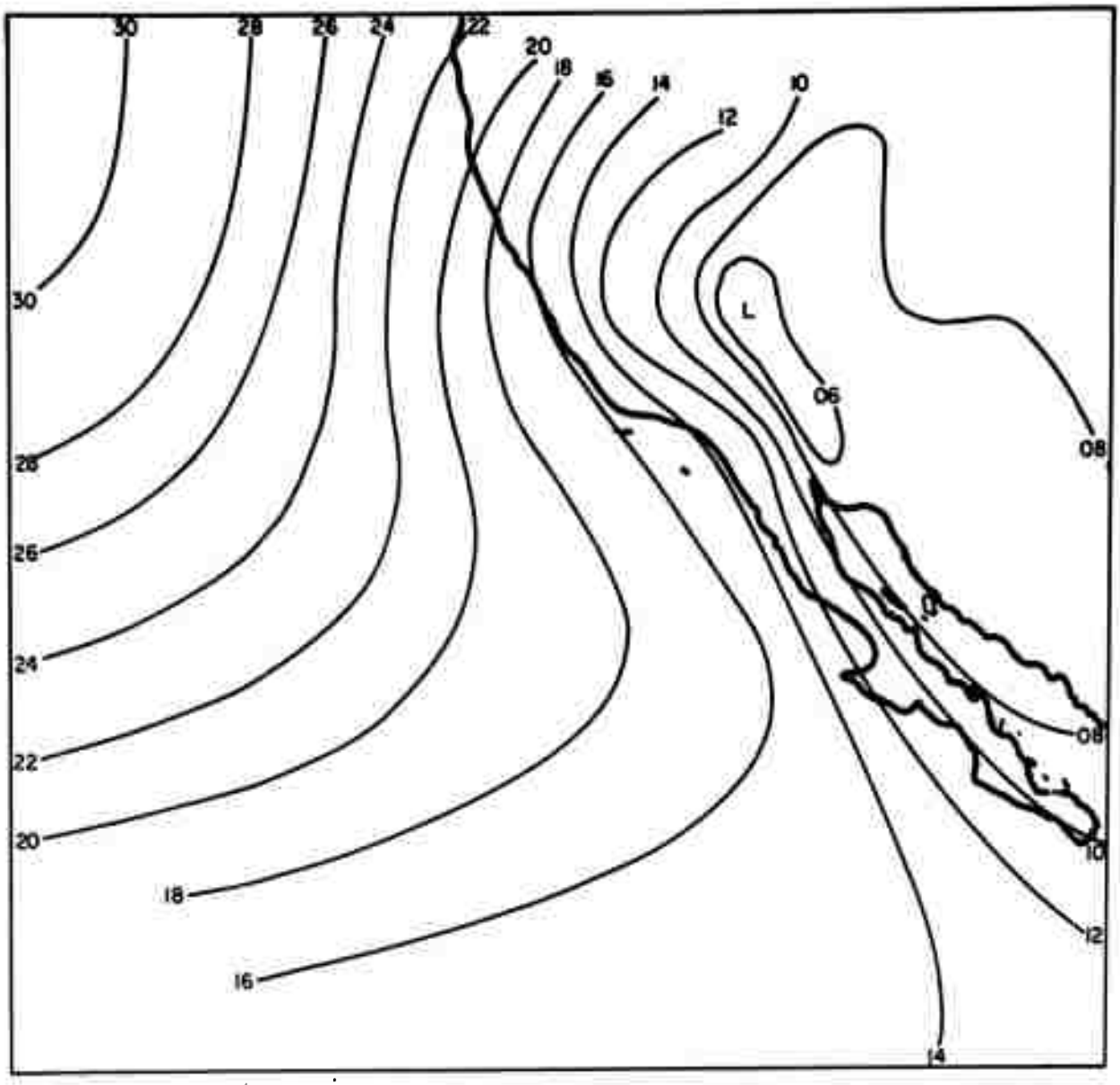

FIG.20

TIROS I PHOTOGRAPH AND RECTIFICATION SHOWING WAKE PATTERN

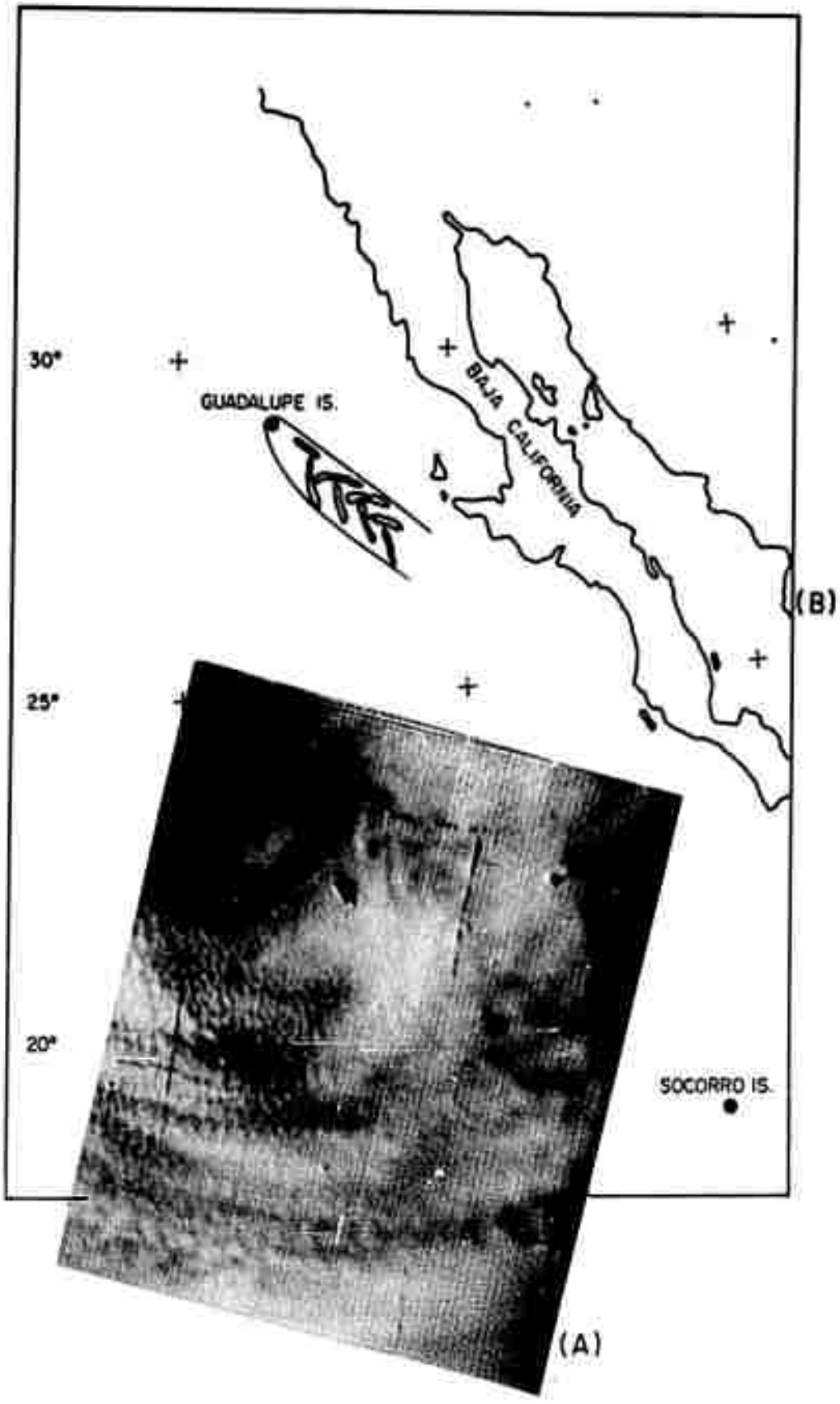

TIROS I NARROW-ANGLE PHOTOGRAPH SHOWING GUADALUPE AREA

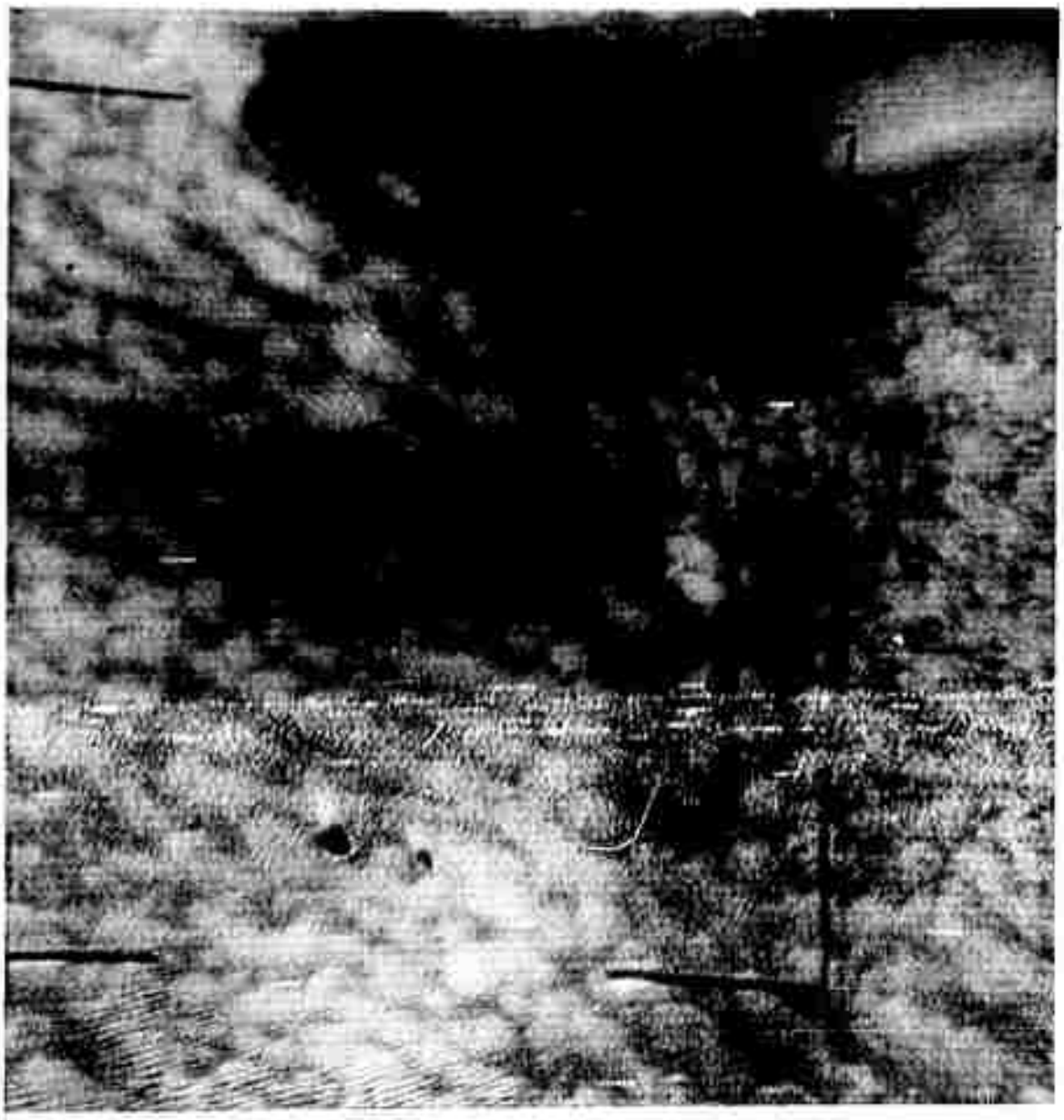

to Guadalupe within a field of low stratiform clouds - probably stratocumulus. A portion of the first cloud band is visible at the upper right; it is seen to be a smooth band, differing sharply from the broken banded clouds in the region.

4.2.3 Theory

A point disturbance travelling at a supersonic speed, v, has a wake confined to a cone. The half angle at the cone vertex is given by

$$\theta = \sin^{-1} \frac{1}{M}$$

where M, the Mach number, is v/c, and c is the speed of sound. The angle is plotted in Figure 22 for different Mach numbers.

A blunt-shaped object travelling at supersonic speeds is accompanied by a wave front, or shock wave ahead of the object. The half angle at the forward portion of the shock wave may be considerably greater than the Mach angle, θ.

In Figure 20, the shock wave is apparent as a parabolic shaped boundary enclosing the wake in the immediate vicinity of Guadalupe. Farther downstream the boundary becomes a straight line with a half angle of 32°. The first waves within the wake are curved indicating a changing Mach number, but the later ones become parallel to the wake boundary. The half angle of 32° is evidently the Mach angle for the flow beyond the first 60 nautical miles. From Figure 22 this angle corresponds to a Mach number of 1.9.

According to the theory of Freeman, a wave disturbance at an inversion of height, H, will travel at a speed, c, given by

$$c^2 = (1 - T/T_1)\, gH$$

where T and T_1 are the respective temperatures of the air below and above an inversion of negligible thickness, and g is the acceleration of gravity. The values of c, which constitute equivalent speeds of sound in the supersonic analogy, are plotted in Figure 23 for various inversion heights and temperature discontinuities (assuming T_1 = 300K).

Data from a ship radiosonde north of Guadalupe Island gives the inversion base at 450 m with ΔT about 3°C. According to Figure 23 this corresponds to c = 6.7 m sec^{-1}. The Mach number of 1.9 then corresponds to an undisturbed flow speed of 13 m $\cdot$ $sec.^{-1}$.

Wind speeds observed at Point Arguello, California, below the inversion

FIG.22

MACH ANGLE vs MACH NUMBER

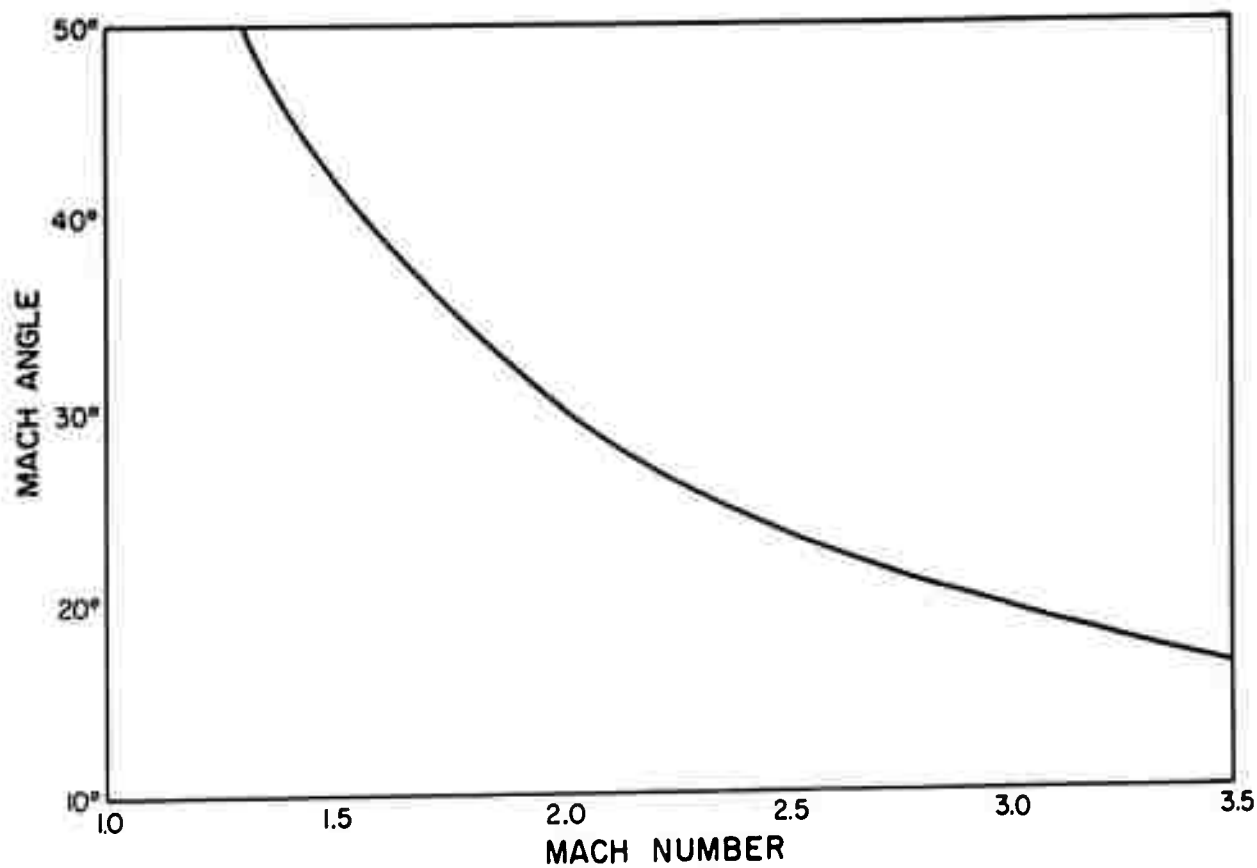

FIG. 23

EQUIVALENT SPEED OF SOUND FOR INVERSIONS AT DIFFERENT HEIGHTS AND TEMPERATURE DIFFERENCES

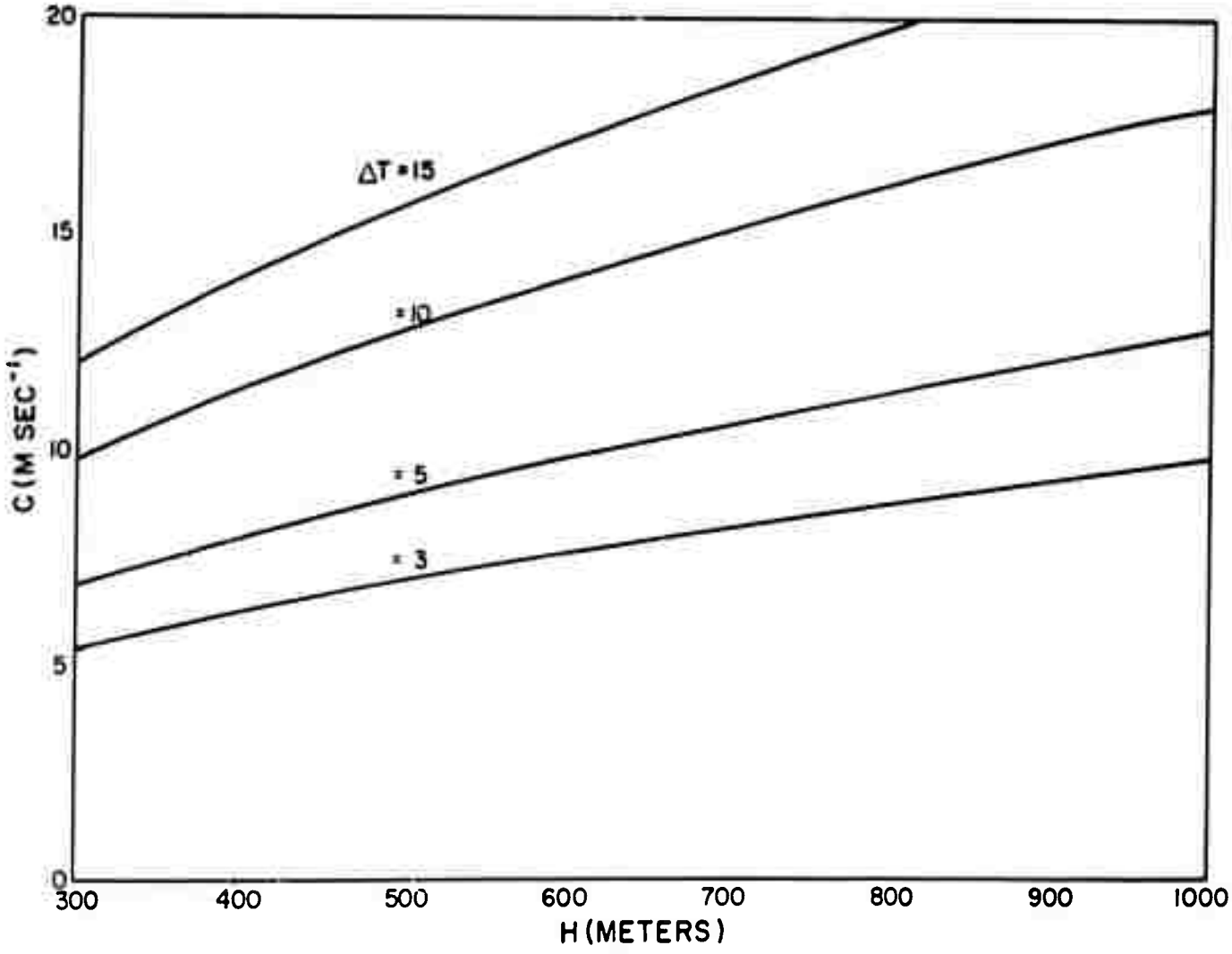

at 0000Z 19 May were about 14 msec^{-1} from the north-northwest, which is in good agreement with theory. The geostrophic winds in the vicinity of Guadalupe were estimated to be of that order, but the sparsity of data precludes a good estimate. Winds below the inversion at San Diego were evidently subject to local effects since they were light southwesterly.

4.2.4 Discussion and Conclusions

The TIROS photographs of the criss-cross pattern in stratocumulus clouds off the California coast provide further evidence of the validity of the analogy between supersonic flow and flow beneath an inversion. They also indicate that relatively small islands may cause a visibly disturbed wake for distances of several hundred kilometers downstream.

The criss-cross pattern is probably not an unusual phenomenon in stratiform clouds. The wake phenomenon associated with Guadalupe Island was observed on five successive days. It has been observed twice at Socorro Island, also off the lower California coast, some 1370 km to the southeast of Guadalupe (see Figure 20b).

The observation of this phenomenon from TIROS photographs enabled the determination of the approximate wind flow over a large area in the Pacific. While this is an unusual situation, it points to the potential of satellite cloud photographs in observing and interpreting atmospheric flow patterns.

We are indebted to the sharp eyes and inquiring mind of Allied Research's Clinton J. Bowley for discovery of this phenomenon.

SECTION V

THE STATUS AND FUTURE OF OPERATIONAL SATELLITE METEOROLOGY

5.1 Introduction

At the time of this writing, satellite meteorology, dating from the firing of TIROS I, is one year old. It was the privilege of the author of this section to be present at that time to assist in the processing of some of the first pictures. The impact that TIROS I and its successors would have on the science of meteorology was immediately obvious to all present. Equally obvious was the great amount of research and technology that would be required to put this new observational tool to effective use.

Now that a year has passed, a better view of the nature of this task and of the future of satellite meteorology is possible. It is the purpose of this section, then, to provide a brief critical review of the year's progress and, based on this progress to date, to estimate the immediate future of satellite meteorology.

5.2 An Evaluation of Present Status of Satellite Meteorology

5.2.1 General

The basic aim of the TIROS experiments has been completely fulfilled. This was to demonstrate that useful pictures of the earth's atmosphere and its clouds could be telemetered back to earth. More importantly, it has demonstrated that a large amount of observational material can be obtained via the satellite which is unobtainable by any other observational system. Some partial demonstration has been made of the applicability of these satellite observations to many problems of weather forecasting.

But many new problems have been created by the satellite observational tool. These fall largely into two categories, one dealing with the mechanics of data processing and data handling, the other with the integration of satellite data with other more conventional classes of meteorological data.

9.2.2 Television Observations

By far the most impressive results of the TIROS satellites to date have come from the televised pictures showing the grand organization of meteorological systems and the complex interrelationship between the smaller elements and the larger scale organizations of which they form part.

Data abstraction systems had been set-up previous to the launch of TIROS I which served to bring the television observations, more or less on a real-time basis, to an ever-widening group of meteorological forecast centers. Since transmission of the abstracted material, usually via facsimile, was necessarily performed on a somewhat erratic basis, practical utilization of the material was also somewhat erratic. But even with this handicap, sufficient number of forecasts were performed on the basis of the abstracted TIROS material to amply demonstrate its utility. In most cases, these were forecasts of cloud cover or forecasts where the cloud cover element was important.

The optical accident to the wide angle television system of TIROS II provided an interesting insight. It was found that the televised material, while suffering in clarity and definition, was nearly as useful operationally as was the case with the much clearer pictures of TIROS I. Two interpretations of this situation are possible, each probably true at least in part. First, the techniques used for the abstraction and depiction of material from the televised pictures for transmission via the facsimile network degrade the information content to a degree that makes high resolution of the original material rather unnecessary. A second interpretation is that the operational meteorologist has, as yet, little use for knowledge of the detailed structure of weather systems. The suggestion is strong, that improvements are required either in data handling methods or in data utilization techniques, most likely in both.

A tremendous library of pictures covering a wide variety of meteorological situations has been acquired. Those of TIROS I, in particular, contain a wealth of meteorological information. A fair amount of work has been done on various case studies, such as those reported in earlier sections of this report, but as yet a relatively small amount of work has been done on systematization of the mass of observational material. It is probable that a considerable amount of case study work will be required before a meaningful descriptive organization can be achieved.

The televised pictorial information is presented to meteorologists in a form that has a small-scale counterpart in radar meteorology. The basic value of the material lies in the pattern represented. While advanced digital computers are being taught very elementary pattern recognition, pattern in the meteorological sense remains an essentially non-quantitative property. Thus, just at a juncture when quantitative meteorology is making significant headway in such areas as numerical weather prediction, a whole large new class of qualitative information is being made available. It is a small wonder that those whose interests are largely quantitative tend, in their more pessimistic moments, to view the meteorological satellite as something of a backward step in the science of meteorology.

A more constructive point of view is that the satellite pictures provide just the sort of basic pattern material which must be used to inject an element of realism into numerical procedures, which tend to ignore the smaller scales and the more complicated aspects of atmospheric motion.

5.2.3 Infrared Observations

TIROS II contains a battery of sensors to measure the emission of the earth and its atmosphere in various bands of the infrared and visible spectrum. In anticipation of these observations, a fair amount of work has been done on the interpretation of the infrared emission using computationally simulated data. It has been found that the pattern of observed radiation will probably be of more practical significance than the absolute values of the radiation observed. The absolute value does, however, produce a third dimensionality which may in certain cases be diagnostically useful.

At the time of writing, only a limited amount of reduction of actual TIROS II data has been achieved. Comparison with what might have been predicted on the basis of the interpretive studies shows few suprises. More detailed evaluations of the TIROS II material, now planned or in progress, should result in demonstration of the general utility of this class of observation.

5.2.4 Observations by Radar and Other Radiations

Various proposals have been made to increase the scope of satellite meteorological observations to include such features as active radar. It would appear that a satellite-borne weather radar is marginally feasible, although the width of the swath beneath the orbit that could be adequately

surveyed might be quite restricted. Serious question exists, however, of the potential scientific or practical utility of the material that might be obtained by such an observing system. It is probable that this doubt can only be resolved by a suitable experiment.

Other potential observations, such as those of radio emanations (sferics), back-scattered ultraviolet, and solar observations, appear quite feasible and potentially quite useable. Presumably these will appear on such satellites as NIMBUS and its successors.

5.3 Outstanding Problems

5.3.1 Introduction

The meteorological satellite has posed many new problems in addition to providing much new information about the earth's atmosphere. Lest the catalogue of problems that follows appear overwhelming, it should be pointed out that it is easy to define relatively isolated areas of difficulty, whereas the description of the great mass of affirmative knowledge that has accrued from the meteorological satellite experiment must necessarily be more general.

5.3.2 Photo Interpretation

The TIROS satellites have provided pictures of broad areas of the earth's atmosphere which are rather tantalizing in the sense that one can almost, but not quite, discern the detail required to determine cloud types. The narrow angle pictures provide sufficient detail in most cases, but the pictures are spaced far apart and generally sample areas of lesser interest. Accordingly, those charged with the abstraction of data from the wide-angle pictures have been faced with the characteristic problem of the photo-interpreter--that of reconstructing information from pieces of somewhat indirect evidence. Like all photo-interpretation, this has become somewhat of a personal art, various data abstracters differing widely in ability and adventurousness.

It should be noted, parenthetically, that cloud type recognition is not completely essential to succesful use of satellite pictures. In probably the majority of cases, cloud type can readily be inferred from location in the overall pattern along with such partial clues as may be present in the pictures. For general analysis purposes the implications of cloud pattern transcend any great need for cloud type identification.

Progress to picture-taking systems of higher resolution will provide only a partial solution to this problem, as there will always be a requirement, real or fancied, for detail finer than that which can be resolved. The art of the meteorological photo-interpreter is thus likely to become a permanent one, being in a sense quite similar to that of the skilled meteorological analyst. It may be anticipated that a problem will exist in providing a uniformly high standard of meteorological photo-interpretation and a sufficient level of general education and experience, so that all who have occasion to consult meteorological photographic information can make reasonably good use of it.

It would appear that the best exercise of the talents of the meteorological photo-analyst and data abstracter would be in a weather central, where the results of his efforts could best be integrated with the other activities of the center, and whence the abstracted material that he prepares can be readily disseminated to the meteorological world.

5.3.3 Photogrammetry

A vexing problem of TIROS I, and to a lesser extent of TIROS II has been the establishment of the location of meteorological features seen in the pictures. An equivalent problem exists in establishing the appropriate locations of the infrared observations of TIROS II. While the state of this art has increased materially during the year since the launch of TIROS I, errors as great as 2° of latitude can still be incurred under unfavorable circumstances.

Basically the photogrammetric problem is one of trigonometry. Knowledge of all the required distances and angles, however, has been somewhat poorer than might be desired. This stems in part from relatively minor deficiencies in attitude sensing systems, in part from orbital uncertainties, and to a fair degree from uncalibrated distortions present within the pictures themselves. All of these represent non-basic engineering problems which should be resolved in future satellites.

The actual techniques of photogrammetry employed have in the past been slightly inconvenient. The techniques are now advancing rapidly, and for the future TIROS satellites it is believed that distraction of the photo-interpreters by essentially photogrammetric details can be minimized.

5.3.4 Picture Data Reduction and Transmission

In the TIROS system, picture data reduction occurs at the two data read-out stations where signals from the satellite are received at the ground. Residual problems of photo data reduction and transmission have stood in the way of the fullest utilization of TIROS pictures. The principal bottleneck is the impossibility of transmitting the great amount of information contained in the pictures through conventional communication channels. As a result, it is necessary to abstract or condense information from the pictures at the data acquisition sites and to disseminate the abstracted material by facsimile where possible, or by verbal or numerical teletype where facsimile does not reach.

5.3.4.1 Information Content and Pattern

The first problem of data abstraction is the selection and isolation of useful information. While, in a quantitative information sense, the pictures contain many bits of information, a high degree of redundancy is present so that a satisfactory description of the picture can in principal be made with a much smaller amount of basic information. In addition, much of the nominal information content of the picture is patently useless for meteorological purposes.

The difficulty arises in isolating that part of the information contained within the picture which is of significance to a wide class of potential operational users. In general, the most important features are those loosely described as "pattern." Of nearly equal interest may be the nature and extent of cloud cover and gross details of distribution of cloud masses that form the pattern. Also of frequent interest are certain key details of relatively small scale.

Abstraction of pattern and of the key details could in p inciple be performed objectively. However, it is hard for human photo-interpreters to avoid insertion of an element of subjectivity, in that it is difficult to avoid meteorological interpretation of at least the more clear-cut patterns. Because of restricted communication with the consumer of the information, such subjective interpretation may in fact be highly desirable to insure that the consumer is led to the best reconstitution of the condensed material available to him.

In general, pattern recognition poses relatively few problems once a reasonable amount of experience has been obtained. Problems of perspective, relative scales, and geographical interrelationships are ameliorated by the photogrammetric aids provided the data abstracters.

5.3.4.2 Depiction

Once the meteorological data abstracter at the satellite read-out site has a clear idea of the meteorological content of a TIROS picture, he is still faced with the problem of imparting this information to the more-or-less anonymous consumer at the other end of a one-way communication line. Since facsimile transmission has proved to be the principal means of transmitting this information, the problem can be termed one of depiction. An analogous problem exists whether transmission be by numerical code, abridged plain language code, or verbal description.

General techniques have evolved for depiction which have permitted a good degree of standardization and a diminished dependence upon the artistic capabilities of the data abstracter. However, comparison of facsimile abstractions with the original photographic material indicates that further improvement of graphical depiction is highly desirable.

It should be recognized that it is quite possible to make the depiction overly pictorial. In this case, the eventual consumer may be faced with the task of finding the material meteorologically relevant to his activity in a picture of degraded quality, a task for which he may have neither training, time, nor taste.

One suggested solution of the problems of data abstraction and depiction would be to have representatives of the principal operational users at the data acquisition sites. The efficiency of such representation would be dubious, probably adding to the considerable confusion that tends to prevail in the data abstraction centers. Because of this probable impracticality, it is desirable that all consuming services having specific requirements for satellite meteorological data should make the detailed nature of these requirements clear to the data abstraction personnel.

5.3.3.4 Infrared Grammetry and Interpretation

The infrared sensors on TIROS II scan the earth's surface by virtue of the rotation of the satellite. The optical axes of these sensors are oriented at 45° to the spin axis, so that the path on earth swept out by each rotation

of the satellite is quite complicated. Successive scans fit fairly closely together, so that reconstitution of a "picture" is possible. The geometry of this reconstitution is so complex that it has been found necessary to resort to the use of a large-scale digital computer to handle any significant fraction of the information. The success of the computer program is quite dependent upon the accuracy with which the attitude of the satellite is known- a problem already discussed.

It is believed that a considerable amount of digitally reduced information will presently become available. In the meantime, it has been possible to perform a few hand reductions of infrared data over restricted areas. However, residual uncertainty about location has made interpretation of these reduced data relatively general.

A problem also exists in depiction of the infrared data in a form which can readily be grasped. A number of attemps have been made, which have been deemed marginally satisfactory by their authors. A good depiction scheme will be a material aid to interpretation.

5.4 Operational Utilization

5.4.1 Present Status

In general, practical utilization of TIROS observations has been relatively casual. This is a direct result of the irregularity of appearance of TIROS observations of any given area. Vagaries in the communication of abstracted material, particularly during TIROS I operations, did little to encourage active use. Nevertheless, in those instances when timely TIROS data were available for an operational need (or were used in a postmortem), it was obvious that the potential utility of the information ranged from fair to outstanding. Thus, if the problems of timeliness can be resolved, there can be small doubt that heavy dependence upon satellite meteorological data will occur.

5.4.2 Techniques

The relatively casual operational utilization of TIROS data has done little to encourage the development of specific techniques for using satellite meteorological data. One of the more difficult techniques required is that of integrating the cloud data with conventional observations. While simple map superposition is feasible, joint interpretation may still be somewhat difficult. A further difficulty is engendered by the fact that the satellite

meteorological observations are not synchronous with conventional observations, and of course one orbit laps another with a time difference of some 99 minutes. The meteorologist accustomed to his two-dimensional smoothed snapshot depiction of meteorological phenomena, experiences considerable difficulty in dealing with this mass of information, unsynchronized with the conventional synoptic data.

While the development of techniques for coping with these problems will actively be pursued, a sobering lesson can come from the experience of radar meteorology. Here, after 15 years of experience, integration of radar observations with conventional observations is just now beginning to occur on other than a sporadic basis. In this case, integration has been achieved only through the development of special techniques for handling conventional meteorological information.

5.4.3 The Place of the Satellite in Meteorological Practice

It is interesting to speculate at this point on the eventual role of the satellite in meteorological practice. In some cases, where the element to be forecast is cloud cover or weather, such as for longer-range operation of winged aircraft, the satellite can well become the principal data source. Also in regions in which either no observations are made, or observations are made at relatively great expense, the satellite may once again become the prime data source for all classes of forecast. But in situations in which ample quantities of conventional information are and will continue to be present, the role of the satellite observations is not as clear. Its principal use would seem to be as an adjunct to conventional analyses, helping to clarify situations and provide the necessary observational detail for appropriately detailed forecasts. Large-scale pattern, not detectable by other means, as well as important details that slip between observing stations would permit this expansion of forecast capability.

In time of war, the role of the meteorological satellite is fairly obvious. Most military operations, whether on land, on the sea, or in the air, or even space missions, are vitally dependent upon the weather elements graphically displayed by satellite pictures. (In the event of doubt about the weather dependence of intercontinental missilery, the relation between cloud cover and the effect of nuclear devices should be reviewed.) The meteorological satellite provides a ready way of obtaining nearly all required information, other than wind data, that may be required over battlefields or enemy territory.

Telemetering from the satellite to directional antennas at appropriately located ground stations is relatively jam-proof. There is little need for security, since the same information is available to the enemy's satellites.

Perhaps the greatest utilization of the meteorological satellite may be found in its indirect effect on meteorological practice. The relation of characteristic weather patterns seen by the satellite to synoptic systems of the conventional weather map is becoming generally known. Armed with knowledge of the detailed structure of such systems, the forecaster is better enabled to interpret otherwise apparently anomalous observations in terms of pattern details, and thus to prepare more detailed and adventurous forecasts than have previously been possible. The degree to which forecasting skill can thus be improved remains yet to be demonstrated.

5.5 Research Utilization

Here we are not concerned with research specifically in problems of satellite meteorology, but rather with the impact of the satellite on meteorological research in general. Research results have already been achieved, using satellite pictures as basic data, which have clarified the meteorologist's view of the atmosphere and its phenomena. An example is a start toward a better understanding of the life history of the extra-tropical cyclone. Other atmospheric structures have been examined in detail with significant results.

The research potential of the meteorological satellite pictures is enormous. In all of the pictures one sees repetitive patterns and obviously non-accidental details of structure, nearly all of these features are without a sufficient explanation. There can be little doubt that when adequate quantitative "explanations" for the phenomena observed by the satellite have been obtained, our new understanding of the atmosphere will make possible far better forecasting than we now enjoy. It is possible that this understanding will culminate in the long-sought control of weather.

5.6 A Look Into the Future

It is not idle speculation at this point to look beyond the TIROS series of satellites, through the NIMBUS satellites, to the eventual future of satellite meteorology. The prime concern of the eventual meteorological satellite will be operational observation. Accordingly, the satellite system will be organized in such fashion that it can maintain all or a large fraction of the globe constantly under surveillance. This must be achieved within a reasonable economic structure.

Two alternatives seem to exist. One is a small number of satellites flying at extremely high altitudes, such as the projected AEROS satellite in a 24-hour earth-synchronous orbit at 22,000 miles. A small number of these satellites could satisfactorily cover the earth. At this distance, considerable problems of communication exist. If it is desired to maintain a fixed geographic position, fine orbital adjustment must be provided. Active earth stabilization is probably required. All of these features suggest a fairly heavy satellite. The lifting of such a satellite to a great height is likely to continue to be expensive even with improvement of the state of the booster art.

An alternative scheme would make use of large numbers of low-flying satellites. Here, coverage would be on a statistical basis rather than truly continuous. An entirely different type of communication problem would exist, which might be resolved if a similar number of communications satellites are flying in similar orbits. A large-scale computer installation would be required to keep track of locations of the many satellites and to interpret the data in terms of location. Passive gravitational stabilization of these satellites may be feasible, so that they could be relatively simple and light. Failure of a few out of a large number of such satellites would pass virtually unnoticed.

Accordingly, this prognosis of the future operational meteorological satellite system sees a large number (30 or more) of small satellites on a group of random 300 to 400 mile high orbits interspersed with a similar number of communications satellites. Interrogation of the meteorological satellites would be achieved by already established routing techniques through the communications satellites, the meteorological data returning over the same route to a central ground station. Branching routes could be established to feed the information to a number of world meteorological centers. The communications load represented, while by no means insignificant, would not seriously tax the capacity of the communications satellite system. The same computer center used to establish locations and routings through the communications satellite system would serve also to keep track of the locations of individual meteorological satellites so that they can be interrogated at the proper locations and times and could be used to superpose location information on the pictorial information received.

It is not immediately obvious at this time how observations will be achieved at night. Present infrared scanning devices appear to be far too clumsy for operational use. The development of a satisfactory infrared vidicon would appear indicated; it would be even more attractive if it could be used in day time for observation in the visual wave lengths. Data processing will undoubtly follow the general lines now envisaged for conventional data. Initial processing and distribution will be almost completely automated. For purposes of general forecasting, where digital computers will play a larger and larger part, the photographic and infrared material will be introduced into the computer system as a part of the data to be handled. At such time as generalized baroclinic forecasting becomes possible, cloud cover and infrared emission will become important inputs.

A presentation to human forecasters will also be provided. Here, the many specialized applications will be performed by appropriate techniques, most of which have yet to be developed.

Reviewing the economics of the probable future satellite system, it would appear that much of the expense will be found in the communications and data processing aspects. With launch into orbit becoming fairly routine, and with standardized satellite packages, the currently astronomical cost of merely orbiting a satellite may well become secondary. Accordingly, it may not be too soon to start consideration of the eventual operational meteorological satellite data processing and communications system. In particular, since material revisions to the handling of conventional data are proposed by the implementation of system 433L, close coordination with this system to assure compatibility with potential satellite inputs is now recommended.

In conclusion, the meteorological satellite has already demonstrated its utility as both an operational and a research tool. Much of the effort in the future must be devoted to rendering the operational aspects economically feasible. A reasonable prognosis would suggest that an integrated, economical world-wide system can be implemented on a time scale of 10 to 15 years.

Institution of an operational meteorological satellite system will lead to no meteorological millennium. It will, however, facilitate the steady progress of the science and the art of meteorology.

APPENDIX A

ATTITUDE DETERMINATION FROM TIROS PHOTOGRAPHS

A.1 Introduction

A fundamental problem with TIROS pictures has been that of determining the location of the objects whose images are found in the picture, the results being expressed in any way convenient for the user. An evaluation of the meteorological significance of the objects is equally important for TIROS pictures, and in current practice the two problems are usually attacked simultaneously, but in the present discussion the latter aspect of the work is ignored.

To determine picture locations one needs to know the location of the camera, the direction in which it is pointed, the picture's object-image relation i.e., its distortion, the extent to which it deviates from the straight-ray geometry of the pin-hole camera and some additional information to add the third dimension to the two-dimensional information from the picture itself.

The distortion problem has been especially severe for TIROS pictures because of the unknown and varying distortions superimposed by the telemetry on to pictures taken by a camera which was not originally intended as a metric instrument. With sufficient care a surprising amount of this distortion can be taken into account, and this is an important preliminary step for good accuracy from the procedures discussed below. However, the present exposition does not cover this topic, all derivations being based on straight-ray geometry.

In the present treatment the third dimension is treated by assuming all identified objects to lie on the surface of a spherical earth and assuming the height of the satellite to be known.

This assumption introduces errors due to the topography of the earth and the height of the clouds above the surface, but they are small relative to other errors in TIROS picture interpretation, and in any event they will be unavoidable until some accurate method appears for determining the height of clouds seen in photographs from satellites. Refinements for the figure of the

earth are likewise small, but they can be made by including correction terms in the programs for actual operational calculations.

The position of the satellite will be assumed known from an accurate orbit determination together with an accurate picture time.

The remaining element of information, the camera direction or "attitude", is the principal subject of the present discussion. This work was started because of the failure of the horizon sensor system which was planned to provide calculated attitudes for TIROS I pictures, and the subsequent discovery that landmark images are seen too infrequently to permit complete reliance on attitudes deduced from them. The meteorologists faced with the deluge of TIROS pictures, quickly discovered that the horizon images and the ample overlap between pictures permitted fairly accurate intuitive rectifications, and soon thereafter they developed this to an art which was quite adequate for the initial meteorological work. The present discussion is the outgrowth of an attempt to provide a rigorous foundation for the intuitive methods, to provide maximum accuracy, to provide graphical aids for quick approximation, and to adapt the methods to whatever degree possible for automatic digital computation.

An initial report of this work was published earlier (Ref. 1). A few changes in nomenclature have been made for the present report.

A.2 Basic Geometry

A.2.1 Coordinates

In our basic geocentric reference system (Figure A-1) X passes through perigee and Y cuts the orbit beyond perigee, in the direction of motion of the satellite. The Z-axis is normal to the orbit, forming a right-handed system. The axes are fixed to the orbital ellipse and follow its secular changes. The satellite position is described relative to these axes by its true anomaly, w, (the polar angle, $w = \arctan(Y/X)$), and by its distance from the origin, r.

The sense of rotation of the satellite about its spin axis is immaterial for the present purpose. We choose the positive direction along the spin axis to be that going into the satellite camera lens i.e., that of the ray of light producing the central image of the picture; the unit vector $\underline{P}$ describes this direction. We define this directed line segment to be the principal axis, its intersection with the earth's surface (or with the celestial sphere, if it misses the earth) to be the principal point in object space (PO), the image

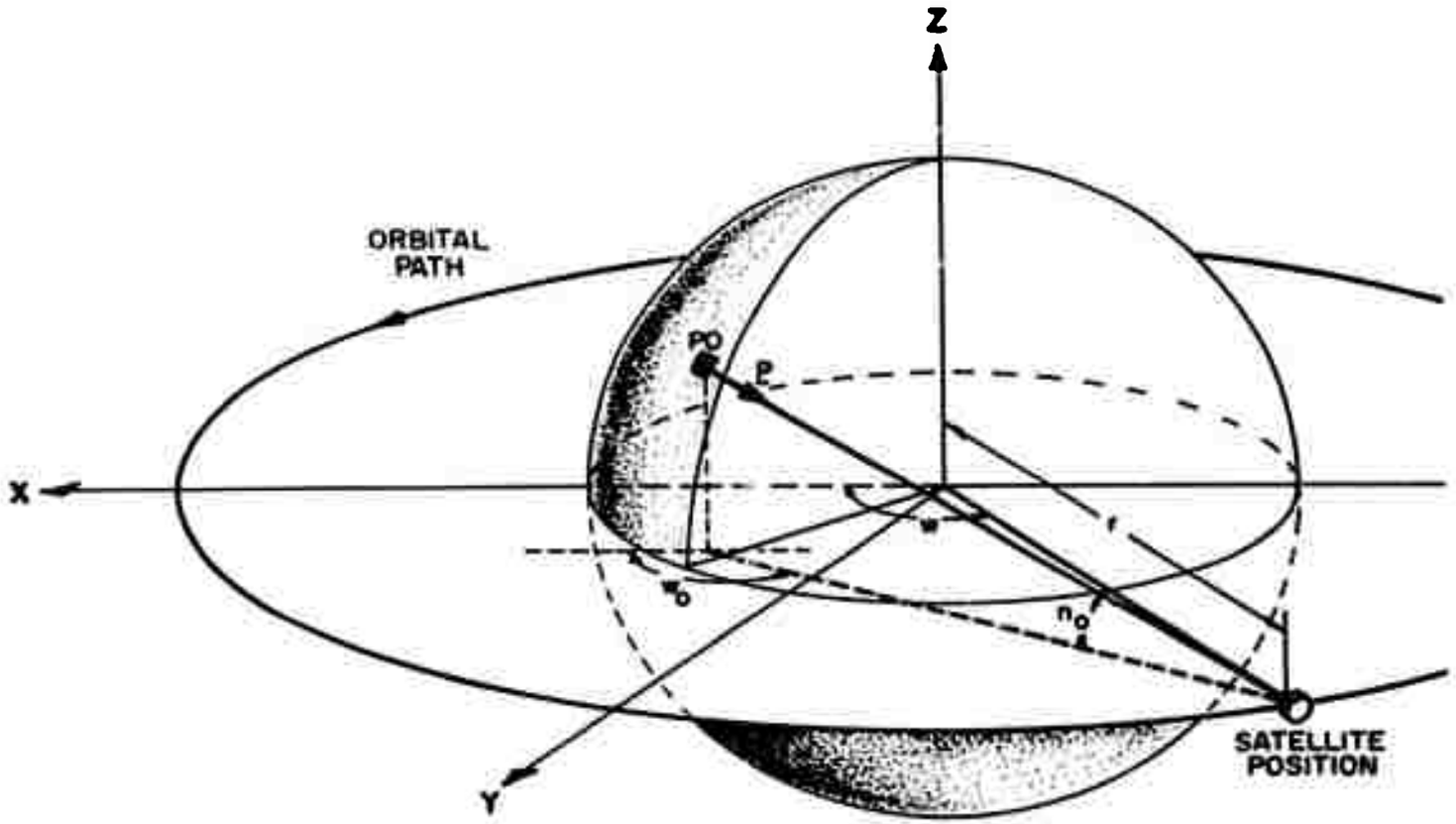

BASIC COORDINATES

FIG.A-1

of PO by the camera lens to be the principal point in image space (PI). If the optical axis is not parallel to the spin axis these definitions differ from the usual optical convention. Our choice is made to simplify the relation between successive pictures in a sequence, and any misalignment of the optical axis will be considered as an additional fixed picture distortion.

The angle of rotation of the camera around the principal axis will be discussed later.

The direction of the principal axis is expressed by the angle between it and the XY plane, n_o, and by a true anomaly, w_o. A sign is affixed to n_o to make it positive if $\underline{P}$ points toward the negative Z hemisphere, and negative otherwise; thus $\sin n_o = -(\underline{P} \cdot \underline{Z})$. The angle w_o is the true anomaly of the projection on the XY plane of a directed line from the origin parallel to the principal axis. These two angles change slowly with time. One contribution to the motion is artificial, due solely to the secular change in orientation of the coordinate system. The other (of the same order of magnitude, for TIROS) is the slow change of the satellite spin axis due to torques exerted by its environment.

A local coordinate system is used for interpreting each picture. A suitable reference frame for it, xyz, is derived from the basic XYZ system above by a rotation of angle w around the Z axis, to make the x axis pass through the satellite (Figure A-2). The angle between the principal axis and the positive x axis is the nadir angle, n. We shall use an azimuth angle, ξ, measured between the ($\pm x$, $+ y$) half-plane and the half-plane which contains the principal axis and the entire x axis; the choice of sign is such as to give $0 < \xi < 90^\circ$ when the PO lies in the ($+x$, $+y$, $+z$) octant. In effect, n and ξ are spherical polar coordinates having their origin at the satellite and their polar axis along $\underline{x}$.

Although defined here with reference to the principal axis, a nadir and azimuth may describe any ray from the earth to the camera lens. When necessary to distinguish between these two uses, the subscript, r, will denote the values for rays other than the principal axis.

A.2.2 Object-Image Relations

We consider each image point to be the intersection with a plane surface (the focal plane) of a straight ray from the corresponding object point through the nodal point at the center of the lens. We may translate the xyz frame to place its origin at this nodal point, to describe any point in object

FIG. A-2

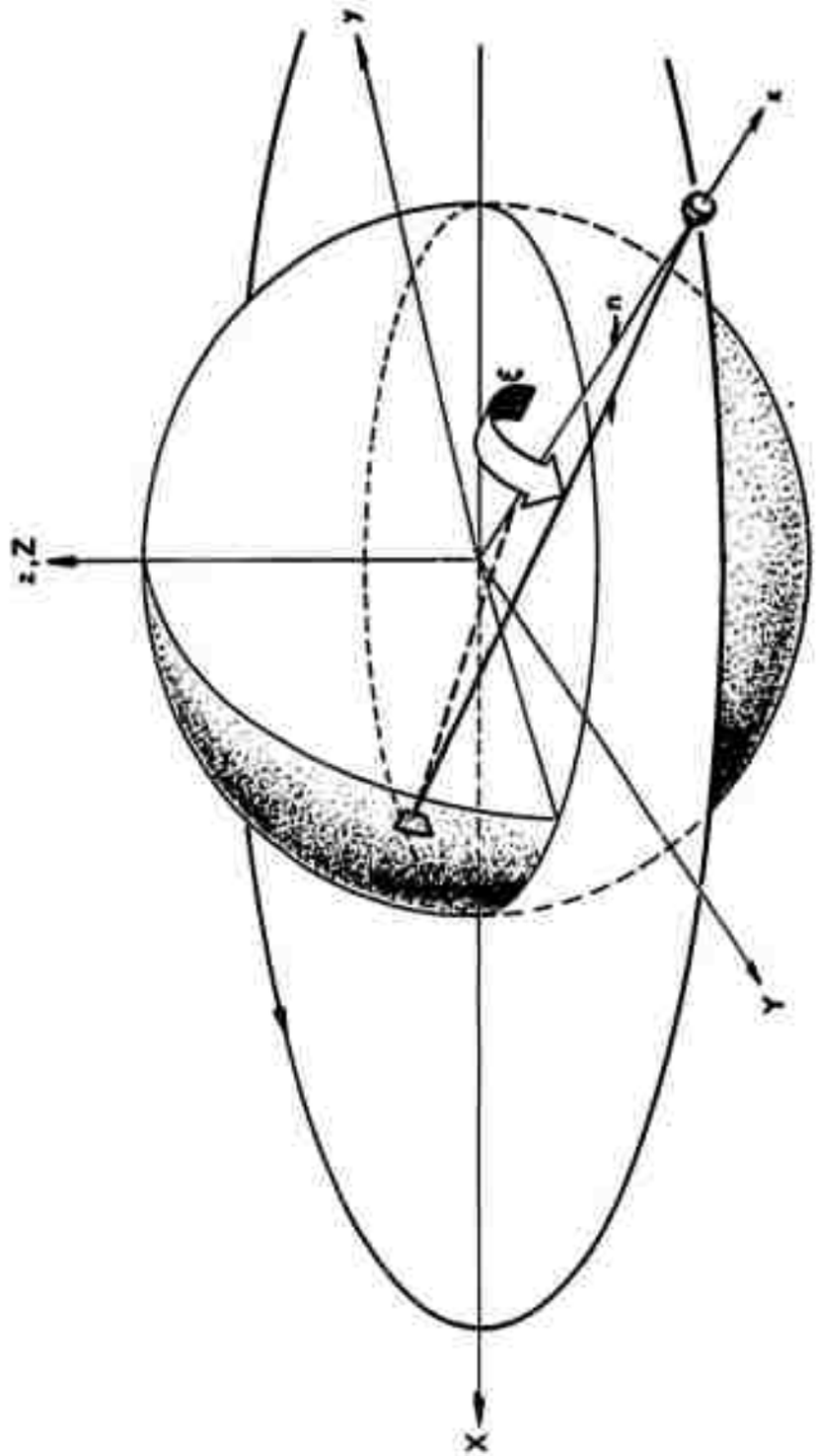

LOCAL COORDINATES

space by $(x', y', z') = (x-r, y, z)$. If the nadir angle of the principal axis, n, is not zero, we now rotate these axes by $\xi - 90^{o}$ around the x axis, then rotate by n, around the new y axis direction. Denoting coordinates relative to these axes by x", y", z", we have

$$\begin{Bmatrix} x'' \\ y'' \\ z'' \end{Bmatrix} = \begin{vmatrix} \cos n & -(\sin n)(\cos \xi) & -(\sin n \sin \xi) \\ 0 & \sin \xi & -\cos \xi \\ \sin n & (\cos n)(\cos \xi) & (\cos n)(\sin \xi) \end{vmatrix} \begin{Bmatrix} x-r \\ y \\ z \end{Bmatrix} \quad (1)$$

The case $n = 0$ is singular and must be treated separately whenever it occurs.

It can be seen then the "+x" axis parallels +P. Thus the y" z" plane parallels the focal plane, and each image point lies at coordinates (f, y''_i, z''_i), where f, a positive number, is the focal length. Similar triangles give the relations between each object point and its corresponding image point:

$$b = (y''_i/f) = (y''/x'') \quad (2)$$

$$c = (z''_i/f) = (z''/x'')$$

where we introduce the picture coordinates, b, c, normalized to unity focal length. Equations (1) and (2) together describe the image position for any point in object space.

The z" axis lies in the plane defined by the principal axis and the original x axis. This choice is convenient because this is the plane of symmetry for the camera-earth system (we assume a spherical earth). Since the visible portion of the earth is bounded by a circular horizon centered on the x axis, the rays from the horizon form a right circular cone whose apex is at the nodal point of the lens. Thus the image of the horizon is the section cut from this cone by the focal plane, and by symmetry the major axis of the conic section lies along the c axis of the picture coordinates. The intersection of the conic section with the negative c axis is the nearest point of the horizon image to the principal point, PI, (the negative sign is simply the normal inversion of an image in a camera system). Denoting the absolute value of this intercept by c_o from Figure A-3 we find the relation

$$n = \arcsin(1/r) - \arctan c_o \quad (3)$$

FIG. A-3

HORIZON AND NADIR ANGLES

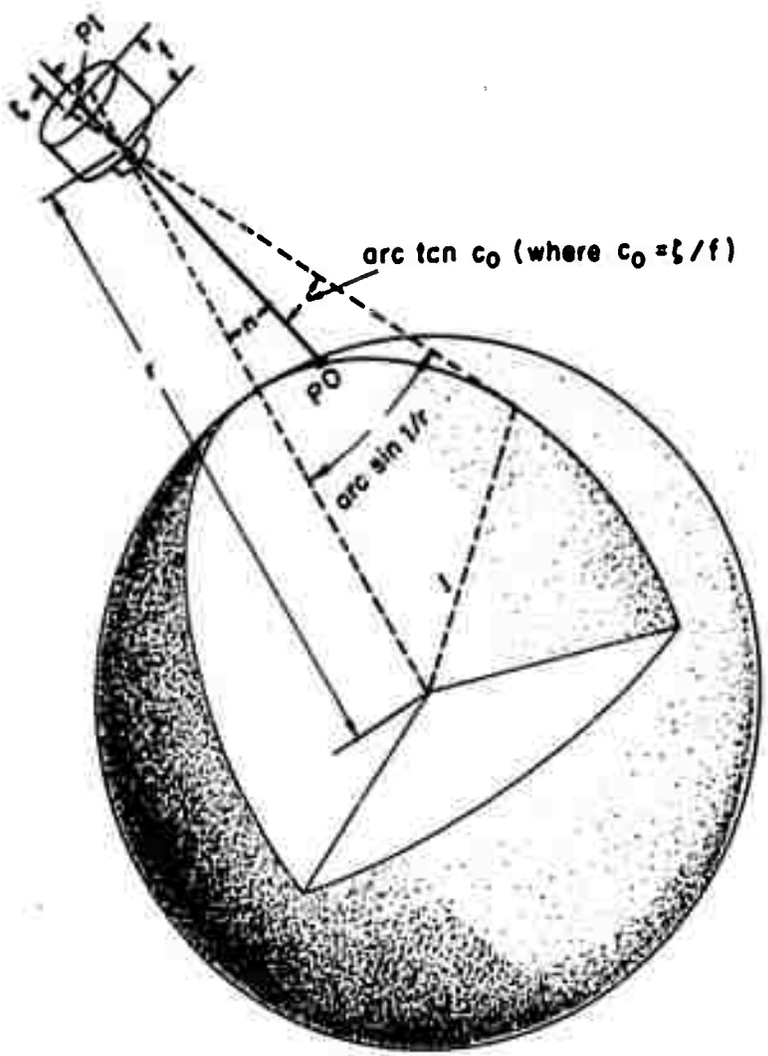

in which we have used unity for the radius of the earth.

Using an angular parameter, β, to trace out the circular horizon in object space, we use Equations (1) and (2) to find the horizon image:

$$\begin{aligned} b &= -(\sin \beta) / D \\ c &= \left[(r^2 - 1)^{\frac{1}{2}} \sin n - \cos \beta \right] / D \end{aligned} \tag{4}$$

where

$$D = (r^2 - 1)^{\frac{1}{2}} \cos n + \sin n \cos \beta$$

This is most easily derived by noting that the azimuth is irrelevant here, so that the general case is obtained from the formulae for $\xi = 90^{\circ}$.

The figure of the earth must be used explicitly to find the location of an object point from the location of the corresponding image point, since the image position furnishes only two coordinates, b and c. We shall use a sphere for this purpose.

We shall require the location of an object point, given n_r and ξ_r, for a ray from it to the camera. The nadir angle defines a right circular cone about the x axis which intersects the earth along a small circle x = constant. The relations are seen in Figure A-4, from which we can derive

$$x = r \sin^2 n_r \pm \cos n_r (1 - r^2 \sin^2 n_r)^{\frac{1}{2}} \tag{5}$$

We discard the negative solution, which is the circle of intersection hidden from view beyond the horizon.

The azimuth angle prescribes a particular point on the circle defined by n, and thus completes the description of the point in the local coordinate system:

$$\begin{aligned} y &= (1 - x^2)^{\frac{1}{2}} \cos \xi_r \\ z &= (1 - x^2)^{\frac{1}{2}} \sin \xi_r \end{aligned} \tag{6}$$

The subscript, r, signifies that these hold for any ray direction. The principal axis nadir and azimuth may be used, of course, to calculate the principal point.

OBJECT LOCATION

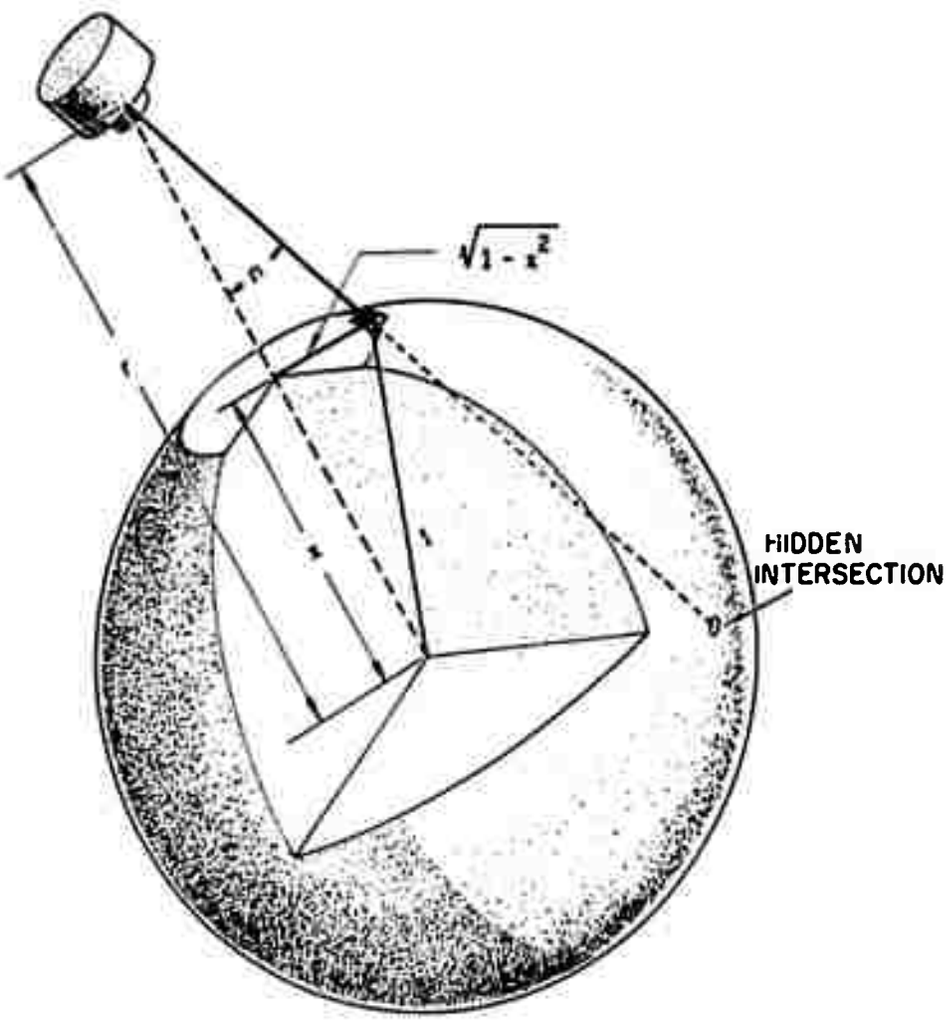

In passing we note that the nadir which grazes the horizon is that which makes the radical vanish in Equation 5, i.e.,

$$\sin n_h = 1/r \tag{7}$$

and thus, for horizon circle, we have the further result

$$x_h = 1/r = \sin n_h \tag{8}$$

Elsewhere we require the object position, given the position of its image (b, c), and the azimuth and nadir of the principal axis (n, ξ). For this we first calculate the nadir and azimuth of the ray (n_r, ξ_r); Equations (5) and (6) will then complete the calculation. We transform the image coordinates by

$$\begin{Bmatrix} x_i - r \\ y_i \\ z_i \end{Bmatrix} = \begin{vmatrix} \cos n & 0 & \sin n \\ 0 & 1 & 0 \\ -\sin n & 0 & \cos n \end{vmatrix} \begin{Bmatrix} 1 \\ b \\ c \end{Bmatrix} \tag{9}$$

in which the nadir angle of the principal axis is used. From these follow the nadir and relative azimuth angles of the ray to a given image point:

$$\begin{aligned} \sin n_r &= \rho/d \\ \cos n_r &= (x_i - r)/d \\ \sin \xi_r &= -z_i/\rho \\ \cos \xi_r &= -y_i/\rho \end{aligned} \tag{10}$$

where positive roots are taken in the definitions

$$\rho = (y_i^2 + z_i^2)^{\frac{1}{2}}$$

$$d \begin{cases} = ((x_i - r)^2 + y_i^2 + z_i^2)^{\frac{1}{2}} \\ = (1 + b^2 + c^2)^{\frac{1}{2}} \end{cases} \tag{11}$$

A.2.3 The Variation of Azimuth and Nadir Angles

In our idealized model of TIROS the principal axis remains essentially fixed in space during the period of one revolution of the satellite around the earth, whereas the local coordinate system rotates through 360°. The angle between the principal axis and the xy plane remains fixed, however. Thus, from the point of view of the satellite, the principal axis appears to describe a right circular cone with its apex at the satellite and its axis parallel to the Z axis. Since this apparent motion is simply the inverse of the rotation of the local coordinate system, it is measured by the true anomaly of the satellite, w.

The minimum value of the nadir angle occurs when $w = w_o$, and this value is $n_{min} = n_o$. Simple trigonometry yields the relations

$$\cos n = \cos n_o \cos (w-w_o)$$
$$\operatorname{ctg} \xi = \operatorname{ctg} n_o \sin (w-w_o) \qquad (12)$$
$$0 \leq n \leq 180$$
$$0 < \xi < 180 \text{ for } n_o > 0$$
$$0 > \xi > -180 \text{ for } n_o < 0$$

Graphs of the functions n(w) and $\xi(w)$ are shown in Figure A-5. Since w(t) is simply the motion of the satellite, assumed known, these formulae provide (n, ξ) as functions of time. Secular changes are taken into account exactly if n_o and w_o are inserted as known functions of time.

These relations will also determine n_o and w_o from observed values of the other quantities. For illustration, we differentiate the first of Equations (12) with respect to w (ignoring secular changes), square the result, and add it to the square of the original equation; after rearrangement we have

$$\cos^2 n_o = \cos^2 n + \frac{dn}{dw} \sin^2 n \qquad (13)$$

Thus n_o, and subsequently w_o, can be determined in principle by two measurements of n(w), slightly separated in time. Measurements of ξ can be used similarly. Alternatively, simultaneous values of ξ and n can be used with the formulae

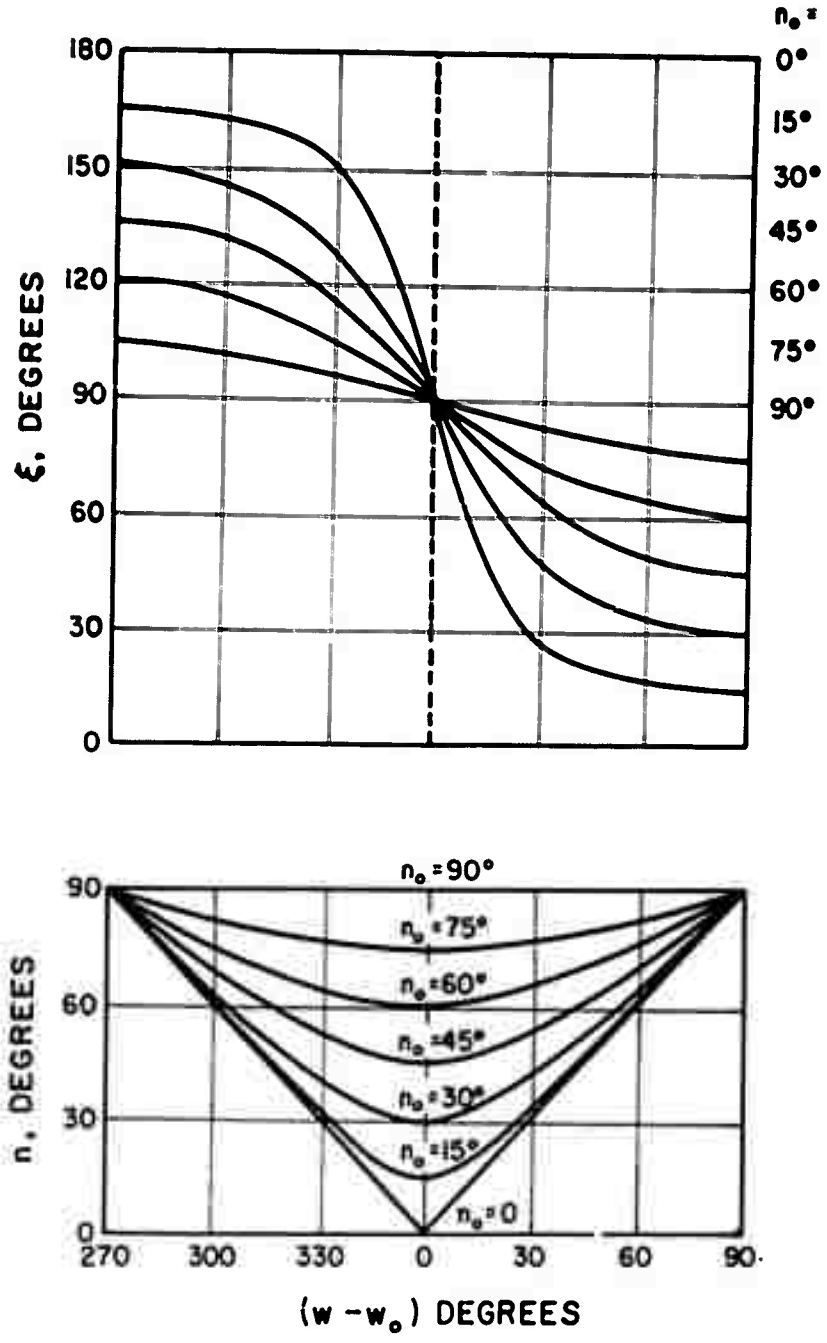

Fig. A-5 ATTITUDE NOMOGRAM

$$(w - w_o) = \arctan \left\{ \cos \xi \tan n \right\}$$
$$n_o = \arccos \left\{ \cos n / \cos (w - w_o) \right\} \qquad (14)$$

A.3 Data Extraction From Pictures

A.3.1 Nadir Angle Measurement and Use

In normal TIROS operation more than thirty pictures are obtained from each orbit that passes within telemetering range. In practice a majority of these contain an image of the horizon.

The picture coordinates defined in Section A.2.2 require the c axis to be placed along the axis of symmetry of the horizon image. Let us assume 400 line resolution in the picture and an angular field of view of 100°, approximately the TIROS values. An uncertainty of 1 line in locating the horizon image near the edge i.e., at about 200 lines from the principal point yields the estimate of about 1/200 radians or about 0.3° as the order of precision with which the picture coordinates might be oriented on a given picture. By similar arguments the measurement of c_o and the use of Equation (3) might give n to about 0.3° precision. The picture distortions introduced by the scanning and telemetry electronics make these precision estimates rather fanciful for most TIROS pictures, but nonetheless they suggest the limits which might be approached in favorable cases.

The redundant nadir angle data from a sequence of pictures can be processed in various ways to obtain best-fit values of n_o and w_o from the first of Equations (12), depending on objectives and facilities. However, the horizon is not in the field of view for low nadir angles. These occur when n_o is small, but this is also the case in which data near the time of minimum nadir angle are required ($w \doteq w_o$) in order to obtain a good value for n_o (see the graph in Figure A-5). The severity of this requirement depends on the uncertainty of the nadir angle data, but the fundamental problem is always present. A similar problem appears to exist in determining w_o for n_o near 90°, but this is not physically important since this is merely analogous to an uncertain longitude value for a point near the pole.

A.3.2 Azimuth Data from Overlapping Pictures

As shown by Figure A-5 the information from azimuth data essentially complements that from nadir angles. Unfortunately, however, there is no simple and normally available counterpart to the horizon image as a reference

from which to deduce azimuth for individual pictures. On the other hand, the actual displacement of the satellite between pictures is known with ample accuracy to serve as such a reference, and even if the picture timing is uncertain, the direction of the displacement is known. Since the apparent motion of identifiable objects in overlapping pictures is essentially the inverse of this displacement, azimuths can be obtained from such sets of pictures.

We outline two methods which are similar but which differ in detail. The first is a brute force technique primarily intended for automatic digital computation, although Section A.4.2 contains a graphical version of it. The second can be used in various forms ranging from approximate graphical work to detailed automatic computation which is essentially a variant of the first method given.

A.3.2.1 Object Space Calculations

Consider a picture with an image of the horizon, so the nadir angle and the orientation of the image plane coordinate axes are known within the picture. We assume that the image coordinates (b, c) of certain picture elements (landmarks or cloud features) can be measured accurately. However, we assume that the azimuth angle of the camera is not known. By applying the sequence of Equations (9) through (11), (5), and (6), the relative locations of the corresponding object points can be located on the spherical earth, regardless of what azimuth value is used. The subpoint is known on the sphere, since it is at the intersection with the x axis i.e., at (1, 0, 0). However, the location of the y and z intersections are not known relative to geographic coordinates. For the following developments we make the explicit choice $\xi = 90^{o}$ in applying these calculations; this artifice allows a slight simplification in determining the true azimuths.

Now let a picture taken a short time later in the same orbit contain images of some of the same object points, and let it also contain the image of the horizon. Again the relative location of the object points can be found on a sphere, but this time with the new subpoint position at (1, 0,0), and with new and again unknown geographic positions for (0, 1, 0) and (0, 0,1). It is apparent that the new version of object space can be derived from the previous one by a simple rotation of the sphere, and that this rotation will transport the first subpoint to a new position along an arc which is in fact the locus of subpoints over which the satellite has passed. This locus differs from an instantaneous intersection of the orbit plane with object space because

the technique identifies the previous subpoint relative to surface features which have been carried along by the earth's rotation during the interval between pictures. However, this effect as well as the tiny contribution due to secular change in the orbit are easily accounted for. This detail is treated in Section A.3.2.3.

Let $\underline{r}_j^{\,1}$ and $\underline{r}_j^{\,2}$ be the object space locations of the j^{th} picture element as determined from the first and the second pictures, respectively. Imagine both sets of j vectors plotted on a common coordinate system i.e., superimpose the two different versions of object space as seen by the satellite. Let $\underline{\underline{M}}_{12}$ be the matrix which rotates the first picture results into the second i, e., let $\underline{\underline{M}}_{12}\,\underline{r}_j^{(1)} = \underline{r}_j^{(2)}$ for each j. The determination of $\underline{\underline{M}}_{12}$ is discussed below. Now $\underline{\underline{M}}_{12}\,\underline{x} = \underline{\underline{M}}_{12}\,(1,\ 0,\ 0)$ is the first subpoint as it should be plotted relative to the second picture. Let us use ξ' for an azimuth uncorrected for earth rotation. The reference direction of $\xi'^{(2)}$ (the superscript $(_2)$ denotes second picture) is the great circle arc from $\underline{\underline{M}}_{12}\,\underline{x}$ to (1, 0, 0), since the forward direction along the orbit was chosen in Section A.2.1. Because of our choice "$\xi = 90^{o}$" in the previous paragraph, the vertical projection of the principal axis onto the earth at the time of the second picture, relative to the $\underline{r}_j^{(2)}$, is the great circle arc from the x axis toward the z axis (strictly, it is this arc with the opposite sense, but the present sense is correct for the azimuth calculation here). Thus $\xi'^{(2)}$ is the angle measured from the $(\pm x,\ -\underline{\underline{M}}_{12}\,\underline{x})$ half plane to the $(\pm x,\ +z)$ half plane, the angle being measured positive for a positive right handed rotation about the +x axis.

Let $\underline{\underline{M}}_{12}\,\underline{x}$ have the components $(\alpha_2,\ \beta_2,\ \gamma_2)$. Now $(0, \beta_2, \gamma_2)\,/(\beta_2^{\,2} + \gamma_2^{\,2})^{\frac{1}{2}}$ is a unit vector such that

$$\begin{aligned} \cos \xi'^{(2)} &= -\gamma_2 / (\beta_2^{\,2} + \gamma_2^{\,2}) \\ \sin \xi'^{(2)} &= -\beta_2 / (\beta_2^{\,2} + \gamma_2^{\,2}) \end{aligned} \qquad (15)$$

In general the azimuth for picture 1, $\xi'^{(1)}$, differs from that for picture 2, according to Equation (12). It could be computed from the plane of the reference arc used above, $\underline{\underline{M}}_{12}\,\underline{X}$ to $\underline{x}$, to the plane defined by $\underline{\underline{M}}_{12}\,\underline{x}$ and $\underline{\underline{M}}_{12}\,\underline{z}$. Alternatively one would consider the inverse matrix i.e., $\underline{\underline{M}}_{12}^{-1}\,r_j^{(2)} = r_j^{(1)}$. Let $\underline{\underline{M}}_{12}^{-1}\,\underline{x}$ have the components $(\alpha_1,\ \beta_1,\ \gamma_1)$; we find

$$\cos \xi'^{(1)} = +\gamma_1 / (\beta_1^2 + \gamma_1^2)$$
$$\sin \xi'^{(2)} = +\beta_1 / (\beta_1^2 + \gamma_1^2) \qquad (16)$$

In principle, of course, it suffices to determine either $\xi'^{(2)}$ or $\xi'^{(1)}$, since the same data are used and the final results should be related through Equation (12).

To determine the matrix $\underline{\underline{M}}_{12}$, let two object points, j = 1, 2, be visible in both pictures. A rotation w_1, with $\cos w_1 = \underline{r}_1^{(1)} \cdot \underline{r}_1^{(2)}$, around the axis parallel to $\underline{r}_1^{(1)} \times \underline{r}_1^{(2)}$, will carry $\underline{r}_1^{(1)}$ into coincidence with $\underline{r}_1^{(2)}$. We denote this rotation by the matrix $\underline{\underline{M}}_a$. A single further rotation, $\underline{\underline{M}}_b$, about an axis paralled to $\underline{r}_1^{(2)}$ should complete the transformation i.e., $\underline{\underline{M}}_b \underline{\underline{M}}_a = \underline{\underline{M}}_{12}$. However, in general the experimental errors in the actual data will prevent perfect alignment of $\underline{\underline{M}}_{12} \underline{r}_j^{(1)}$ with $\underline{r}_j^{(2)}$ except for j = 1. As an approximation let us choose the amount of rotation w_b to place $\underline{\underline{M}}_b \underline{\underline{M}}_a \underline{r}_2^{(1)}$ in the plane defined by $\underline{r}_1^{(2)}$ and $\underline{r}_2^{(2)}$, that is,

$$\cos w_b = (\underline{r}_2^{(1)} \times \underline{r}_1^{(2)}) \cdot (\underline{r}_2^{(2)} \times \underline{r}_1^{(2)}) / \left| \underline{r}_2^{(1)} \times \underline{r}_1^{(2)} \right| \left| \underline{r}_2^{(2)} \times \underline{r}_1^{(2)} \right| \qquad (17)$$

In an alternate procedure we note that all axes of rotation which can carry $\underline{r}_1^{(1)}$ into $\underline{r}_1^{(2)}$ lie on the mirror plane between them. This plane can be defined by the two unit vectors $\underline{A}_1 = (\underline{r}_1^{(1)} + \underline{r}_1^{(2)}) / \left| \underline{r}_1^{(1)} + \underline{r}_1^{(2)} \right|$ and $\underline{B}_1 = (\underline{r}_1^{(1)} \times \underline{r}_1^{(2)}) / \left| r_1^{(1)} \times r_1^{(2)} \right|$, such that any unit rotation vector can be written $a_1 \underline{A}_1 + (1 - a_1^2)^{\frac{1}{2}} \underline{B}_1$. Similarly we can construct the unit rotation vectors $a_2 \underline{A}_2 + (1 - a_2^2)^{\frac{1}{2}} \underline{B}_2$ from $\underline{r}_2^{(1)}$ and $\underline{r}_2^{(2)}$. Thus the axis of rotation for $\underline{\underline{M}}_{12}$ can be taken as the solution of $a_1 \underline{A}_1 + (1 - a_1^2)^{\frac{1}{2}} B_1 = a_2 \underline{A}_2 + (1 - a_2^2)^{\frac{1}{2}} \underline{B}_2$; the amount of rotation can be shown as the average of those indicated by j = 1 and by j = 2.

Careful analysis of individual cases would be needed to determine the most suitable way to obtain a best-fit $\underline{\underline{M}}_{12}$ from redundant data which are inconsistent due to measurement errors. For a best-fit superposition of the two vector sets in a chosen section of the picture e.g., near $\underline{\underline{M}}_{12} \underline{x}$ relative to the $\underline{r}_j^{(2)}$ one may evaluate an $\underline{\underline{M}}_{12}$ from two object points dispersed fairly symmetrically about it. The empirical discrepancy, $\underline{r}_j^{(2)} - \underline{\underline{M}}_{12} \underline{r}_j^{(1)}$ as a function of position can then be smoothed to permit correction by interpolation for the desired vector.

We point out that identifiable landmarks in the pictures concerned would permit at least an approximate orbit determination based on the

preceding work. Conversely, the technique can be viewed as one which locks pictures together in such a fashion as to permit the relative location of geographical objects.

A.3.2.2 Image Space Calculations

The preceding work deals explicitly with the locations of points in object space, as deduced from two overlapping pictures. For some purpose it is useful to work instead in terms of image space for one of the pictures. Here an apparent azimuth is measured within the picture, relative to the satellite displacement established by apparent cloud motions; the result is then modified to take picture perspective into account.

The distortions near the edge of the TIROS pictures and their restricted field of view make it difficult to deal directly with the subpoint image. However, it is possible to modify the calculations to deal with the path of principal points, which of course, passes through the center portion of the picture where the least distortion is expected.

In the simplest approach the location of the principal point in one picture is determined relative to sharply delineated picture elements (cloud features or landmarks). Since TIROS pictures usually have enouh overlap for the same picture elements to occur in several pictures on one sequence, one can locate and mark on one picture the principal points from several adjacent pictures. The result furnishes what is in fact the image of the path of principal points. The angle, γ, between this path and the picture b axis is to be compared with theory to derive ξ; that and the known n together specify n_o and w_o.

The theory is most readily written down in the opposite order, leading to a numerical solution by successive approximations. We take n as known from the horizon in the given picture, and we select a reasonable value for ξ; these values imply $(w - w_o)$ and n_o, which are calculated from Equation (14). Since w is known (we assume throughout that the ephemeris for picture time is well known), w_o follows. These form the first trial values of the unknowns.

An approximate principal point is now calculated for a slightly later time i.e., for a slightly different anomaly, $w_1 > w$. First n_1 and ξ_1 are found from Equations (12), then the principal point is calculated from Equations (5) and (6), in terms of local coordinates at the new (later) picture time. What we require is this principal point in the local coordinates at the original

picture time; thus the calculated principal point is rotated about the z axis by $(w_1 - w_0)$. This position must be corrected for the earth rotation, etc., as described in Section A.3.2.3. Finally Equations (1) and (2) provide the image of the new principal point in the original picture $(b_1\ c_1)$ we calculate γ from the definition:

$$\sin \gamma = b_1 / (b_1^2 + c_1^2)$$
$$\cos \gamma = c_1 / (b_1^2 + c_1^2) \qquad (18)$$

This is compared with the measured γ, a revised value for ξ is determined, and the calculations repeated, the cycling being continued until satisfactory agreement is rendered. A simple correction for the new ξ is $\xi_2 = \xi_1 + (\gamma - \gamma_1)$, where γ_1 is the value computed from the previous azimuth, ξ_1 and γ is the observed value. This is based on the rough similarity in meaning of γ and ξ. Although not examined theoretically for convergence properties, it has worked well in trials.

Because of the curvature of the image of the principal point path it is well to compute a second value of γ based on a second choice of w_1, with $w_1 < w$. The average of the two computed values is used as the correct γ. Alternatively, γ can be found from the line joining the two offset principal points, but the amount of calculation is about the same; the choice depends on programming efficiency.

Useful results can be obtained from principal point paths which have been determined by simple inspection of the picture sequence, in cases where the image detail is sufficiently profuse near the principal point. For less favorable cases an empirical transfer function can be constructed which relates the available image detail in one picture to that in the next, and the principal points transferred from one picture to the other by interpolation. The most thorough and precise transfer method would appear to be essentially that of the preceding section, but it would seem that the simpler theory involving subpoint track would be preferable if this amount of detail were to be used. It is felt that the present method has its principal advantage where γ can be measured fairly simply by inspection, and where sufficient accuracy can be achieved by the use of nomograms based on the above calculations, as discussed in Section A.4.

A.3.2.3 Correction for the Earth Rotation

It is necessary to take into account the rotation of the earth when data from overlapping pictures are used in conjunction with theory based on orbital coordinates. An object which is recognized in two successive pictures has been moved an appreciable distance by this rotation during the interval between pictures. Thus, for example, a locus which has been contructed in one picture by identifying the position of adjacent principal points relative to clouds or landmarks in general is not parallel to the locus of those principal points in space relative to an inertial frame or to the orbital frame.

As noted earlier, an explicit correction for this effect should be included in the calculations of Section A.3.2.2. This correction, of course, is a small rotation around the north pole, the orientation of which can be specified relative to the local coordinate system for this purpose. Strictly, one should take into account the motion of the north pole relative to the local frame during the time for which this rotation is calculated. For overlapping pictures from the TIROS altitude, however, the interval between overlapping pictures can only be the order of a minute or two. Thus the correction for the rotation of the earth is fairly small, and this further refinement is quite trivial.

In other cases this effect is most readily included by noting that azimuth data from overlapping pictures are simply measured from an incorrrct reference direction. According to Section A.2.1 the proper reference direction at any instant is given by the unit vector $\underline{k} = (\overset{o}{w} \times \underline{r}) / \left| \overset{o}{\underline{w}} \times \underline{r} \right|$, where $\overset{o}{w}$ is the orbital rotation vector, taken along the +z axis. Neglecting the effect of orbit precessions, this is simply the direction of the tangential component of the satellite velocity in space. The reference in overlapping pictures, however, is the direction of this component of satellite velocity relative to the earth's surface at the subpoint, expressed by the unit vector, $\underline{k}' = ((\overset{o}{w} - \Omega) \times \underline{r}) / \left| (\overset{o}{w} - \Omega) \times \underline{r} \right|$, where Ω is the earth's rotation vector, positive toward North. The difference between azimuth and the apparent azimuth measured from pictures is simply the angle between these vectors, and is easily evaluated from the scalar product $(\underline{k} \cdot \underline{k}')$. Figure A-6 shows a graph of the correction which must be added to measured apparent azimuth to provide true azimuth, for typical TIROS parameters.

In principle, further azimuth corrections are required because the reference direction is defined relative to the orbit, whereas the velocity of the

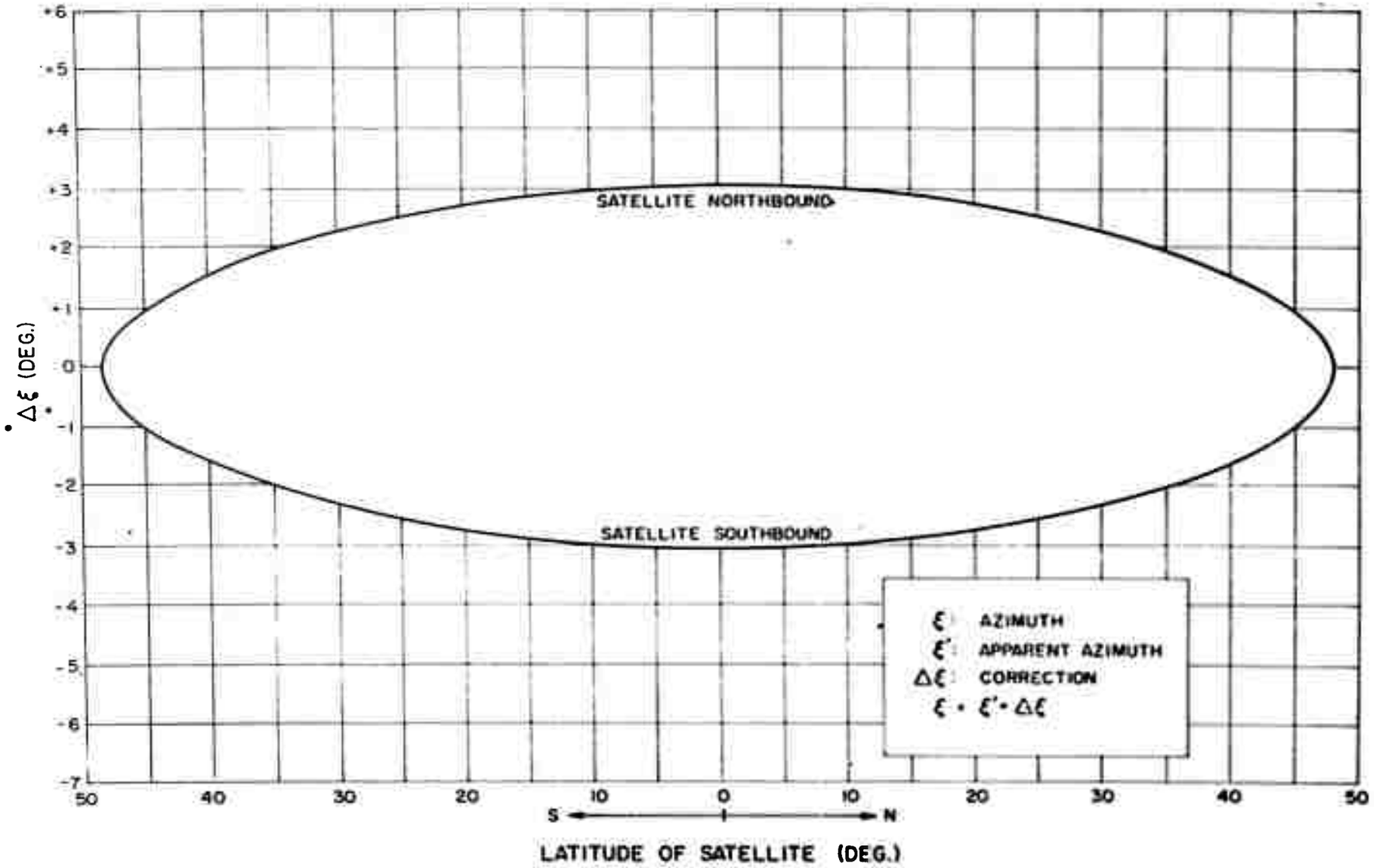

AZIMUTH COMPENSATION FOR ROTATING EARTH

FIG. A-6

satellite relative to earth has contributions due to orbit precessions. However, these are trivial for TIROS picture applications. These precessions are typically the order of 5° per day, leading to tangential velocity contributions of the order of 15 mph, even less than typical cloud velocities or in the effect of parallax on assessing surface velocity due to uncertain cloud height.

A.4 Graphical Methods for Approximate Attitude Determination

The graphical methods described here are intended to give reasonably accurate attitude determinations with a minimum of time and labor. Designed originally to provide attitudes for the TIROS I operational use program, they have continued to prove useful in subsequent research work and in the operational program for TIROS II.

The fitting of nadir angles measured from the pictures to the theoretical curves of Figure A-7, a procedure which was described earlier (Ref. 1) has been the most widely used of these methods. We review this method first because it best exemplifies the characteristics sought for graphical work. The other graphical procedures suffer by comparison, for they either have inherent inaccuracies, or demand much more labor, or both. However, they are useful at times, when the results are needed but the the automatic digital programs are unavailable.

A.4.1 Sequence of Nadir Angles

Figure A-7 shows a plot of horizon images for standard nadir angles, based on Equation (4) but incorporating the lens distortion for TIROS. With a picture projected on this plot at the proper magnification, one can match the horizon image in the picture to one of these curves to determine the nadir angle. This procedure is quite accurate because with reasonable care one essentially takes into account every horizon image element in the picture so as to arrive at the best overall horizon fit.

Let nadir angles be measured in this way for several pictures in a sequence, taken at known values of true anomaly. These values are plotted against true anomaly at the same scale as used in Figure A-5. The value of w_o is assumed unknown at first, of course; it is determined by moving the plot of observed nadirs sideways (keeping the n = 0 baselines superimposed) to achieve the best fit of the plotted points to one of the theoretical curves. The value of n_o is determned as that of the theoretical curve which provides the best fit.

FIG. A-7

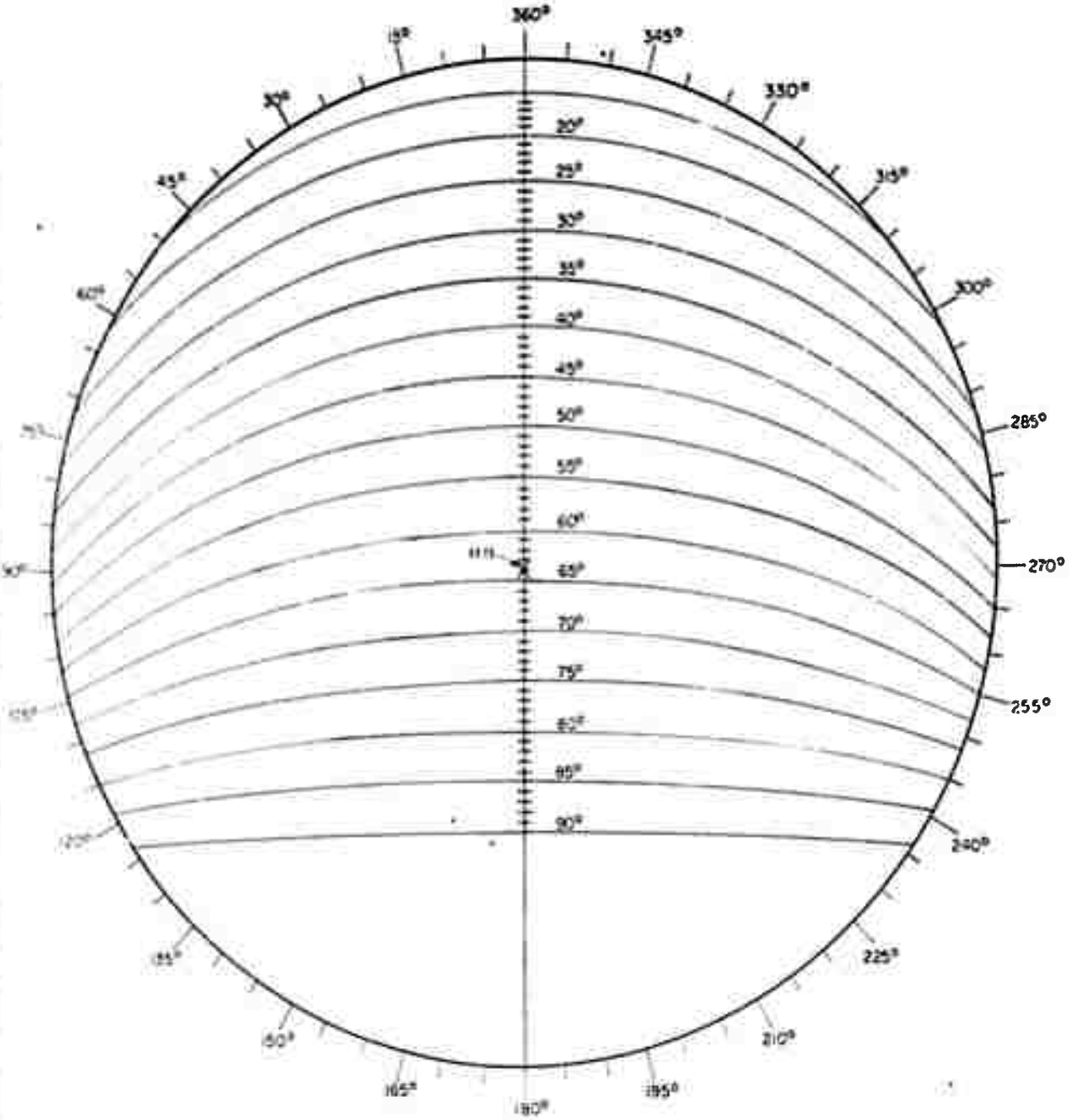

NADIR ANGLE INDICATOR

450 STATUTE MILES

The use of true anomalies has been inconvenient because the position of a TIROS satellite in its orbit has generally been furnished to the user only in terms of the time after ascending node. For convenience, therefore, a circular orbit approximation generally has been used, where the $(w - w_o)$ scale in Figure A-5 is replaced by a linear $(t-t_o)$ scale. In so doing, one deals with t_o, the time at which minimum nadir angle occurs, rather than w_o, the true anomaly at which it occurs. The error resulting from the use of linear time scale is not serious for TIROS I or II, within the precision sought for the early operational use programs. In any event its practical effect is minimized when one regularly deals with pictures from the same restricted segment of the orbit.

Part of the time this method is sufficient by itself. However, it is inadequate for cases of small n_o, because the horizon image is generally missing from the pictures for small nadir angles, which are indispensible for accuracy in determining n_o when n_o is small.

From the graph of azimuth angle against true anomaly (Figure A-5) it is apparent that the sequence of azimuth angles would be the ideal counterpart to the preceding method; it also would employ a simple curve-fitting scheme, and the azimuth data is orthogonal to the nadir data, in the sense that the one set provides whatever information the other set indicates poorly. Unfortunately, azimuth data require a picture analysis which goes well beyond the use of horizon images that furnish nadir angles. Except when landmarks or an accurately interpretable sunglint image can be seen, the picture must contain some representation of the known satellite velocity vector to provide a reference against which the azimuth of the principal line can be measured. In practice therefore, one must rely on some analysis of the regions of overlap between successive pictures. Simple graphical curve-fitting can be used finally, but the points to be fitted to theory must be derived from the pictures by a fairly laborious analysis.

A.4.2 Matching Individual Rectified Pictures

A direct parallel to the mathematical treatment of Section A.3.2.1 was described in an earlier report (Ref. 1). The use of the perspective grid-transfer grid technique of Allied Research (Ref. 9) permits the rectification of any single picture containing a horizon image on to a planar representation of the earth's surface. Except for the subpoint, true latitudes and longitudes are unknown under our assumption of no prior azimuth information, but the

rectified picture can be drawn satisfactorily on a blank sheet of paper with the aid of the transfer grid. The same thing is now done on a separate sheet of paper for another picture containing images of a portion of the same object space. The two rectified sketches are placed together to provide the best coincidence of rectified images in the region of overlap. Since the principal points or the subpoints, or both, can be marked on each of the sheets for the corresponding satellite position, the path of subpoints and the path of principal points is easily derived. From the path of subpoints and the direction of the principal lines of the two pictures the azimuth is measured directly. This is not the true azimuth because the subpoint path is affected by the rotation of the earth (see Section A. 3. 2. 3), but on the other hand it is precisely the azimuth required for transferring the cloud data directly to a map on which the path of subpoints has already been prepared from orbit calculations.

This procedure has the unfortunate effect of introducing yet another transfer of cloud information between maps, in addition to the standard set of such transfers that is already used in the TIROS meteorological analysis. Aside from the additional time required, this has the disadvantage of allowing more errors to occur in the usual course of operations. However, with sufficient time and care, this procedure should provide good overall rectification. The rectification of the individual pictures must be done in painstaking detail, to insure ample positive identification of the image details to be matched in the regions of overlap.

A.4.3 Image of the Principal Point Path

As noted just above, the difficulty in matching the representations of object space from two pictures is the need to construct those representations with accurate fine detail, a nuisance when only a portion of the detail has meteorological significance. An alternative is to work directly in image space i.e., to perform the graphical construction directly on one of the pictures. In many sequences the pictures contain enough fine detail to permit an accurate location of the principal point in a picture relative to either cloud or landmark features. In these cases the same details can be identified in adjoining pictures from the sequence, and thus it is a relatively simple task to spot on to a print of one picture the principal points from one or several adjoining pictures. Preferably one would do this for the subpoints, but the fact that they are typically near the edge of any picture with enough horizon image for accurate picture orientation, means that they can seldom be either

located or transferred from picture to picture with satisfactory accuracy or frequency.

Principal points can be transferred as described on to a perspective grid when only a single positive film is available, containing all the pictures of interest. However, for good accuracy one again needs to construct an accurate sketch of one picture in order to compare its details with the next picture. Ideally the principal points are transferred between individual enlarged prints, permitting all of the detail in the original pictures to assist in an accurate transfer.

Figure A-8 illustrates an image of the principal point path which has been derived in this manner. Also shown is the principal line image, ostensibly chosen as the shortest line from principal point to the horizon for this picture, but in practice traced from the principal line of the horizons chart (Figure A-7) after the best-fit horizon has been chosen. The angle in object space between the principal line and the path of principal points i.e., this angle as it would be measured directly on the earth approximates the desired azimuth angle because in general the path of principal points is roughly parallel to the path of subpoints. The image of this angle i.e., the angle, γ, which is shown measured directly on the picture, is of course modified further by the picture perspective. Nevertheless the relation between γ and ξ can be calculated, and Figure A-9 shows γ as a function of $(w - w_o)$ for selected values of n_o, in a manner directly analogous to the azimuth angle graph of Figure A-5. The curves do not extend to the point $w - w_o = 90^o$ because the principal axis misses the earth for the higher nadir angles.

Unlike the azimuth angle curves, the curves of γ are different for different satellite heights, so that a universal curve cannot be drawn, at least in any simple fashion. Also because of this it is not possible in general to produce curves of γ for a specific elliptical orbit, since one must anticipate secular changes in the location of minimum nadir angle, relative to perigee, w_o. A further difficulty is the fact that the effect of the earth's rotation cannot be incorporated in a single set of γ curves, both because of the secular change in the location of perigee relative to the ascending node, and because of the changing w_o.

If one can tolerate inaccuracies of a few degrees in azimuth, however, one may measure γ as indicated by a sequence of pictures, plot them, and fit

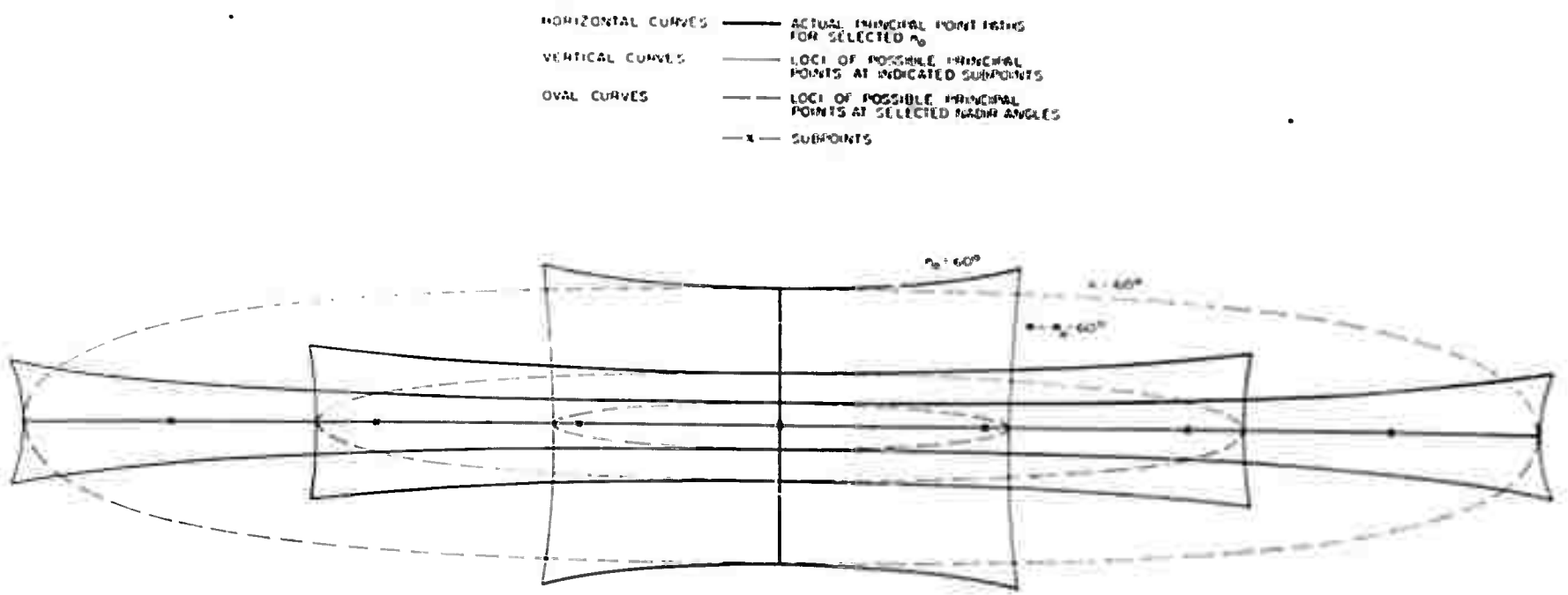

PRINCIPAL POINT PATHS IN OBJECT SPACE

FIG. A-8

FIG. A-9

THE FUNCTION $\gamma(\phi, n_o)$ FOR TIROS I
(ONE QUADRANT ONLY)

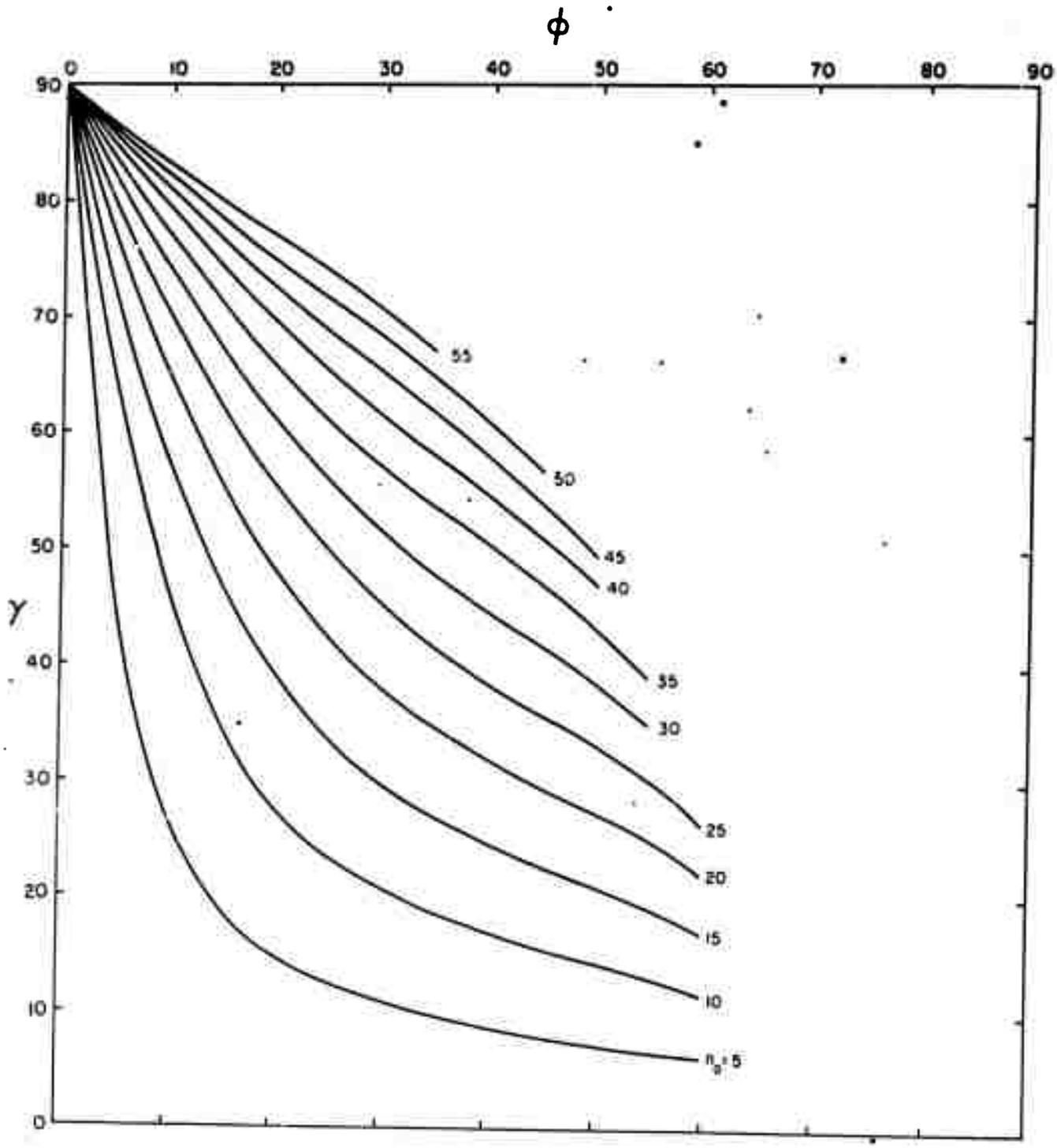

them to curves of γ as shown in Figure A-9, which have been drawn for a suitable TIROS I approximate circular orbit. This fit provides indicated values of n_o and w_o in the same fashion as did the fit of nadir angles described above. Although inherently less accurate overall, the indicated azimuth information can be more reliable than that from nadir angles when n_o is quite small.

An alternative method is to use n and γ for one picture to calculate n_o graphically. The algebra is similar to that of Equation (14), but modified at some length to include picture perspective and the distinction between the use of subpoint path and principal point path as the reference direction for the measurements. A nomogram for such a solution is shown in Figure A-10. Although the solution is unique, a normal graph is awkward because the curves overlap. To remedy this, a sliding baseline is used in effect, to spread the curves apart in Figure A-10. To use this nomogram, one first evaluates the parameter m for the given n and γ; then one finds $n_o = m - n$.

In this procedure one may equip oneself with an assortment of curves for selected satellite heights in order to be prepared for elliptical orbits. However, no simple compensation seems possible for the rotation of the earth. This procedure has been used with reasonable success for a few orbits, several values of n_o being obtained for each orbit by using the (γ, n) values measured from several pictures, and an averaged value calculated after a qualitative allowance was made for the varying probable accuracy of the individual measurements.

A.4.4 The Principal Point Path on an Oblique Mercator Map

Figure A-11 shows principal point paths on an oblique Mercator projection of the earth, for selected values of n_o. These paths were calculated for a circular orbit at the average height of TIROS I. Also shown are loci of principal points for given nadir angle values, and loci of principal points for given values of true anomaly, as well as the subpoints for those true anomalies. This chart can be used in various ways to evaluate attitude or to assist directly in picture rectification. Like other aids described above, a single chart is sufficient only if one can tolerate the circular orbit approximation and ignore the effect of the rotation of the earth. If these effects must be taken into account, a special chart is required for the proper value of the argument of perigee and the proper value of w_o.

FIG. A-10

THE FUNCTION $n_o(\gamma, n)$ FOR TIROS I (ONE QUADRANT ONLY)

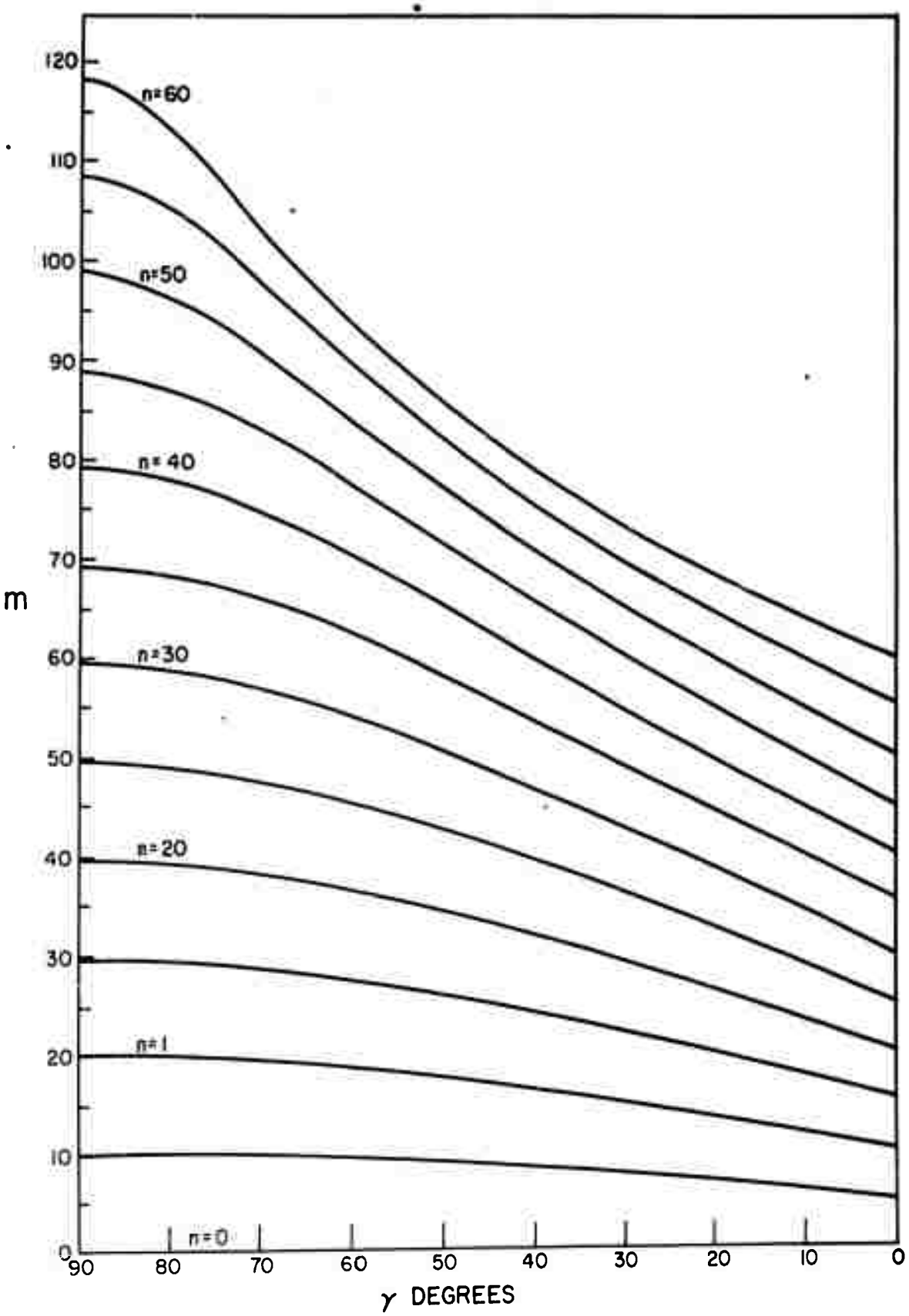

PRINCIPAL POINT PATH IN IMAGE SPACE

This chart is intended primarily for use in conjunction with the image of the principal point path, located by comparing overlapping pictures as described in the preceding section. In rectifying pictures by means of the Allied Research perspective-grid, transfer-grid technique (Ref. 9) one simply requires that the rectified sketch derived from each picture be rotated about the subpoint to place the rectified principal-point path from the picture in proper alignment with the theoretical curves provided by the chart of Figure A-11. As a rule of thumb, it can be seen that the principal point path on the map in fact is roughly parallel to the subpoint path over a great deal of the chart, so that one normally gets approximately correct results by simply lining up the rectified principal point paths from the pictures in this way.

The other loci on the chart assist in deriving further information in the course of the above operation. Consider a single pucture which has been rectified onto a blank sheet of paper. The principal point to subpoint distance is fixed by the nadir angle, which we assume to be known from the horizon image in the picture. The angle between the principal line and the path of subpoints rectified from the photograph is known. Now let us move the principal point along the locus for the proper nadir angle, meanwhile keeping the subpoint on the subpoint path. It can be seen that the rectified picture must be rotated as this is done; the correct position for the rectified picture is that which properly aligns the rectified track of principal points. With the picture placed correctly, one can read the indicated value of n_o and of $w - w_o$ from the chart; with w assumed known, w_o is fixed.

A.5 Automatic Computation of Latitude-Longitude Grids

When the attitude of the camera is known it is possible to construct latitude-longitude grids to match each picture. This is probably the most efficient way of applying the information at present. It allows the cloud information to be transferred directly from the pictures to a standard base map, eliminating the need for the transfer grid and the special oblique Mercator map which must be used with the perspective grids.

Equations (1) and (2) give the image location for an object which is described in the local coordinate system, x, y, z. We apply this to the positions of the intersections between standard parallels and meridians which lie in the field of view of the camera. The transformation from geographical

coordinates to our local coordinates is a single rotation, easily compounded of a rotation by the longitude of the orbit ascending node, around the north pole, a rotation by the inclination of the orbit, around the ascending node, and a rotation by the argument of the latitude of the satellite, about the direction normal to the orbit.

As programmed for the Bendix G-15D computer, the horizon is plotted first, using Equation (4). After this the computer starts from a grid point known to be in the picture, and calculates points in each direction until it arrives at either the horizon or at a predetermined radius chosen as the edge of the picture. The program was arranged to do this in a fixed order, and to drive the associated incremental plotter so as to draw the entire grid automatically. An example is given in Figure A-12. Here the plotter also has been made to draw the West coast of North America. The same computer program is used for this as for the grids, except that the sequence of points is drawn from memory instead of incremented along a standard grid.

FIG. A-12

LATITUDE-LONGITUDE GRID WITH COASTLINE

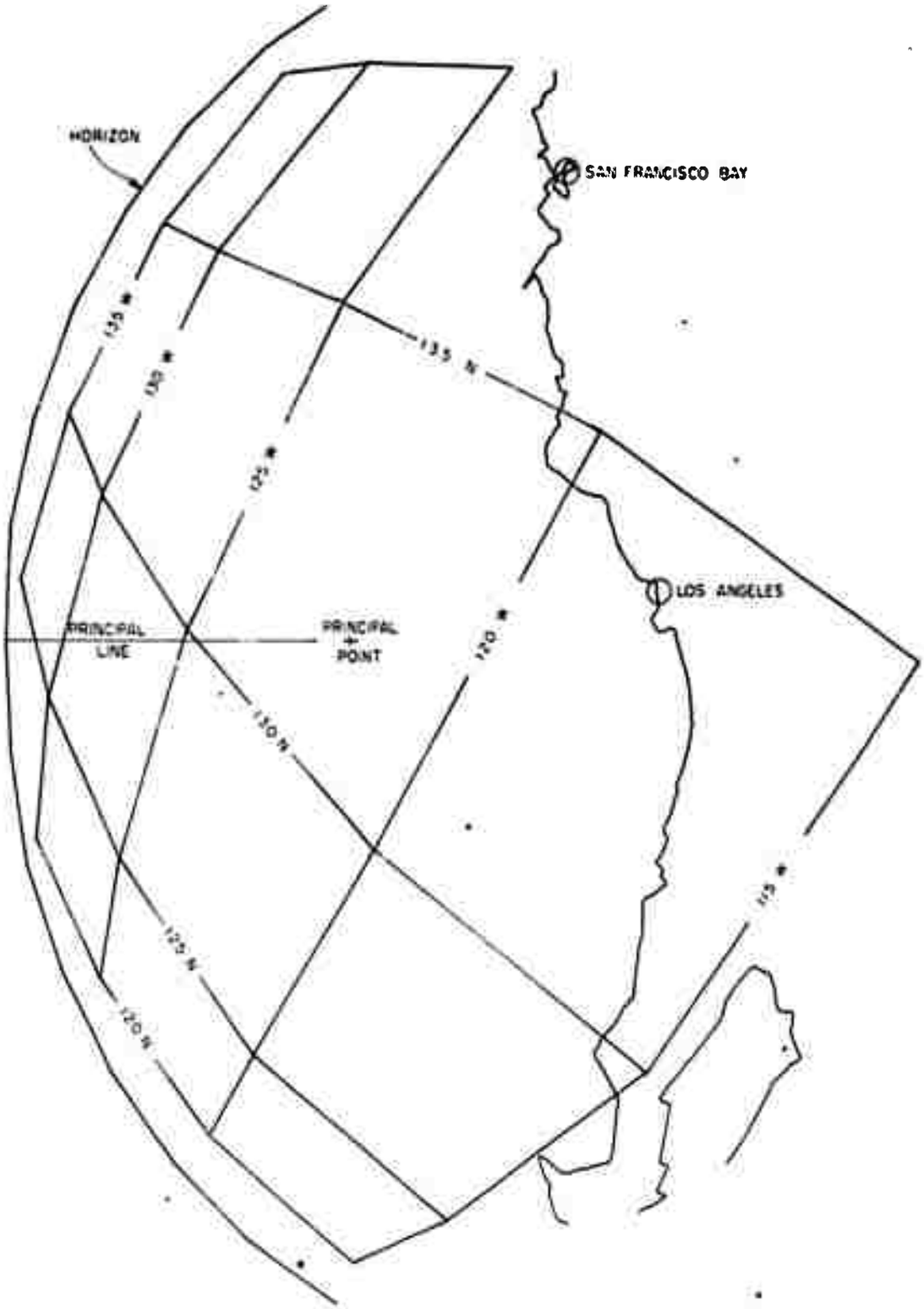

APPENDIX B

A CRITIQUE OF THE TIROS II IMMEDIATE OPERATIONAL USE PROGRAM AT BELMAR, NEW JERSEY

B.1 Facilities and Pre-Launch Activities

The facilities for TIROS II were essentially the same as for TIROS I with the following exceptions: At the antenna site, a small photographic darkroom was set up in the control building, and a direct teletype line to TIROS Technical Control at NASA was installed for transmission of the horizon information obtained from one of the infrared channels.

A "nixie" light clock calibrated to milliseconds and tuned to WWV was installed near the backup programmer. It was the time standard at the read-out site. A small spring-driven, sweep-second-hand clock was installed to be in the field of view of the monitor display panel. This "read-out clock", set to nixie light time, was used to time "direct" pictures.

At the meteorological analysis center, Bldg. 4, the equipment available was similar to that for TIROS I, though the facsimile machines had been changed to Alden facsimile rather than Times facsimile as previously. The photo-facsimile circuit to TIROS Technical Control was put on a separate line with a provision for telephone communication between the two sites.

The primary special equipment in Bldg. 4 consisted of the following:

Two teletypewriters, one at a time on line to Spacon (NASA Space Communications Center) for retransmission to the Weather Bureau at Suitland, Maryland, Point Mugu read-out site, etc.

Two Alden facsimile machines (one on line) direct to the Weather Bureau at Suitland, for transmission of Mercator maps depicting cloud cover; also one recorder for monitoring the transmission.

One high resolution wire photo machine for transmission of polaroid prints of 35 mm positives to TIROS Technical Control to be used for publicity and to illustrate areas viewed by IR sensors.

Three modified Simmon enlargers for projecting the TIROS 35 mm film positives.

Working schedules provided for two shifts a day, to be rotated among the three four-man teams so that each would work approximately a 40 hour week, while providing seven-day coverage, two-day vacations for two teams each week plus one four-day vacation for each team every six weeks. The first shift performed most of the rectifications and the associated facsimile and teletype transmissions. The second shift would make the last few remaining rectifications (if any) and transmissions and prepare for the next sequence of passes.

B. 2. Early Post-Launch Activities

TIROS II was launched from Cape Canaveral at 0613E on 23 November 1960. Reports of the launch were received over the telephone from NASA TIROS Technical Control. The first two stages were exactly on predicted course, but the last signal from the third stage indicated it might be off course. This was verified later in the day, when it was established that TIROS II was orbiting successfully, but with a much greater orbital eccentricity than was desired. Apogee and perigee were approximately 455 and 385 statute miles, respectively.

The first pictures, "directs" taken on orbit 1, showed no earth. The nadir angle was too high and the pictures were taken west of the sunrise line. Narrow-angle pictures from succeeding orbits were excellent, but wide-angle pictures were of poor contrast. Late in the day, and increasingly over the next few days, the contrast was enhanced electronically, making the pictures more usable.

By measuring nadir angles from frames having horizons, the value of minimum nadir angle (n_o) was estimated (by comparison with the theoretical curves of Dr. C. Dean of Allied Research) to be about 10 degrees. The minimum nadir angle occurred about 40 minutes after ascending node. The first successful rectification, over the eastern U. S., was made on 26 November. It was not retransmitted by the Weather Bureau because

of possible location errors. On 28 November, the first rectification was retransmitted from Suitland. The number of rectifications transmitted to Suitland increased day by day until by 4 December and thereafter every pass with usable pictures was rectified, transmitted to Suitland and retransmitted over the national facsimile network.

B.2.1. Spin-up

After the satellite had been de-spun from its third stage spin rate of about 120 rpm, its spin rate was 7.9 rpm. This was below the design range of 9-12 rpm and a slight wobble was detected. On 25 November the satellite was spun-up to 10.8 rpm after a previous attempt at spin-up on the 24th had failed. Wobble was still noticeable, as verified by the picture analysis, and had possibly even increased. On the same day the satellite was spun-up a second time to about 14 rpm. This greatly reduced or eliminated the wobble.

B.3. Late Post-Launch Procedures

As of mid December, procedures of the set-up team, for remote pictures only, were roughly as follows:

Team members check both Belmar and Point Mugu programs for the next sequence of passes for completeness and consistency. Via direct phone to TIROS Technical Control at NASA, they resolve any discrepancies or omissions.

They select the oblique Mercator map(s) appropriate to the pass. Using ascending node time and longitude, necessary calculations are performed to establish time and longitude for master subpoint map.

From observations of n_o and t_o, n_o and t_o are predicted for all passes to be read out at Belmar. A separate data sheet is prepared for each pass tabulating the necessary attitude and rectification data.

About 15 minutes before satellite acquisition, one or two members of the analysis team arrive at the antenna site. At the antenna site, they check the settings of the clock pulses on the "programmer" to be used on the pass against the program, check the programmed alarm times, and on direct pictures check the time of the read-out clock against the nixie light clock.

During acquisition, these people observe the operations in general while checking alarm times, observing the monitor scope to see whether remote pictures with horizons are being received, that the correct number of set pulses is sent out to the satellite, etc. After the pass, they discuss with the read-out team how the acquisition went, noting any significant departures from normal. While a photographer is processing the 35 mm film in Unibath, they help one of the read-out team members determine time of first remote picture from IR tape on the Brush recorder.

If, as usual, processed (positive) film quality is satisfactory, they then drive to the meteorological analysis site with film plus negative film of preceding pass. If film is unsatisfactory, a rerun from tape is requested.

Examine film for such features as number and labelling of frames, picture resolution and contrast, visible horizons, rotation rates, landmarks, clouds, noise, etc.

At the meteorological analysis site, team members measure nadir angles, using the nadir angle indicator sheet corresponding to the satellite height at time of picture taking. From the curve of best fit the minimum nadir angle (n_o) is estimated, along with the time of minimum nadir angle (t_o) with respect to a frame of known time, (usually Frame 32-the first remote picture taken). Observed and computed minimum nadir angles and times are compared. In general, if predicted azimuths of principal lines with respect to subpoint track (ξ) are within three degrees of those "observed", the predicted (plotted) ξ's are accepted. In the event of greater differences, principal lines on the oblique Mercator map are replotted.

Rectification can now begin. This followed earlier practice.

B.4. Magnetic Attitude Control Switch

During operations with TIROS I the spin axis remained nearly in the plane of the orbit for most of the passes. This was unanticipated and inexplicable for many weeks until it was discovered that fortuitously the wiring of the satellite formed a D. C. loop which produced a net restoring force by interaction with the earth's magnetic field.

For TIROS II, it was planned to control the attitude of the satellite by regulation of current through a special loop oriented so as to cause a

perturbing force through interaction with the earth's magnetic field. The magnetic attitude control (MAC) stepping switch was to regulate the current flow through the loop, hence the rate of change of attitude. It had been expected that after the MAC switch was stepped the spin axis (in celestial coordinates) would move due south rapidly. This would reduce the minimum nadir angle while greatly increasing the time after ascending node at which it occurred. The switch was not to be stepped until two weeks after launch, but during the first week it frequently stepped itself out of the "off" position, presumably by responding to noise. This trouble gradually rectified itself.

By 7 December, two weeks after launch, minimum nadir angle was 38 degrees, increasing about two degrees per day, while time of minimum nadir angle was 55 minutes after ascending node increasing about one minute per day. The MAC switch was stepped to position two on pass 203 about 0800Z on 7 December. The results were soon apparent. Minumum nadir angle reached 40 degrees but then almost stopped increasing. Time of minimum nadir angle after ascending node began increasing at about two minutes per day. Thus the switch was partially effective, but less so than anticipated.

B. 5. Horizon Scanner

There was an infrared sensor aboard TIROS II mounted at right angles to the spin axis, which scanned the earth as the satellite rotated. During direct passes the respective scan times for earth and space were recorded in milliseconds on teletype tape. Spin rate was obtainable directly from these data. With known height (from NASA computer) the nadir angle at a particular time could be computed from the relative earth to earth-plus-space scan times. When minimum nadir angle was occurring in the southern hemisphere, the Dean nomogram could be used to obtain maximum nadir angle and time of maximum from a plot of nadir angle vs. time. The minimum nadir angle was obtained as the supplement of the maximum. The time of minimum could be found by determining latitude of maximum nadir angle from ephemeris data, and from the same data source, finding time of satellite arrival at the corresponding southern latitude.

Starting 12 December one or more determinations per day of minimum nadir angle were made at Belmar using horizon scanner data. This was time consuming work, requiring one to two hours per determination. The results scattered somewhat, but were in substantial agreement with the photo attitude determinations, though in the mean giving minima perhaps a degree higher than those indicated by the photo attitude data and occurring about a minute earlier. Provided the satellite heights from the ephemeris data were correct, it was believed that the photo attitude determinations were more nearly correct.

B.6. NASA Computation Center Activities

For portions of orbits within antenna range and portions of orbits within which remote pictures may be taken, the NASA computer provides minute-by-minute predictions of subpoint latitude and longitude, heights of the satellite, nadir angles, principal point latitude and longitude, ascending node time and longitude for each pass. However, for a period of several days four of NASA's five computers were inoperative, so ephemeris data were sketchy, possibly leading to some misplaced subpoints.

Ascending node elements, subpoint coordinates, and heights of the satellite were satisfactory, but nadir angle and principal point predictions were not usable through 16 December. At first, minimum nadir angle predictions were 5-10 degrees too high and times of minima a few minutes late. Later, predicted minima were 8-10 degrees lower than observed with times still late. A third set of predictions gave minima within a few degrees of those observed, with times still late by one to two minutes.

B.7. Picture "Noise"

In addition to poor resolution and contrast, the wide-angle pictures suffered from "noise" of various sorts. Ignition and other local noise was present, but was probably less than for TIROS I. Pulses from the sun sensors appeared as bands stretching across the whole image. Within the bands, noise lines were oriented diagonally to the band boundaries but parallel to one another. This noise was not too serious.

Noise appeared in various other guises: As a herringbone pattern, as squares, and as an apparent great increase in resolution giving a

"billowy cloud" appearance. Rectification through this noise was impossible. It became a serious nuisance for several days in early December, though it had been observed from time to time previously. It was diagnosed by Signal Corps representatives as a result of low beam voltage on the satellite vidicon. This analysis seemed to fit the facts since the December occurrence coincided with heavy programming which had reduced voltage. When programming was reduced this noise decreased also.

B.8. Impressions

Despite such limitations as poor contrast and resolution, and an elliptical orbit, TIROS II rectifications were completed in a shorter time and with better accuracy than TIROS I. After the first ten days every pass with usable film was rectified. These results were due partly to the larger staff but mostly to the much better attitude determination for TIROS II. High minimum nadir angles made it unnecessary to attempt to rectify frames without horizons, thus simplifying the attitude determination and rectification technique.

TIROS II nephanalyses probably reached meteorological field "users" several hours earlier than did the TIROS I nephanalyses. Faster data distribution resulted from time saving procedures such as high speed photographic processing techniques and increased availability of transmission time on the national weather facsimile circuits.

The transmitted Mercator maps were on scales of either 1:10,000,000 or 1:20,000,000. Most analysts were somewhat hesitant about using the latter, feeling that significant cloud features were so reduced in size as to appear insignificant in casual inspection.

The enthusiasm of the staff had been aroused by training with TIROS I film. When the comparatively poor quality of TIROS II film became evident, loss of enthusiasm occurred (though the success of the attitude determination nomograms gave some satisfaction), Consequently, some of the rectifications were performed in a mechanical manner without much attempt to relate the cloud features to meteorological phenomena. Around mid December, vortices began to become evident and rekindled some of the lost enthusiasm.

APPENDIX C

A CRITIQUE OF THE TIROS II IMMEDIATE OPERATIONAL USE PROGRAM AT POINT MUGU, CALIFORNIA

C.1 Pre-Launch Activities and Facilities

Three teams of four men each were formed to provide complete service during all TIROS data acquisition times. Each man had been previously trained in most of the essential phases of the operation as developed by the Meteorological Satellite Laboratory (MSL) of the U. S. Weather Bureau. The initial TIROS data reduction and rectification was to be handled by methods developed by MSL.

The TIROS II I.O.U. project was housed in the Naval Aerology Building. Working space and materials were adequate. The RCA van containing the tape recorders was located about 100 feet from the Aerology Building and was always accessible to the meteorological staff. The location of the photographic laboratory necessitated about a two-minute car ride from the RCA van. It required only fifteen minutes to get the film from the van, have it processed at the photography laboratory and return it to the meteorologists in the Aerology Building. Film processing was never required of the meteorologist as was initially feared.

The primary transmitting and receiving equipment was located on San Nicolas Island - some 40 miles off the coast from Point Mugu. Incoming picture signals from the satellite were transmitted from San Nicolas Island to the RCA van via a microwave hookup. The microwave link caused no additional problems of any significance. Occasionally, however, some minor line distortion was noted in the pictures.

It was rather unfortunate that the receiving equipment was located on San Nicolas Island. Some information recorded there would have been useful to the meteorologist. For example, it was not possible to have ready access to the Events Record and the Brush Instrument Record. The former provides data on the time of "direct" pictures and the number of "remote" pictures, whereas the latter record provides remote picture times.

C. 2. Post-Launch Activities

After launch an inspection of the first TIROS pictures (wide-angle) revealed that the images were not clear. The pictures lacked contrast and sharpness resulting in an image which appeared to be out of focus. The fiducial marks (which were etched onto the vidicon) were very clear and in sharp focus; this means the image which passed through the lens system (preceding the vidicon) was blurred. In addition, the vidicon itself may have been faulty. A series of bands with identical orientation was noted on each picture. These "ripples" were most clearly visible against an image towards the white end of the gray scale. Thus a white cloud mass would appear to be a series of cloud billows.

Attempts to increase picture contrast met with only marginal success. Contrast was boosted nearly to the limit of the ground monitor capacity. The range of the gray scale was also shifted towards the white. All these adjustments provided an apparent improvement in gross image recognition with an attendant loss of image detail.

The narrow-angle camera performed satisfactorily. It should be noted that narrow-angle camera pictures may appear greatly overexposed due to the attempted electronic enhancing being applied to the wide-angle camera pictures, which were on the same film strip. However, the original narrow-angle pictures stored on the magnetic video tape are probably of good quality requiring only normal processing.

Meteorological utilization of the TIROS II pictures during the first few days of acquisition was negligible. Utilization gradually improved to the point where large-scale cloud features were consistently transferred to base maps and transmitted on the facsimile. Cloud types were not generally recognizable. Only cloud cover data were available.

The pictures were generally kept well "squared-up" as indicated by minimal shifting of the fiducial marks. However, during the week of 10 December, an increasing displacement of the fiducial marks was noted. During this same time period there were many failures of the 60-foot antenna.

Initial picture rectification was attempted with MSL techniques. It was immediately obvious that the predicted attitude data from the NASA Computing Center was in error. MSL techniques were also greatly

hampered due to the lack of landmarks in the pictures. During these first few days it was possible to deduce some of the parameters required in the Allied Research method of attitude determination. Over a period of two or three days the attitude determinations were at least internally consistent. Some of the attitude determinations were independently verified by the Allied Research representative at Belmar, New Jersey. Gradually the entire meteorological staff at Point Mugu was trained and most of the attitude determination techniques developed by Allied Research were instituted as standard operating procedure.

Confirmation of the validity of the Allied attitude determination and rectification system was obtained at a later date when a landmark (Australia) became visible. Extrapolation of required parameters (n_o, t_o) was fairly reliable. The only difficulties encountered were when the magnetic attitude control switch position was changed. This resulted in a change in slope of the two critical parameters, n_o and t_o.

During the week of 12 December the automated drawing of latitude-longitude grids for geographic location and rectification was instituted by Allied Research. The grids were produced by a Bendix G-15D Computer driving an incremental line drawer. The accuracy of the grids was found to be excellent when landmarks were available for comparison. A serious handicap was presented due to the excessive time required for the plotter to produce the grids. Three to four hours were required to obtain ten grids with latitude-longitude intervals of 2-1/2 degrees. As a result of the time required to produce the grids only one remote sequence of pictures could be rectified by using latitude-longitude grids. A grid was prepared for every third frame.

A new grid program was subsequently prepared by Allied Research personnel. This program was identical to the original with the exception that latitude-longitude lines were drawn for 5 degree intervals. This program reduced the required plotting time by nearly a factor of four. It permitted the generation of ten grids in fifty minutes, making it feasible to generate grids for all four passes during the day.

The time saving advantage provided by the second grid program has not yet been fully realized. Using the first grid program it was necessary to assign one man to spend an additional 3 to 4 hours with the computer.

However, since one remote sequence can now be generated in less than one hour (about 50 minutes), it may be possible to generate grid sequences between successive data acquisition times.

The ability to generate grids between acquisition times (instead of 6 to 12 hours prior to the time of the first read-out pass) permits one to check any last minute changes in programmed picture timing. It also permits verification of the predicted daily values of n_o, t_o after the first picture sequence has been rectified.

A further reduction of grid-generating time would be highly desirable from many aspects. At present, grids are generated for every third frame. However, in some situations it might be more advantageous to generate grids for alternate frames. Another reason for a decrease in grid-generating time is to permit the start of grid generation a few minutes after data acquisition. During this short delay it would be possible to obtain a verification of remote picture time from the Brush Instrument Record, thus enabling the programmer to feed a more accurate time input into the computer resulting in even more exact grids.

For expediency it would be desirable to have the Bendix computer and plotter in the same location as the meteorological analysis team. Thus each grid could be removed from the plotter upon completion instead of being delayed until all grids for a pass were completed.

Utilization of the latitude-longitude grids during the rectification process reduced analysis time from 2-1/4 hours to approximately 1-3/4 hours.

The problem of uncorrected picture distortion (both optical and electronic) became quite evident when picture rectification was accomplished through the use of the latitude-longitude perspective grid. In one case a cloud element was observed towards the center of a picture. The geographical latitude and longitude of this cloud element were obtained from the generated perspective grid. Some frames later, on the same picture sequence, the cloud element appeared towards the edge of the picture. Using the appropriate perspective grid for this latter frame it became obvious that the cloud element was no longer near the originally determined coordinates. Although the latitude-longitude perspective grids contained a first order distortion correction, it is apparent that further investigation into eliminating the distortion to a much greater extent is required.

C. 3. Summary

The TIROS II experiment was extremely valuable proving the validity of the various data reduction techniques and the feasibility of generating latitude-longitude perspective grids on an operational basis.

REFERENCES

1. Glaser, A. H., TIROS I: An Operational Evaluation of a New Meteorological Tool. Second Semi-Annual Technical Summary Report, Contract AF 19(604)-5581, Allied Research Associates, Inc., 1960.

2. Glaser, A. H., The Temperature Above An Airport Runway On a Hot Day. Sci. Report No. 3, Contract AF 19(604)-997, Texas A and M Research Foundation, 1955.

3. Glaser, A. H., Elliott, W. P., and Druce, A. J., The Study of Small Scale Modification of Air Passing Over Inhomogeneous Surfaces. Final Report, Contract AF 19(604)-997, Texas A and M Research Foundation, 1957.

4. Sverdrup, H. U., Oceanography for Meteorologists. New York, Prentice Hall, 1942.

5. Glaser, A. H., Meteorological Utilization of Images of the Earth's Surface Transmitted from a Satellite Vehicle. Final Report Phase II, Contract No. AF 19(604)-1589, Blue Hill Meteorological Observatory, Harvard University, 1957.

6. Fitz Roy, R., The Weather Book. A Manual of Practical Meteorology, Second Edition. London, 1863.

7. Bergeron, T., Methods in Scientific Weather Analysis and Forecasting. The Atmosphere and the Sea in Motion. New York, The Rockefeller Institute Press, 1959.

8. Freeman, J. C., An Analogy Between the Equatorial Easterlies and Supersonic Gas Flows. J. Meteor., 5 138-146, 1948.

9. Glaser, A. H., A System for the Meteorological Operational Use of Satellite Television Observations. First Semi-Annual Technical Summary Report, Contract AF 19(604)-5581, Allied Research Associates, Inc. 1960.

UNCLASSIFIED